

Semiconductivity  
in  
Cadmium Telluride

by  
John Leete Stull, B.S., M.S.

A Dissertation  
submitted in candidacy  
for the degree of  
Doctor of Philosophy  
in  
Ceramics  
at  
Alfred University

State University of New York  
College of Ceramics

June 1958

ERRATA

<u>Page</u>	<u>As is now</u>	<u>Should read</u>
3, eqn. 1	$(\hbar^2/2m)k^2$	$(\hbar^2/2m)k^2$
6, eqn. 3	$\hbar/m, m = \hbar (d^2E/dk^2)$	$\hbar^2/m, m = \hbar^2 (d^2E/dk^2)$
8, line 11	bottom of the conduction band	top of the valence band
9, eqn. 8	$(u_p + u_m)$	$(U_p + U_m)$
22, lines 4 and 13	$Cd^{-2} = Te^{+2}$	$Cd^{-2} = Te^{+2}$
23, line 8	Garlick	Gorlich
54, line 6	low temperatures	high temperatures
60, line 1	conduction	condition
80, refr. 17	P. E. Klaus	P. E. Kaus

## ACKNOWLEDGMENT

The author wishes to express his appreciation to Professor T. J. Gray, without whom this work could not have been undertaken. His stimulating advice throughout the course of the research has been a constant source of inspiration. Thanks are also expressed to Professor D. P. Detwiler for many helpful discussions of band theory and the calculations used in semiconductor research, and to Professor W. G. Lawrence, for his encouragement and his help in interpreting crystal structures.

Some of the early measurements were performed under the supervision of Dr. P. C. Bailey, then Senior Research Fellow, and his help and guidance are gratefully acknowledged, as are that of E. A. Giess, Senior Research Fellow of the ARDC Diffusion Program. Additionally, thanks are expressed to C. E. McNeilly and Dr. J. L. Miles, who prepared the single crystals and hot-pressed specimens, to S. W. Burt, who constructed the vacuum equipment, and to Mrs. D. A. Stevens and C. M. Bloomquist, who made the production of this thesis possible.

This research was supported by the United States Navy, through the Office of Naval Research, Contract Nonr 1503(01), Project No. NR 015-215. This financial aid is gratefully acknowledged. Reproduction in whole or in part is permitted for any purpose of the United States Government.

## TABLE OF CONTENTS

	page
I. INTRODUCTION	1
A. ELECTRICAL CONDUCTION IN SOLIDS	1
1. Ionic Conductors	1
2. Electronic Conductors	1
Metals	1
Semiconductors and Insulators	6
B. ELECTRICAL MEASUREMENTS	16
1. Resistivity	16
2. Hall Coefficient	18
C. CADMIUM TELLURIDE	21
II. EXPERIMENTAL	28
A. PREPARATION OF SPECIMENS	28
1. Single Crystals	28
2. Hot-Pressed Specimens	31
B. CUTTING AND ELECTRODES	33
C. APPARATUS	39
1. Atmosphere	39
2. Sample Holders	41
Hall Coefficient	41
Quenching Unit	45
3. Measurement Techniques	45
III. MEASUREMENTS	48
A. CONVENTIONAL HALL AND RESISTIVITY MEASUREMENTS	48
1. Pure Crystals	48
2. Bismuth Impurity Crystals	48

3. Hot-Pressed Specimens	49
4. Copper Impurity Samples	50
5. Indium Impurity Samples	51
6. Silver Impurity Crystals	52
B. ANOMALOUS RESISTANCE CHANGES	53
1. "Polarization" Phenomena	53
Resistivity	53
Hall Measurements	65
2. "Quenching" Experiments	67
IV. DISCUSSION	71
A. CONVENTIONAL HALL AND RESISTIVITY MEASUREMENTS	71
B. POLARIZATION AND QUENCHING EXPERIMENTS	73
V. SUMMARY	79
VI. BIBLIOGRAPHY	80

## I. INTRODUCTION

### A. ELECTRICAL CONDUCTION IN SOLIDS

#### 1. Ionic Conductors

The electrical conduction of a crystalline solid can be described as one of two general types of process, depending upon the identity of the predominant current carriers. In some materials, electrons are so strongly bound to their parent nuclei as to be, for all practical purposes, immobile, even under the influence of such forces as can cause movement of the parent nuclei. These materials come under the heading of ionic conductors, and owe their distinctive conductivity type to their greater ionic than electronic mobility. The current carriers consist predominately of the ions of the crystals themselves, the movement of which, because of their charged condition, constitutes an electric current.

Varying degrees of ionic character exist, and therefore, the classification of a compound as being "ionic" is not clear-cut (1). However, the classification "ionic conductor" includes those materials in which the preponderance of the current is carried by the ions themselves.

#### 2. Electronic Conductors

Metals -- The other broad classification of materials is "electronic conductors". In these materials, although motion of the nuclei may take place, the preponderance of the current is carried by electrons.

Within this classification, a material may be classified as either a metal, a semiconductor, or an insulator. The consideration of these three types will begin with a discussion of metallic conduction.

Much of the behavior of metals can be explained by considering a metal as a group of positively charged ions, whose lost valence electrons are free to move through the crystal. Their systematic movement through the crystal constitutes an electric current, from which arises the high conductivity of a metal.

A further analogy is the consideration of the electrons as a gas which pervades the interionic space in the metal (2) and whose interaction with the lattice ions can be explained by considering the potential energy of the electrons as being constant within the metal, that is, not subject to the periodicity of the lattice.

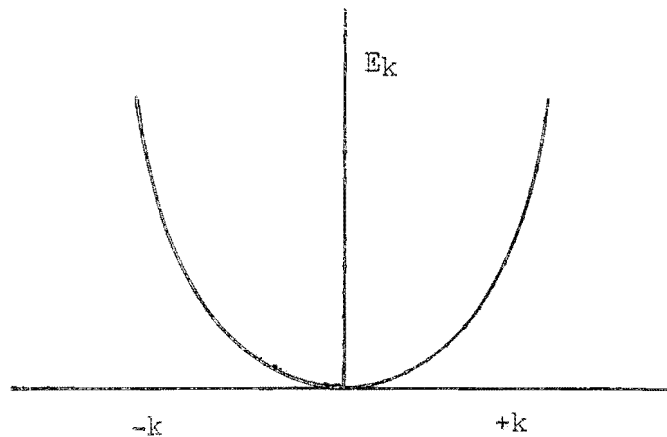
However, if this electron gas is treated in the same manner as a classical gas (3), errors result, particularly as regards the high specific heat to be expected of such a gas. This error arises because of two assumptions, made in the classical treatment of gases, that is, that any number of molecules can have exactly the same energy, and that the molecules are individually distinguishable. In this case, the distribution of the energies of the molecules will shrink about the zero energy point at low temperatures, and in general will have an average value consistent with the value of the temperature. This assumption is valid for gases, whose molecules are relatively far apart, and relatively heavy.

However, electrons are extremely light, and extremely concentrated in a metal ( $10^{22}$  or more/cc). These facts led to a quantum mechanical treatment (4), in which only discrete values of kinetic energy are available to the electrons, the occupancy of each of these energy levels is limited to two electrons of opposite spin (Pauli exclusion principle) and the individual electrons are considered as

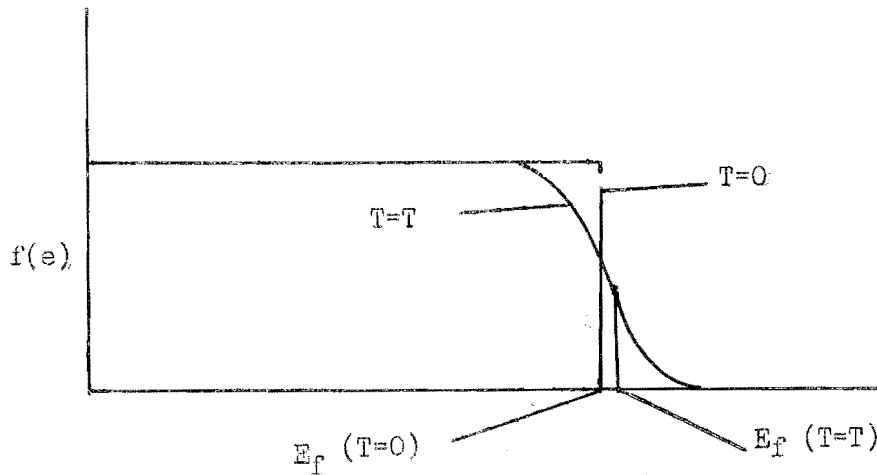
being undistinguishable. These assumptions result in the Fermi-Dirac statistics. Implicit in this quantum-mechanical treatment is the possession by the individual electrons of a wave-like character, which can also be demonstrated experimentally by such phenomena as electron diffraction (5). The electron can then be thought of as possessing a momentum  $p = mv$ , or a wavelength  $\lambda = h/p$ , where  $h$  is Planck's constant, and  $\lambda$  is commonly called the de Broglie wavelength (6). The energy of the electron will then be

$$E = \frac{1}{2}mv^2 = p^2/2m = h^2/2m\lambda^2 = (h^2/2m)k^2 \quad \text{---- (1)}$$

where  $k$  is the wave number. A plot of  $E$  vs the wave number  $k$  for the free electrons in a one-dimensional crystal will look thus



The distribution of electrons among the various kinetic energy states in a metal is governed by the limitation imposed by the Pauli principle, so that even at 0°K many of the electrons must occupy high energy states for lack of empty levels at lower energies. The distribution of electrons in the possible energy states is shown by



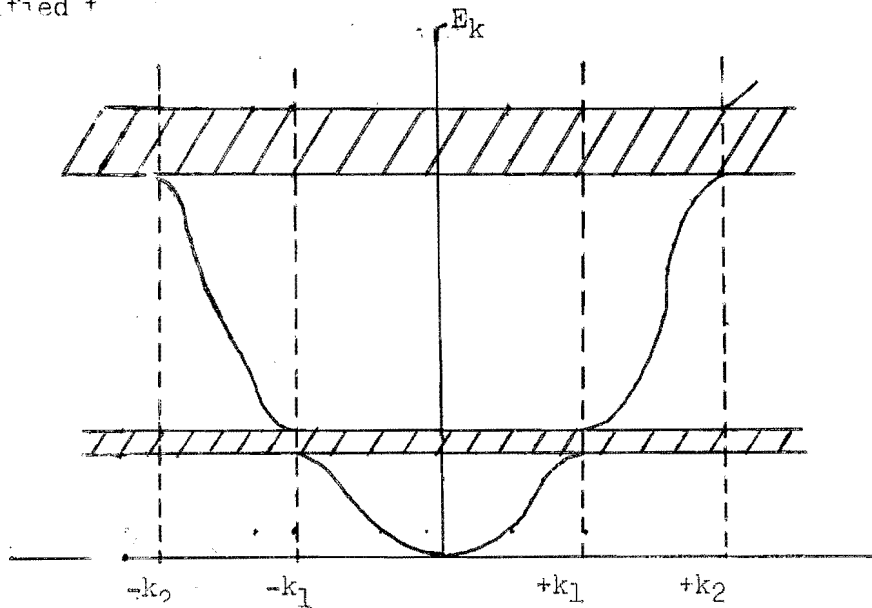
where  $f(e)$  is the average number of electrons per state. The energy  $E_f$  is defined as the Fermi energy, which is the energy at which one-half of the possible energy states are filled with electrons. An expression can be deduced by means of a statistical treatment (7) which gives the value  $f(e)$  at any energy  $E$  and temperature  $T$ , viz.

$$f(e) = \frac{1}{\exp(E - E_f)/kT + 1} \quad (2)$$

In metals, the average electronic kinetic energy at  $0^\circ\text{K}$  has a value which corresponds to the average value of the classical distribution at extremely high temperatures (many thousands of degrees (8)).

This inability of the electron distribution to attain an average value in keeping with the temperature of its surroundings means that, even at the melting point of the metal, relatively few electrons will receive the extra energy necessary to break away from the top surface of the energy distribution, and consequently the electronic specific heat will be almost insignificantly small.

The above considerations apply to a metal crystal within which the electronic potential energy is constant. If this potential energy is assumed to have a term which varies with the periodicity of the lattice, then solution of the appropriate equations discloses that the relationship between energy and wave-number is no longer continuous (9). Rather, values of  $k$  exist at which a further infinitesimal increase in  $k$  is accompanied by a discontinuous change in energy. The  $E_k$  vs  $k$  curve is modified +



where the shaded portions represent a "band of forbidden energy", and the clear areas are "bands of permitted energy". The values of  $k_1$ ,  $k_2$ , etc. occur when  $k = n\pi/a$ , where  $a$  is the lattice constant in the direction of reference, and the situation can be thought of as an interference effect involving the periodicity of the lattice and the wave-like character of the electrons. A generalization in three dimensions of one allowed band in the distorted  $E_k$  vs  $k$  curve is called a Brillouin zone.

Another result of the distortion of the  $E_k$  vs  $k$  diagram is shown by double differentiation of equation (1),

$$d^2E/dk^2 = \hbar/m, \quad m = \hbar/(d^2E/dk^2) \quad \text{---- (3)}$$

Under ordinary conditions (i.e., when the  $E_k$  vs  $k$  curve is a parabola), the right-hand term of this equation is constant. However, the distortion of the parabola produces changes in the second derivative which seem to indicate a change in the mass  $m$  of the electron. It can be seen that near the upper edge of the allowed bands, the second derivative is negative, indicating a negative mass. This phenomenon is expressed by assigning an "effective" mass  $m^*$  to these not-quite-free electrons.

The appearance of effective masses different from the electronic mass or with negative sign has been shown experimentally by measurement of such things as diamagnetic susceptibilities and electronic heat capacities of metals (10). Another instance is the conduction in certain metals, which indicates charge transfer by movement of positively charged particles (a condition which can be shown equivalent to negative electronic masses). This effect occurs in metals whose uppermost Brillouin zones are nearly filled (with electrons), the vacant electronic energy levels behaving as positively charged "holes", which are the current carriers.

Semiconductors and Insulators -- The concept of alternate forbidden and allowed energy bands completes the basic picture necessary for the division of non-ionic conductors into metallic conductors, insulators, and semiconductors. In metallic conductors, the uppermost allowed band is only partially filled with electrons which, under conditions of zero

applied electric field, lie in the lowest available levels in the band. This is not to say that these electrons are stationary, since the band represents not positions, but momenta of electrons, and the flat top of the distribution indicates merely that, for every electron traveling in the positive  $x$  direction with momentum  $p$ , another electron somewhere in the crystal has the same momentum, but an exactly opposite direction of travel; thus, there is no net charge transport. In order for a current to flow, some of the electrons at the top of the distribution must move to higher levels, where they can have momenta more or less parallel to the direction of the applied field, so that the distribution of momenta is no longer completely random, but has a net resultant in the direction of the field. This can be effected by the application of a potential across the crystal.

In an insulator, however, the uppermost band is completely filled, and the absence of vacant levels prohibits the production of a net resultant current flow within this filled, or "valence" band (so-named because of the occupation of this band by the valence electrons of the atoms in the crystal). In this case, the nearest empty levels lie in the bottom of the next allowed band (the "conduction" band), which is separated from the valence band by the energy gap represented by the interposed forbidden band which, in insulators, is of the order of one or more electron volts wide.

A source from which electrons can acquire enough energy to cross this gap is the thermal energy possessed by the crystal lattice. Since the thermal energy available is of the order of  $kT$ , which is only about 0.025 eV at room temperature, very few electrons will find themselves able to make the jump at room temperature, and the conductivity of the material will be extremely low.

In an intrinsic semiconductor, on the other hand, the energy gap is relatively small, perhaps of the order of only one-tenth electron volt, and the thermal energy of the lattice is enough to excite a significant number of electrons to the vacant conduction band. If the zero of energy is taken at the bottom of the conduction band, the number of electrons so excited can be calculated from (2) above to be

$$n = C_n \exp \left[ (E_f - E_g)/kT \right] \quad \text{---- (4)}$$

where  $C_n$  depends upon the density of states in the bottom of the conduction band and  $E_g$  is the width of the energy gap (11). This equation assumes that  $E_f - E_g \gg kT$ , so that

$$\frac{1}{\exp \frac{(E_g - E_f)}{kT} + 1} \approx \frac{\exp(E_f - E_g)}{kT}$$

The evaluation of  $E_f$  depends upon the fact that, for each electron excited to the conduction band, a positive hole is formed in the valence band. The number  $p$  of such holes is given by

$$n = p = C_p \exp (-E_f/kT) \quad \text{---- (5)}$$

where  $C_p$  is related to the number of states in the top of the valence band. The product of (4) and (5) is

$$np = C_n C_p \exp \frac{E_f - E_g - E_f}{kT} = C_n C_p \exp (-E_g/kT) \quad \text{---- (6)}$$

Since  $n = p$  for intrinsic conduction, then

$$\sqrt{np} = n = p = \sqrt{C_n C_p} \exp(-E_g/2kT) \quad \text{---- (7)}$$

The conductivity of an intrinsic semiconductor can be calculated from these and other equations to be

$$\sigma = |e| (p\mu_p + n\mu_n) = |e| \sqrt{C_n C_p} \exp(-E_g/2kT) (\mu_p + \mu_n) \quad \text{-- (8)}$$

where  $|e|$  is the numerical value of the electronic charge, and  $\mu_p$  and  $\mu_n$  are the mobilities of a positive hole and an electron, respectively, expressed as  $\frac{\text{average drift velocity}}{\text{applied electric field}}$ . Although  $\mu_n$ ,  $\mu_p$ ,  $C_n$  and  $C_p$  are all temperature dependent, the temperature dependence of (8) is controlled primarily by the factor  $\exp(-E_g/2kT)$ , so that the temperature dependence of  $\sigma$  for an intrinsic semiconductor, when plotted as  $\ln \sigma$  vs  $1/T$ , will have a slope very nearly equal to  $-E_g/2k$ . This allows the calculation of  $E_g$  from a series of measurements of  $\sigma$  at different temperatures.

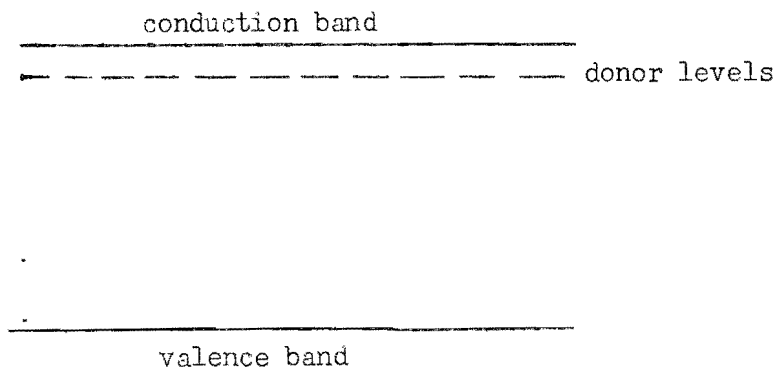
An assumption which is implicit in the above treatment is that the number of electrons in the conduction band is relatively small, so that the classical statistics can be used in the consideration of their movement. In certain cases, such as at very high temperatures or in materials with a very small forbidden gap, the density of electrons in the conduction band is so great that the Fermi-Dirac statistics must be applied to them. In this case, the electron distribution in the conduction band is said to be degenerate. The analogy with the state of affairs in a metallic behavior leads to the classification of this phenomenon as "pseudo-metallic" behavior.

It has been seen that the division between pure insulators and intrinsic semiconductors is a function of the width of the energy gap in each. There is, then, no clear-cut division between the two since, even in an insulator having a very large gap, at least a few electrons will be excited to the conduction band. The distinction is arbitrary, and can be applied according to personal preference.

The consideration of intrinsic semiconductors has been undertaken with one further implicit assumption; that is, that the materials under consideration are perfectly pure, perfectly stoichiometric single crystals. In practice, this assumption is not valid, due to the presence in the crystal of foreign atoms and lattice vacancies, both of which exert a profound effect on the conduction process.

One example of this is the replacement of a cation with an ion of higher valence (for instance,  $\text{In}^{+3}$  in place of  $\text{Cd}^{+2}$  in  $\text{CdTe}$ ). In order to fit into the bond arrangement in a manner similar to that of the normal cation, two of the three available valence electrons will be used. This leaves a surplus of one electron outside the last full quantum shell of the replacement ion, which is bound to the ion by coulombic attraction. The energy of interaction of the ion and the extra valence electron can be calculated from a Bohr-like model, but it turns out to be much smaller than in the free atom, due to the surroundings in which the atom finds itself (12). The host lattice is a dielectric, and the force of attraction, from elementary considerations, is inversely proportional to the dielectric constant. Thus, the orbit of this "extra" electron will be much larger than in the free atom, and the energy of interaction will be correspondingly smaller.

Thus, only a small energy need be given to this extra electron in order that it may break away completely from its parent ion, and become a free electron, able to take part in electrical conduction. Its energy is then represented by the bottom of the conduction band. The energy of the electron when still bound to the parent ion (or donor center) can be represented by a discrete energy level below the bottom of the conduction band, the distance being equal to the energy of interaction.



As in the case of intrinsic materials, the electron can be excited into the conduction band by the thermal energy of the lattice in a manner to be considered below.

Substitution of a cation of valence lower by one has somewhat the opposite effect. This cation (or acceptor center), having given all its valence electrons to bonds with its neighbors, still requires one extra electron to complete the bonding. An extra electron can be supplied by its removal from a normal bond somewhere near the impurity cation. The energy required is less than that necessary to excite it into the conduction band by the amount of the energy of interaction between it and the impurity cation, and can be represented by a discrete "acceptor" level somewhat above the valence band.

Conduction Band

---

----- Acceptor Levels

---

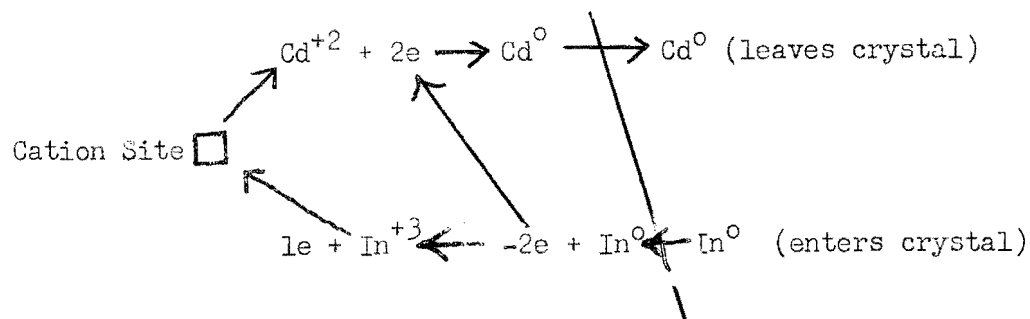
Valence Band

The removal of an electron leaves behind a positive hole, which is actually the absence of an electron in the valence band, and which can move about when an electron from a neighboring bond moves into the vacancy, thus leaving a vacancy on the site from whence it came. This positive hole, as a result of its ability to move, can take part in the conduction process and, as has been considered above, can be treated for most purposes as a positively charged particle.

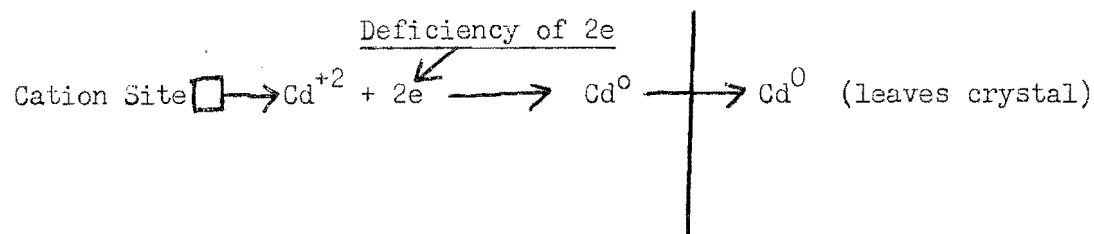
It must be pointed out that the electrons and positive holes are originally bound to the impurity ions, and that they can move only after being excited to the conduction and valence bands, respectively.

This discussion has dealt only with the replacement of cations. Anion replacement is also possible, the mechanism responsible for the generation of electrons and positive holes being essentially the same. A similar treatment discloses that vacant cation sites will act like cations of lower valence, and vacant anion sites will act like anions of lower valence, and may contribute positive holes and electrons, respectively, to the crystal.

The production of positive holes and electrons in the crystal as a result of the replacement by ions of different valence is one mechanism by which the charge neutrality of the crystal is maintained (13,14) and its operation is easily understood by considering the replacement of a free atom by another free atom. The process for the substitution of an indium ion for a cadmium ion would then be pictured thus:



The process of formation of a cadmium vacancy would be



and so on.

Another mechanism by which charge neutrality can be preserved is by simultaneous incorporation of lattice vacancies of the proper type to "cancel out" the effect of the high- or low -valence impurities or lattice vacancies (15). In the case of the introduction of In ions into CdTe mentioned above, this would involve, for each two In ions added, the simultaneous inclusion of one Cd vacancy, two monovalent cations, or perhaps even two trivalent, or less likely, one quadrivalent anion. Both of the mechanisms described above are described by Kroger and Vink (16), with particular reference to CdS.

The role played by interstitial ions in semiconducting crystals has received limited consideration (17). It would be expected that they might play a role, but their exact effect does not seem to be predictable in the general case.

The consideration of the thermal activation of electrons and positive holes is treated in a concise manner by Brattain (18). He considers a p-type crystal (one in which conduction is predominately by positive holes) in which are located  $N_a$  acceptor impurities,  $N_d$  of which are occupied by electrons from higher-lying donor levels. The remainder  $N_a - N_d$  of the acceptors are available for ionization by electrons from the filled band.

At any temperature  $T$ , the crystal contains  $p$  holes in the valence band,  $N_d + p$  ionized acceptors,  $N_a - N_d - p$  neutral (unionized) acceptors, and  $N_d$  ionized donors.

The statistics of this are treated by de Boer et al (19), and by Nijboer (20). If  $E$  is the energy necessary to ionize an acceptor, forming a positive hole in the valence band, then the law of mass action gives

$$\frac{p(N_d + p)}{N_a - N_d - p} = A \exp(-E/kT) \quad \text{---- (9)}$$

The solution of this relation has two limiting cases, depending upon the relative numbers of impurity levels.

1. If  $p \ll N_a - N_d$  and if  $p \gg N_d$  (corresponding to low temperature and a negligible concentration of donors) then

$$\frac{p(N_d + p)}{N_a - N_d - p} \approx \frac{p^2}{N_a} = A \exp(-E/kT)$$

or, extracting the square root,

$$p = N_a^{\frac{1}{2}} A \exp(-E/2kT) \quad \text{---- (10)}$$

2. If, on the other hand,  $p \ll N_d$ , then

$$p = \frac{(N_a - N_d)}{N_d} A \exp(-E/kT) \quad \text{---- (11)}$$

There are, of course, intermediate solutions.

The analysis of experimental data will, then, depend upon the relative numbers of impurity centers and positive holes. In particular, the slope of the  $\ln \sigma$  vs  $1/T$  curves will be either  $E/k$  or  $E/2k$ , or some intermediate value. In the present investigation, calculation will follow equation (10).

The development of the above equations has been under the implicit assumption that equilibrium conditions pertain at all times. Deviations due to carrier injection and optical excitation have been, and will subsequently be ignored.

The determination of the number and type of charge carriers present in a crystal constitutes only one of the two factors which determine the conductivity. The other parameters necessary are the mobilities of the electrons and positive holes in the crystal, which have been touched upon above. Once having been produced, the movement of the charge carriers is effected by their interaction with the thermal vibrations of the lattice (21,22) and with impurity atoms (23,24,25). In general, the effect of lattice scattering can be written as

$$\mu_{n,p} = C_1 T^{-3/2} \quad \text{---- (12)}$$

The effect of impurity atoms is essentially due to interaction with ionized impurities (the number of which varies with the temperature), and can be written as

$$\mu_{n,p} = C_i T^{3/2} \quad \text{---- (13)}$$

Although  $C_1$  and  $C_i$  are slightly temperature dependent, the effect of the  $T^{3/2}$  term is usually dominant.

Throughout this section, frequent reference has been made to "the ions in the crystal", "replacement by impurity ions", etc. This is not to say that all semiconductors are to be considered as purely ionic crystals, but that the picture is more easily expressed by reference to ions. Essentially the same considerations apply whether the crystal is considered to be purely ionic, or partly or wholly covalent.

## B. ELECTRICAL MEASUREMENTS

### 1. Resistivity

The most common and straightforward measurement applied to semiconductors is that of the resistivity. The resistivity of a conducting material is perhaps its most descriptive property, serving as the criterion for the classification of the material as either a metallic (or pseudometallic) conductor, a semiconductor, or an insulator. Likewise, the purity of a semiconductor can be qualitatively judged from its resistivity, which depends upon the impurity content.

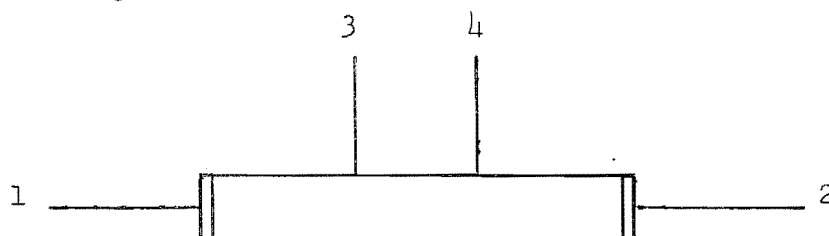
The variation of resistivity with temperature can be used to calculate the activation energy for the conduction process, as described above. In order to do so, the assumption is usually made that the change in resistivity is solely a function of the change in the concentration of current carriers, that is, that the carrier mobility is temperature

independent. This assumption is usually warranted for ordinary precision, as has been indicated above.

In single crystal materials, a dc measurement of the resistivity usually suffices, due to the absence of grain boundaries and other barriers, the analysis of which requires ac measurements. The simplest dc measurement involves merely shaping of the specimen into a bar, attaching electrodes to its ends, and applying a measured potential across them. The current passing through the specimen is measured, and the resistance calculated.

This method has several drawbacks, which result from the inclusion of the current electrodes in the voltage-measuring part of the circuit. Any contact resistance or stray potential generated at the electrode-crystal interfaces will affect the accuracy of the measurement, as will inhomogeneities in the current density near the ends of the specimen, which can be caused by regions of poor contact between the electrodes and the specimen.

An alternative arrangement is the four-probe method, in which the arrangement is thus:



The sample current is passed between electrodes 1 and 2, and the I.R. drop between 3 and 4 is measured by a potentiometric method, so that at the balance point, no current is drawn from the potential probes. Thus, the contact resistances do not affect the balance point (except

that very high contact resistances lowers the sensitivity). The situation of the potential probes near the center of the specimen avoids inaccuracy due to non-uniform current density (above).

## 2. Hall Coefficient

The information supplied by the resistivity measurements, which depend upon both the number of current carriers and the carrier mobility, is incomplete without some independent information about the number of carriers. Hall coefficient measurements supply this information. The Hall effect depends upon the interaction between a magnetic field and a charge moving across the field. In practice, the specimen to be investigated, in the shape of a long rod, is positioned as one of three orthogonal axes, and a magnetic field is applied along one of the other two. As current is passed through the specimen, the current carriers (electrons or positive holes), are deflected by the field, to an extent depending upon their velocity, and in a sense which depends upon their sign. This deflection produces a potential, which appears between the two sides of the specimen which are perpendicular to the third of the orthogonal axes. It is detected by two probes attached to these sides.

This potential is usually measured potentiometrically, again in order to avoid drawing current from the specimen. Alternative methods of measurement of the Hall coefficient include a modification of the dc method (26) in which the Hall potential is chopped and amplified before measurement, and an ac variation (27), which can be used in very high resistivity materials.

The choice of specimen shape is important to the accurate measurement of Hall coefficient. The calculation of results is made with the assumption that the sample is very long with respect to its

dimension along the Hall potential axis. In practice, very little inaccuracy occurs if this ratio is 4:1 or larger, although a correction must be made if the ratio is much less than 3:1 (28,29,30).

Another experimental difficulty arises from the interaction between the current and the magnetic field, which produces thermal gradients in the specimen. These gradients interact with the current and magnetic field, producing anomalous voltages and further thermal effects. These are classified as the Nernst, Ettingshausen, and Righi-Leduc effects, which, if ignored, can introduce some error into the Hall potential measurements. The error can be reduced substantially by averaging the Hall potential for measurements made using two opposite field orientations and two opposite directions of current flow, during which process the Righi-Leduc and Ettingshausen potentials drop out (29). No satisfactory method for eliminating the Nernst effect has been found. However, it usually is small and is commonly ignored.

The Hall coefficient can be expressed in practical units as

$$R_H = 10^8 \frac{V_H d}{IH} \quad (31,32) \quad \text{---- (14)}$$

where  $V_H$  is the Hall potential,  $I$  the current,  $H$  the field and  $d$  the dimension of the specimen in the direction of the field axis. The concentration of current carriers is given by

$$N = \frac{C}{R_H e} \quad \text{---- (15)}$$

where  $e$  is the magnitude of the electronic charge, and  $C$  is a constant which depends upon the predominant scattering mechanism (33,34,35). The value of  $C$  varies between about one and two, the value most often used in semiconductor work being  $3\pi/8$ . This value will be used throughout except where otherwise stated.

Having determined the Hall coefficient, the Hall mobility can be calculated from

$$\mathcal{N} = \frac{R_H}{\rho} \quad \text{---- (16)}$$

where  $\rho$  is the resistivity, and  $\mathcal{N}$  is the Hall mobility, which is also the average drift mobility, if the proper choice of C has been made. The equations above are derived under the assumption that only one type of carrier is present. At temperatures approaching the range of intrinsic conduction, however, significant concentrations of both electrons and positive holes are present. In this case, the Hall coefficient expression becomes

$$R_H = - \frac{3\pi}{8} \frac{nb^2 - p}{(nb+p)^2 e} , \quad \text{---- (17)}$$

where  $b = \mu_n / \mu_p$ ,  $n$  is the concentration of free electrons, and  $p$  is the concentration of free positive holes. Significant information can be extracted from this expression only if additional information is available. Solution of this equation is facilitated by a graphical method developed by Hunter (36).

Another assumption made in the analysis of Hall coefficient data is that the resistivity of the material does not change with the application of the magnetic field (magnetoresistance). This assumption is usually valid except in materials having very high carrier mobilities and small effective masses.

### C. CADMIUM TELLURIDE

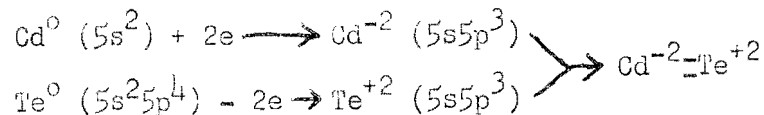
Cadmium telluride is one of a family of similar compounds crystallizing in the zincblende structure. This structure consists of a face-centered cubic array of tellurium atoms with tetrahedral interstices, which are occupied by cadmium atoms. The unit cell length is given as  $6.464 \pm 0.002 \text{ \AA}$  units, with an x-ray density of 5.866 (37).

The phase diagram of tellurium and cadmium is of a simple type, with one compound at Cd/Te = 1/1, the melting point being given between 1041°C (38) and 1050°C (39). This two-component equilibrium diagram would indicate the possibility of straightforward preparation of CdTe, but for the fact that a substantial dissociation pressure of cadmium exists over cadmium telluride at the melting point. This can be roughly estimated at about 1-2 atmospheres from the work of Kroger and de Nobel (40). The presence of a vapor at the melting point is considerably more pronounced in the other two compounds of the group, CdSe and CdS. Of these, CdS melts (at 1750°C) only under a pressure of 100 atmospheres of its vapor (41). An understanding of the phase relationships in this system can thus be obtained only by a consideration of the system solid-liquid-vapor.

The thermodynamic properties of CdTe and other similar materials have been studied by McAteer and Seltz (42), who found for CdTe  $\Delta H_{250C} = -24,530 \text{ cal/mol}$ . The dielectric constant is given for normal temperatures as about 11.0 (43).

The arrangement of the cadmium telluride unit cell is such that each cadmium atom has four tetrahedrally arranged tellurium nearest neighbors, the tellurium atoms being likewise surrounded by

cadmium atoms. This arrangement suggests that a tetrahedral orbital is operative in the bonding. Both cadmium and tellurium can take on the  $sp^3$  hybrid configuration, thus



which, because of its tetrahedral character, is a possibility for the bonding. On the other hand, the ionic radius ratio  $\frac{r_{\text{Cd}^{+2}}}{r_{\text{Te}^{-2}}}$  is of

the proper magnitude for the existence of tetrahedral ionic bonding to form  $\text{Cd}^{+2} \text{Te}^{-2}$ . The electronegativity difference between Cd and Te is small but appreciable (0.6) (44) and leads, from the calculations put forward by Pauling (45) to an estimate of 8% ionic character. It is likely, then, that the bonding in this material is resonant between purely covalent bonding by  $sp^3$  orbitals ( $\text{Cd}^{-2} = \text{Te}^{+2}$ ) and the pure ionic type ( $\text{Cd}^{+2}\text{Te}^{-2}$ ). The relatively low electronic mobility in CdTe (about  $500 \text{ cm}^2/\text{v sec}$ ) in contrast to other of the zincblende compounds (up to  $10^4$  and above) is taken as evidence that the average of the resonant forms is one of at least partial dipolar character since the electronic mobility in such materials is taken to be a function of their dipolar character (46). A further manifestation of dipolar character is the intrinsic activation energy, which is thought to be higher in the more dipolar materials (44,47). Lattice size is also held to be a contributing factor in the activation energy of the series CdS, CdSe, CdTe (48).

Early interest in CdTe and related materials, as well as much of the more recent work, has centered around attempts to produce better infrared photoconductors (49,50,51,52,53,54,55). These materials are of use in detection devices, and in the case of CdTe, a further importance is the size of the band gap (1.45-1.55 eV), which is near the theoretical value desired for most efficient solar energy conversion (56). Schwarz (54), in 1948, prepared CdTe cells sensitive at low temperatures (-78°C and liquid nitrogen temperature). Garlick and Heyne (52) working with evaporated films, produced specimens which, after forming with oxygen at 500°-550°C, showed a temperature-independent sensitivity with maxima both in the red (corresponding to the intrinsic band-gap) and in the blue. This double sensitivity was confirmed by van Doorn and de Noble (55) who, working with single crystals, found a large maximum at about 1.5 eV, and a small subsidiary peak at about 2.5 eV. The change of band gap with temperature was found by transmission measurements to be  $2.34 \times 10^{-4}$  eV/°K at 77°K and  $5.44 \times 10^{-4}$  eV/°K at 800°K. These figures agree well with Bube (57) who had deduced the relation  $E = 1.52 - 3.6 \times 10^{-4}$  eV/°K.

Miyasawa (58) has prepared CdTe in the form of single crystals, from which an activation energy of 1.47 eV was deduced from photoconductive response measurements.

Kretschmar and Schilberg (53) were able to increase the sensitivities of CdTe cells by very slight doping with indium during deposition.

Attempts to obtain a photovoltage from p-n junctions in CdTe have been made by Miles (59), who obtained open-circuit potentials of approximately one volt. Subsequently, Pensak (60) and Goldstein (61) have produced cells with open-circuit voltages of up to several hundred,

by the use of films with many photovoltaic junctions in series. These films were produced by an evaporation technique in which the direction of deposition was at an angle  $\theta$  to the normal of the surface of the film. The voltages produced by these cells increased as  $\theta$  increased from  $0^\circ$  to  $10^\circ$ , and thereafter increased slowly to a somewhat higher value at  $\theta = 60^\circ$ . The mechanism of the production of these multi-boundary films is not known.

Early methods of preparation of CdTe includes reaction of the vapors of the elements (62), growth from the liquid phase under high pressure conditions (63,64), and various wet chemical procedures (64). More recent work has centered on variations of the first two methods.

The first evidence of the effect of added impurities on the electrical properties of CdTe is due to Jenny and Bube (65). These workers found that both n-type and p-type material could be produced, depending upon the impurity added. The p-type activation energies found averaged 0.3-0.5 eV, while the n-type activation energies were extremely small, usually only a few thousandths of a volt. Their explanation for the difference is that in the n-type material the free electrons are liberated from impurity atoms in which they are superfluous to the bonding, which process requires little energy. In p-type material, on the other hand, a hole is generated only by the removal of an electron from a host atom, a process which requires much more energy.

Hall coefficient measurements by these workers indicated a minimum mobility of  $30 \text{ cm}^2/\text{v sec}$  for both electrons and holes, with the probability of electron mobilities being as much as an order of magnitude greater. The value given for the intrinsic gap, as deduced

from transmission measurements, is 1.45 eV.

Appel and Lautz (66,67) have made measurements of dc conductivity in CdTe without intentional impurity as a function of temperature from 300° to 1000°K. Values of the intrinsic gap deduced from the measurements vary from sample to sample between limits of 1.44 to 1.53 eV. In addition, low temperature activation energies of 0.73-0.77 eV and of 0.06 eV or smaller were found, depending upon previous heat treatment. Presumably these were p-type and n-type specimens, respectively. A peculiar feature of all curves shown by these workers is the appearance of smaller (about 0.67 eV) activation energies in the high temperature range above the apparent intrinsic range. In one specimen this slope joins the very low activation energy curve (a few thousandths of an eV) without any trace of an intervening intrinsic region. The cause of this phenomenon is not known, but is believed by the authors to be some sort of chemical process. A further peculiarity is the appearance of another activation energy in several samples at yet a higher temperature. Its slope of 1.98 eV makes it steeper than the intrinsic part of the conductivity curves. The presence of such an activation energy higher than the intrinsic value is not understood. The room temperature values of conductivity for the better behaved specimens vary from  $10^{-5}$  to  $10^{-7}$  mhos/cm. Similar values were obtained by Boltaks (68) for polycrystalline specimens prepared from the melt.

The most exhaustive work to date has been performed by Kroger and de Nobel (40). These workers prepared polycrystalline CdTe by direct reaction at 500°C under 40 atmospheres of argon, followed by melting and re-freezing the product. This material was then melted and zone-purified in a horizontal boat to form a single crystal. The

product, because of its exposure to the free volume of the melting enclosure, was deficient in cadmium in the absence of a cadmium atmosphere. As an approximation, the zone-refining was carried out under a cadmium pressure of one atmosphere. A study was made of the effects of atmosphere upon stoichiometry by equilibrating the specimens at 900°C under various pressures of cadmium vapor. It was found that the resulting crystals could be made either n-type, p-type, or neutral by the use of a corresponding cadmium pressure. Neutral (stoichiometric) crystals resulted when the applied cadmium pressure was 0.56 atmospheres.

It was found that the stoichiometric crystals tended to lose cadmium above 300°C, and that crystals prepared under a cadmium pressure of less than 0.15 atmospheres gave irreproducible results when heated above 150°C. The authors felt that this was due to the separation of excess tellurium.

From measurements of thermal emf, the effective mass ratio in these crystals was found to be

$$\frac{(m_+^*)}{(m_-^*)} = \frac{0.37}{0.14} = 2.65$$

Average Hall mobilities at room temperature were  $\mu_n = 600 \text{ cm}^2/\text{v sec}$ ,  $\mu_p = 50 \text{ cm}^2/\text{v sec}$ . Using the expression

$$\frac{\mu_n}{\mu_p} = \left[ \frac{m_+^*}{m_-^*} \right]^{5/2},$$

the effective mass ratio was calculated as 2.7, in very good agreement with the thermal emf values.

On the basis of these and other measurements, several types of impurity center are postulated to exist in CdTe. In n-type specimens, anion vacancies which have trapped two electrons constitute filled donor ( $V_A^{2-}$ ) centers. Anion vacancies which are empty constitute empty donors ( $V_A^-$ ), which can be compensated by  $V_C^+$  centers or by monovalent impurity atoms.

In p-type crystals, acceptor levels occupied with holes are ( $V_C^{2+}$ ) centers, while unoccupied acceptor levels are ( $V_C^+$ ) levels, which can be compensated by ( $V_A$ ) centers. Copper atoms present in these crystals as an unintentional impurity are thought to contribute levels similar energetically to the ( $V_C^+$ ).

## II. EXPERIMENTAL

### A. PREPARATION OF SPECIMENS

#### 1. Single Crystals

Preparation of the single crystals investigated was carried out by McNeilly (59,69) in this laboratory. These were crystals of cadmium telluride, both "pure" and with intentional impurities of Ag, Bi, In, Sb, or Cu, which were added in the amount of one-tenth mol percent. Starting materials consisted of 99.9997% pure cadmium\* and C.P. tellurium, which was first purified in the laboratory by a zone-refining technique.

The zone-refining apparatus consisted of a fixed silica tube 1.5 inches in diameter and 40 inches long, fitted with water-cooled ground joints and connected to a conventional vacuum system. Provision was made for operation in vacuo or in a purified helium atmosphere. The charge of tellurium to be purified was placed in a recrystallized alumina boat which rested inside the silica outer tube. This precaution was necessary to avoid contact between the molten tellurium and the outer tube, since this contact tended to cause cracking of the tube during the repeated freezing and melting of the charge.

Heating was accomplished by four nichrome tape heaters, which were two inches wide and mounted on four-inch centers. These heaters were mounted on a carriage which constituted the moving part of the system. The carriage moved through the inter-zone distance of four inches in about two hours, the fast return motion being controlled by a clutch mechanism. Thus, in effect, a full molten zone was passed

\*This material was kindly supplied by Imperial Smelting Corporation, Ltd., Avonmouth, England.

through the charge every two hours.

All traceable impurities in the original C.P. tellurium moved with the molten zone, producing a rod whose pure section comprised about three-quarters of the length of the original specimen. Further purification was possible by subsequent re-purification of the pure portions of several charges. Spectroscopic analysis of the purified tellurium showed impurity concentrations of the order of one part per million.

All crystals reported here were grown in a modified Stockbarger furnace, consisting of two independently-wound halves, separated by a conduction and radiation baffle. The temperatures of the two halves were automatically controlled, that of the upper half at about 1080°C and the lower half at about 1010°C (the melting point of cadmium telluride is ~1040°C). The furnace charge, consisting of stoichiometric amounts of cadmium and tellurium, was held in a pointed silica capsule, which in turn was held in an alumina liner which served to protect the outer mullite reaction tube. This outer tube was attached, by means of a glass-mullite seal and a water-cooled ground joint, to a conventional vacuum system. The outer reaction tube was first pumped out hard, and then a purified helium atmosphere was admitted at a pressure which was calculated to increase to just over one atmosphere at the melting point of cadmium telluride. In this way, the diffusion of atmospheric gases through the outer liner at high temperatures was substantially decreased. The inner silica capsule was first pumped out to a pressure of about  $10^{-6}$  mm of mercury, and the contents outgassed at about 200°-300°C, after which the capsule was sealed off.

In preparation for the growth of a crystal, the charge was heated slowly to about 700-750°C, in which range the two reactants united to form cadmium telluride. This reaction must be carried out as slowly as possible, since the reaction is exothermic and can cause the explosion of the charge capsule. The charge was then raised to about 1120°C and held there for a few hours to destroy remaining centers of nucleation. The charge and protective jacket were now held stationary and the furnace raised slowly, so that the freezing front, situated at the division between the two halves of the furnace, passed up through the capsule, beginning at the pointed tip. In the most successful cases, this resulted in the seeding of one crystal at the tip of the capsule, which grew as the furnace was raised further. The usual raising rate was 2 mm per hour.

After the complete solidification of the charge, the resulting crystal was cooled to room temperature over period of several days.

One of the difficulties encountered in the growth of cadmium telluride single crystals is the tendency of the material to lose cadmium at high temperatures, thus producing a non-stoichiometric finished crystal (40). In the method outlined above, however, the charge was enclosed in a capsule having very little free space, which limited the quantity of cadmium thus vaporized. A rough extrapolation of Kroger and de Nobel's results indicated that this loss probably amounted to less than 0.0001 gram of cadmium per gram of charge, or about one part in 5000 of the original cadmium. This discrepancy is hardly enough to affect the stoichiometry of the first material to crystallize. As crystallization continues, the remaining melt will be more and more depleted of cadmium so that the last material to crystallize will be Cd-

deficient. Upon long standing just below the melting point, it would be expected that the cadmium content of the crystal as a whole would be deficient, as a result of the equilibration of the solid phase by means of diffusion of cadmium up through the crystal to the more seriously depleted upper portion. However, in the time available, the geometry of the charge capsule is such that this equilibration is very seriously hampered. This supposition is borne out by the low-temperature measurements of McNeilly (70), which showed some of the crystals to exhibit intrinsic conduction far below room temperature. It is probable that the p-type character found in crystals investigated at high temperature was at least partially produced by evaporation of cadmium during the measurement, and not entirely during the original growth of the crystals.

Spectroscopic analysis of the crystals grown by the above method, together with the occurrence of intrinsic conduction at low temperatures, indicate that the unintentional impurities were of the order of one part per million.

## 2. Hot-Pressed Specimens

The hot-pressed cadmium telluride specimens reported here were prepared by Miles (70) in this laboratory. They were prepared from C.P. materials as part of a preliminary study of hot pressing in general. The specimens were pressed in graphite dies to form disks  $1\frac{1}{2}$  inches in diameter and about  $\frac{1}{4}$  inch thick. Pressing was carried out at  $940^{\circ}$ - $1030^{\circ}$ C, under pressures of 3000-5000 psi. The pressed disks were of nearly theoretical density and quite homogeneous, being easily polished to a mirror-like finish. It was found that by holding the specimens under pressure at  $1030^{\circ}$ C for eight minutes and then cooling to room

temperature in one-half hour, specimens could be obtained with individual crystallites up to three millimeters in size. Both these and specimens with smaller crystallites were investigated.

The purity of these specimens was low, due to their manufacture from C.P. materials, and also due to contamination from the graphite die. It is probable that better specimens could be made by increasing the purity of the raw materials, and preliminary experiments have indicated an improvement could also be obtained by lining the pressing die with boron nitride.

## B. CUTTING AND ELECTRODES

The specimens reported have been prepared for measurement in several different ways. The polycrystalline specimens (hot-pressed) were cut from the original disks by means of a thin, water-cooled silicon carbide-coated paper disk, rotated at about 10,000 rpm. Preparatory to cutting, the hot-pressed disks were mounted on a glass plate in the cutting jig using glycol phthalate.

Single crystal specimens were obtained by first cleaving plates from the grown rods. Cadmium telluride exhibits  $\{110\}$  cleavage (59) which is strong enough that usable plates could be obtained with a minimum of difficulty. All single crystal specimens were cut from these  $\{110\}$  planes. The plates were positioned in a jig and cut into rods about 2 mm square by 8 mm long by means of an S. S. White Industrial, Airbrasive unit, using a narrow rectangular orifice. The Airbrasive unit produces a jet of fine alumina particles driven by 50-80 psi of a dry, inert gas, in this case nitrogen. After cutting, the surfaces of the crystals were lightly abraded with the Airbrasive, since it was found that this slight sandblasting revealed crystal boundaries and planes of twinning. During this treatment and thereafter, the specimens were handled only with forceps, the abrading treatment being relied upon to remove any contamination and debris from the surface. This treatment was felt to be superior to the chemical etch described by other workers, which might leave a contaminating residue.

The literature reports several types of current contacts to cadmium telluride and similar crystals. Some of these are chemically-deposited gold and silver (40), indium-plated metal (40), evaporated gold (58), electrolytically-deposited nickel and copper to which wire

leads were soft-soldered (65), and evaporated copper.

The problem of good electrical contact is one of the major problems in the investigation of semiconductors. The application of low-resistance, noise-free ohmic contacts depends upon the relative work functions of the semiconductor and the metal used, which considerations have been developed in the literature (71). The question of contamination is, however, not so easily dismissed. Generally speaking, any foreign material in contact with a semiconductor must be regarded as a possible source of contamination, especially when the electrode system must be used at high temperatures. Indeed it would seem that any electrode material which fulfills the requirements of good adhesion and good electrical contact must, by the same token, contaminate at least the end portions of the specimen. The use of a four-electrode system, as in the present investigation, partially eliminates the complication of contamination, since the end portions of the specimen are not involved in the measurement. Some contamination must, however, be expected from the potential probes.

The process responsible for the contamination of the bulk semiconductor specimen is the diffusion of the electrode material through the crystal. It has become customary, in some quarters, to neglect the possibility of significant bulk diffusion at temperatures below about 0.5 of the melting point of the host material (the so-called Tammann temperature). At first glance this would seem to rule out contamination due to diffusion of electrode material below about 340°C in cadmium telluride. However, it has been found that, in some cases, contamination can take place in relatively short times in this temperature range (see below). In addition, the possibility of fairly rapid surface

or even volume diffusion must not be disregarded as a contamination mechanism. This proved to be the case in similar materials at temperatures far below the Tammann temperature (72,73,74,75). In view of these aspects, all semiconductor work, the present measurements included, must be examined critically from the standpoint of possible electrode contamination.

During the course of this investigation, several of the electrode materials listed above were investigated in an attempt to secure the best results. Initially, great difficulties were experienced in the matter of current electrodes for Hall coefficient measurements, due to short-term changes in the current flowing through the specimen. These changes produced variations in the I.R. component of the Hall voltage which were, at best, of the same order of magnitude as the Hall voltage itself, and which were aggravated by the high resistivity of the material being investigated. Some improvement was obtained by extremely careful positioning of the Hall voltage electrodes, but the current changes still contributed a very large second-order variation to the measured Hall voltage.

The first current electrodes were made with platinum foil spring-loaded against the specimen. This system entailed perhaps the least possibility of sample contamination. However, although they were reasonably stable, the contact resistance was extremely high, and subject to large discontinuous changes, which limited Hall effect results to the determination of the sign of the current carriers. Further disadvantages were the difficulty of distributing the current flow over the end surfaces of the specimen, and the tendency of the cadmium telluride to attack platinum at high temperatures (above about 300°C). In spite

of this attack, spectroscopic analysis failed to detect any diffusion of platinum into the specimen.

An alternative electrode was made by applying silver paint to the specimen ends and subsequently sintering it on by an instantaneous touch of a small flame. These electrodes had fairly low resistance, although under hard vacuum they tended to crack with age. Another disadvantage was the possibility of diffusion of silver into the specimen at high temperatures (above about  $300^{\circ}\text{C}$ ). This contamination was verified by spectroscopic analysis of one specimen which had been heated as high as  $380^{\circ}\text{C}$  for several hours. Resistivity changes were noted in some specimens which may be attributable to this contamination, but other effects to be noted below may have been responsible.

Evaporation of gold constituted another means of applying current electrodes, the evaporation being carried out from a tungsten spiral under a vacuum of  $10^{-5}$  to  $10^{-6}$  millimeters of mercury. Gold deposited on the sides of the specimens was removed by the abrasion treatment described above. Evaporated gold contacts were found to have extremely high resistances, although they were fairly stable. A further disadvantage was their poor adhesion, which caused them to rub off as a result of the abrasion caused by the different thermal expansions of the crystal and the electrode jig during heating and cooling.

Some of the hot-pressed specimens were provided with copper and nickel current electrodes, which were deposited from solution to a thickness of several microns. In the light of the effect of current flow upon the resistivity of certain of the specimens, these electrodes were abandoned, due to the necessity of passing current through the specimens to effect the plating. These electrolytically-deposited

electrodes proved to have excellent electrical properties in the case of hot-pressed specimens, but attempts to apply them to single crystal specimens were unsuccessful, due to treeing and poor coverage.

Kroger and de Nobel (40) have used both indium-plated electrodes (on n-type specimens) and chemically-deposited gold electrodes (on p-type specimens). These workers found that a good contact could be applied to p-type specimens by applying, at the desired contact point, a solution of gold chloride, which apparently attacked the crystal, replacing cadmium by gold. This system was used for most of the measurements made, in spite of the fact that there is some evidence that it produces changes in the electrical properties of the crystals (70). The use of indium-plated electrodes was not considered, due to the fact that most of the specimens examined were p-type, and the obvious impossibility of using this low-melting metal at high temperatures. An interesting demonstration of the greater applicability of gold electrodes to p-type specimens than to n-type specimens was noted with the indium impurity specimen to be reported below. This specimen was initially n-type, but by suitable heat treatment, its character was changed to the p-type condition. The quality of the contacts proved to be better after the treatment.

Before the change to chemically-deposited gold contacts, the potential probes consisted of fine (0.002 inches) platinum wire, which was heated yellow hot and plunged into the surface of the specimens. Although these probes gave good service, they had two disadvantages. First, the necessity of plunging the platinum wires very rapidly into the crystal made it very difficult to position them properly, as is required in the case of the Hall electrodes, because of the large I.R.

potential mentioned above. Additionally, during the heating of the wires, the specimen was unavoidably heated and, although the surface layer of the crystal was subsequently abraded away to remove the resultant surface film, it was felt that this heating was too strenuous.

Subsequent to the adoption of chemically-deposited gold current contacts, the voltage probes were made by the same process. To accomplish this, two opposite surfaces of the crystal were coated with gold in the desired electrode area. The crystal was then wrapped with one loop of thin copper wire (0.015 inches) and all but the areas so protected were abraded to remove the surplus gold. It proved possible, by this method, to position the Hall electrodes directly opposite each other, to an accuracy of about 0.001 inch.

Following the application of the gold stripes, platinum-rhodium wire leads were spring loaded (by their own elasticity) against the electrode stripes. It was this system of gold electrodes which finally made it possible to measure reproducible Hall coefficients.

## C. APPARATUS

### 1. Atmosphere

A problem common to each of the types of measurement to be made was the preparation and maintenance of an accurately controllable sample atmosphere. In order that results might be more reproducible, it is desirable to have an atmosphere which will not contribute to a change in properties of the specimen during the time of measurement or, failing that, one which will change them in a predictable way.

In cadmium telluride, this problem is aggravated by the tendency of the material to lose cadmium, as has been mentioned above. Since most of the measurements were to be made above room temperature, it would have been desirable to provide as a sample atmosphere a partial pressure of cadmium vapor appropriate to the temperature at which measurements were being made. However, certain obvious difficulties presented themselves. In the first place, this equilibrium pressure has been measured at only one temperature (900°C) (40). Although the equilibration of the specimens reported by these workers occurred in a few hours, the equilibration time would be at least two orders of magnitude greater at 300°C, which is in the upper range of temperatures at which measurements were made. In addition to the above objection, the possible presence of adsorbed cadmium on the surface of the sample holder would cast some doubt on the value of the measurements obtained.

It was therefore decided to abandon the idea of a controlled cadmium atmosphere in favor of some less time-consuming scheme. The first possibility which suggests itself is, of course, hard vacuum. Accordingly, an apparatus was constructed by means of which the sample reaction tube could be evacuated to very low pressure, with additional

provision for the admission of a purified gas atmosphere. This apparatus comprises a conventional high-vacuum system (figure 1), consisting of a high velocity water-cooled mercury diffusion pump backed by a rotary oil fore-pump. This system was also used for the evacuation of the bell jar used in vacuum plating of metal electrodes.

In use, the pressure was kept below  $1 \times 10^{-6}$  mm of mercury, as measured by a standard McLeod gauge. The specimen was protected from mercury from the diffusion pumps and other vapors by two intervening liquid air traps.

In some of the experiments, it proved necessary to use an inert gas atmosphere to act as a transfer medium to facilitate rapid changes in temperature and to permit cooling below room temperature, where heat transfer by radiation was no longer effective. In this case, the system was first evacuated to the highest attainable degree, the stopcock nearest the specimen closed, and the intervening section of the high-vacuum line alternately flushed with high purity helium and pumped out. This procedure was repeated several times, during which two liquid air traps were maintained in the isolated section. Following the flushing the sample tap was opened, and helium admitted to the sample reaction tube, again through two liquid air traps. The helium pressure was generally chosen at about 40 cm of mercury, so that the pressure in the sample section would be less than one atmosphere at the highest measurement temperature.

In the quenching experiments to be described below, it was not possible to pump out the sample holder, due to its design, and therefor it was first flushed with high purity helium, closed off, and kept under a helium pressure of 2-3 cm of mercury. The amount of

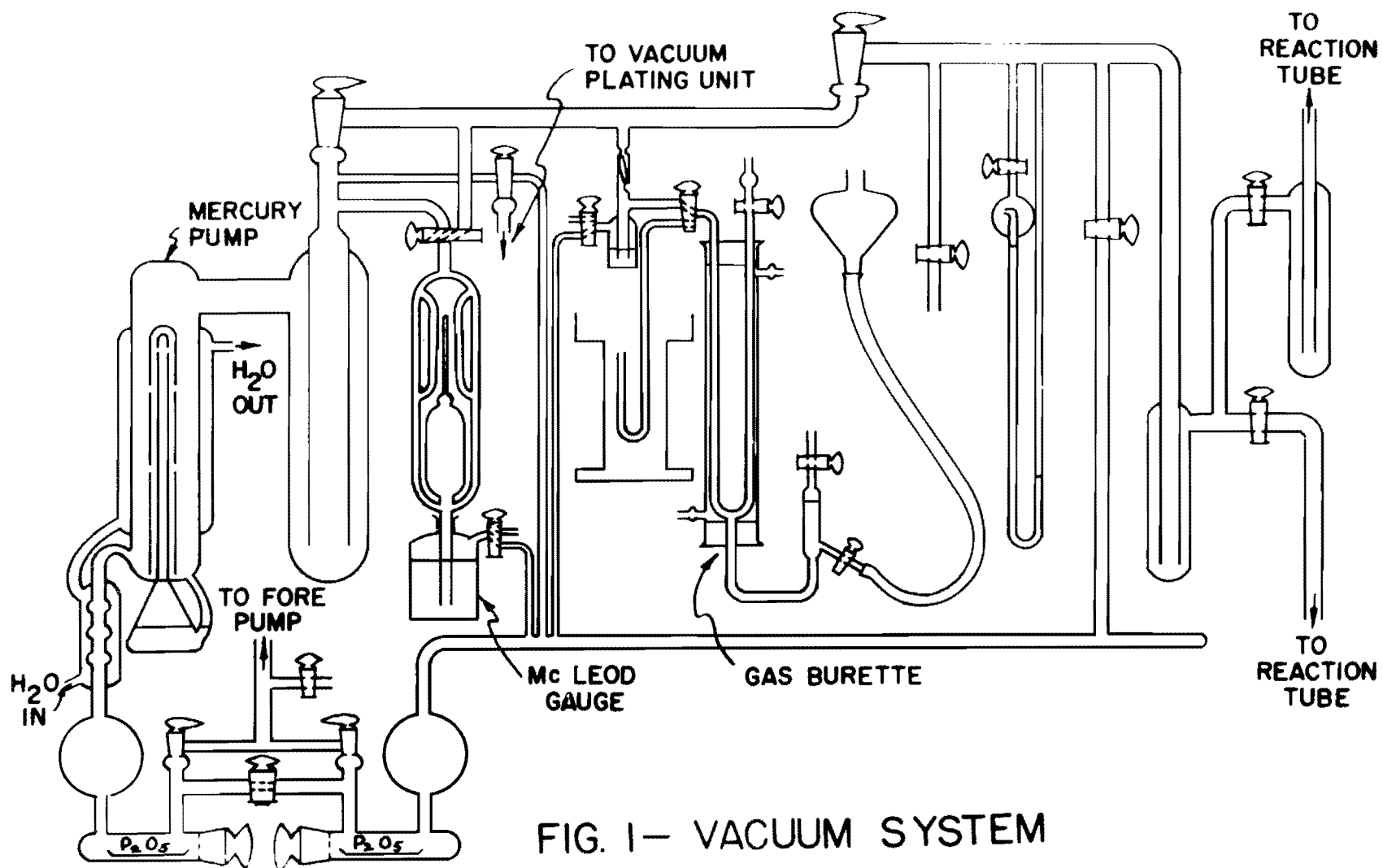


FIG. 1— VACUUM SYSTEM

flushing helium used was about  $10^4$  times the volume of the sample holder.

## 2. Sample Holders

Hall coefficient -- Most of the results reported here were made in a specimen holder designed specifically for the measurement of resistivity and Hall coefficient (figure 2). This holder consisted of a Wonderstone (natural pyrophyllite) jig, suspended in the reaction tube by a bundle of four twin-bore fused silica tubes, which additionally served to insulate the electrical leads from the specimen to the measuring apparatus. Although the bulk resistivity of the Wonderstone material is fairly high, it was decided to sleeve all electrical leads with fused silica. The specimen was held in the desired orientation by two spring-loaded silica rods, the platinum foil current electrodes being held between the silica rods and the specimen. The distance between current electrodes was adjusted by means of the Wonderstone screw shown in the figure. The voltage probes were either spring-loaded against the gold electrode stripes or, in the case of imbedded platinum wire electrodes, welded to these small platinum wires. The thermocouple used, which in most cases was of the copper constantan type, was spring-loaded against the specimen by its own elasticity.

Except where otherwise noted, measurements were made in the dark, the specimen being shielded from ambient radiation by a platinum foil shield wrapped around the sample jig. This shield had an aperture of approximately 1 x 2 cm for the admission of illumination, when desired. The reaction tube itself was of fused silica, and was connected to the vacuum system by means of a Vycor ground joint, below which it was found

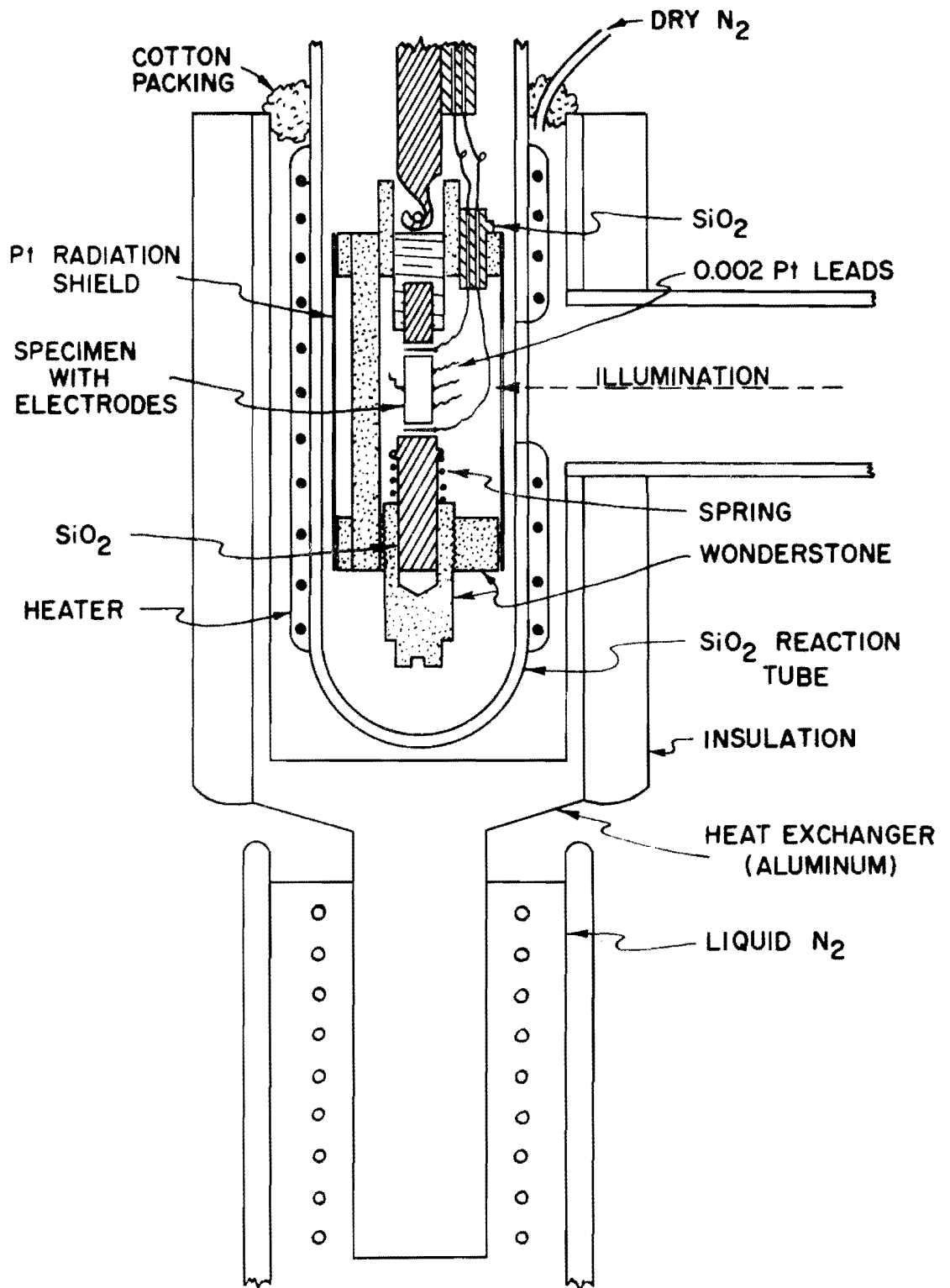


FIG. 2 SAMPLE HOLDER WITH HEAT EXCHANGER

necessary to install a radiation and convection shield to keep the joint cool when the reaction tube was being heated. The reaction tube was equipped with a non-inductively wound platinum heater, insulated and covered by an asbestos-tape-plus-sodium-silicate layer. Additionally, it was provided with a silica window of approximately 1 x 2 cm, for the admission of illumination. When measurements were desired in the presence of such illumination, the reaction tube could be turned in such a way that this window lined up with the aperture provided in the radiation shield mentioned above.

The electrical leads left the reaction tube by means of multiple platinum-to-soft-glass seals, which in turn were joined to the reaction tube head by means of graded Vycor-to-soft-glass seals. By means of the precautions mentioned, it was possible to maintain a leakage resistance of greater than  $10^{10}$  ohms between any two electrical leads at room temperature. This leakage resistance decreased somewhat at high temperatures, but was at least several orders of magnitude larger than the resistances of the specimens at these temperatures.

Measurements at low temperatures without illumination were made by immersing the reaction tube to the required degree in a Dewar flask containing liquid air. The amount of liquid air was chosen so that, when the desired low temperature had been reached, the liquid had been completely evaporated. The space between the mouth of the Dewar flask and the reaction tube was then insulated with cotton batting. The temperature then rose slowly to room temperature at a rate which was found satisfactory for the measurements. When a constant low temperature was desired, some liquid was left in the bottom of the Dewar flask, and the flask lowered to the appropriate degree.

Low-temperature measurements under conditions of applied illumination could not be made by this method, due to the non-availability of a strip-silvered Dewar flask. For these measurements a heat exchanger was made, which is shown in the figure. This unit consisted of an aluminum alloy shell pierced by a one-inch thin-walled Synthane tube. In the bottom of the heat exchanger was incorporated an aluminum rod, which was immersed in liquid air to the extent necessary to obtain the desired temperature. Illumination was admitted through the Synthane side tube. In practice, it was found that the silica window frosted up as the temperature was lowered. This condition was remedied by playing against the window a jet of dried cold nitrogen. This stream, at once cooled and dried, was obtained from a rubber tube connected to a Dewar flask filled with liquid nitrogen. A "leaky" Dewar vessel was used for this purpose, from which the gas evolution was sufficient for the purpose.

The use of liquid air as a coolant in an applied magnetic field sometimes results in a lowering of the temperature of the sample, due to the tendency of the highly paramagnetic liquid oxygen component to drift to the sides of the Dewar vessel facing the pole faces. For this reason, liquid nitrogen was used whenever available, although the effect was found to be negligible with freshly made liquid air, especially since the magnet was used only for short periods.

Magnetic field for the Hall coefficient measurements was provided by a four-inch dc electromagnet, operated manually from a battery system. The magnet was calibrated by comparison of three methods. The first was the conventional ballistic method, in which a search coil is removed quickly from the field, and the induced potential

integrated by means of a ballistic galvanometer. A known field was used for the calibration of the coils. The second was the Quincke (76) method, in which the field is derived from the rise in a capillary of a paramagnetic fluid of known susceptibility. The third method was by use of a laboratory-designed and built double spinning-coil magnetometer. The coils were attached to the ends of a brass rod, which was spun at 3000-5000 rpm by means of an air-driven gyroscope impeller. One coil was placed in the field to be measured, and the other in the field of a Helmholtz coil of known geometry. The emf's produced by the two coils were set in opposition and the Helmholtz field varied until the opposing voltages of the two coils exactly cancelled each other. This point was determined by means of an audio amplifier and oscilloscope. The calibration of the spinning coils was deduced by the use of known fields generated by two identical Helmholtz coils. This method has perhaps the highest potential sensitivity and accuracy, but the necessity of applying corrections for the earth's magnetic field and fringe fields of the two Helmholtz coils during the calibration of the coils makes it difficult to apply. In practice the two other methods were found to be most reproducible and to agree with each other, and were used to the exclusion of the third.

With the pole pieces of the magnet set at a separation allowing the insertion of a Dewar vessel around the reaction tube, the field obtainable was 5000-5400 oe. In cases where higher sensitivities were desired, the maximum field could be raised to 7300 oe, using a narrower pole-gap.

Quenching Unit -- The above apparatus was not applicable to measurements made during the rapid heating or cooling of the specimens, due to its great heat capacity and the thermal insulation properties of its parts. It was therefore necessary to design a new type of sample holder by means of which sample temperature could be changed at rates up to several degrees per second. This holder is shown in figure 3. It consisted of a steel shell with a removable bottom which was affixed by a tapered joint. The specimen was held in a Wonderstone jig between spring-loaded current electrodes, and spring-loaded copper wires constituted the voltage probes. The electrode and thermocouple leads passed out through a Kovar seal.

In order to facilitate rapid changes in sample temperature, two furnaces were constructed, one to be kept at each of the two temperatures between which the specimen was to be heated or cooled. The furnaces were of solid metal, being made purposely massive so as to have large heat capacities.

### 3. Measurement Techniques

Most of the measurements reported here were made by a standard potentiometric technique, using either a Leeds and Northrup type K instrument or a laboratory-constructed unit for the emf measurements. Current was measured by galvanometers and milliammeters having sensitivities up to  $3 \times 10^{-9}$  ampere/division. Resistivities were measured by the usual four-probe method, measurements being made of the current through the specimen and the potential differences between the two voltage probes. In general, these voltage probes were placed in the middle one-third of the specimen, to minimize errors due to inhomogeneities in current density near the ends.

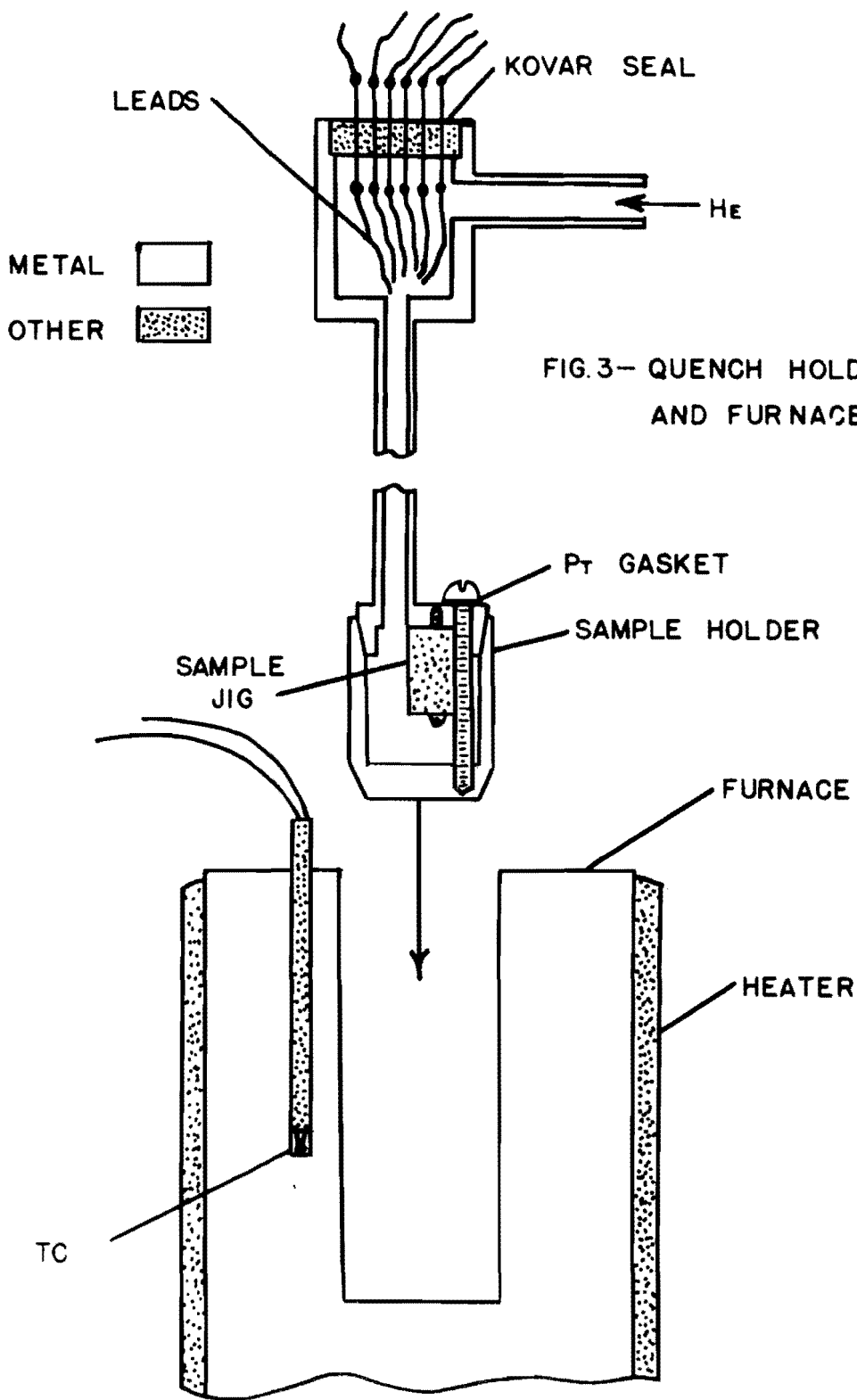


FIG.3- QUENCH HOLDER AND FURNACE

During many of the earlier experiments, the current was allowed to pass through the specimen throughout the time occupied by the measurements. As it was later discovered that current flow could alter the properties of the specimens, this practice was discontinued, except in cases when the effects of the current flow were to be studied.

Hall coefficient measurements were hampered, as has been mentioned above, by a drift in the I.R. component of the Hall voltage. This made it necessary to make the measurements in the shortest possible time, in order to avoid errors due to inaccuracy in the estimation of the I.R. component. Ideally, these measurements should be made under all possible combinations of the conditions (two possible current directions), and (two possible directions of magnetic field) (see Introduction, Hall measurement). However, it was found that during the time required to make the necessary measurements, the drift in I.R. component was great enough to throw serious doubt on the advisability of such multiplicity in measurements. As a compromise, the Hall coefficient measurements reported were made with only one direction of current flow, the direction of the field being the only adjustable parameter. The Hall voltage was measured during the following sequence of magnetic field adjustments: field off, field vector left, field vector right, field vector left --, continuing for several cycles. This permitted fairly precise determination of the true Hall voltage without the interference of the I.R. component.

Potentiometric measurement of the resistivity became extremely difficult when resistivities exceeded  $10^6$ - $10^7$  ohm-cm, due to the high resistances of the voltage probes in such cases. A ballistic method was adopted by which this situation could be avoided. The voltage

probes were connected to a low-leakage condenser by means of a double-pole, double-throw switch, the other throw of which was across a ballistic galvanometer with a sensitivity of  $3.0 \times 10^{-10}$  coulomb. The condenser was first charged from the specimen (to which it presents an almost infinite impedance when fully charged), and then discharged through the galvanometer. The galvanometer-condenser combinations used were calibrated by comparison with the Leeds and Northrup type K potentiometer. Using this method, measurements could be made with specimens whose resistivities approached the limit set by leakage in the apparatus ( $> 10^{10}$  ohms).

Another limitation of the potentiometric measurement of resistance was the necessity during the quenching experiments of measuring very quickly the rapidly changing resistance of the specimen. In order to make these measurements with the smallest possible error in keying the measured resistance to the proper time and temperature, a simple two-probe resistance measurement was resorted to, using a common type of multimeter. During these measurements, the temperature was recorded, being keyed to the resistance measurements later.

The thermocouples used in this investigation were calibrated by comparison with water, carbon dioxide and oxygen in equilibrium with their vapors at atmospheric pressure (results corrected to 760 mm). All thermocouples used were found to be extremely accurate at  $100^{\circ}\text{C}$ , but a slight correction was necessary below about  $(-) 100^{\circ}\text{C}$ .

The bulk measurement of specimens was performed by means of a micrometer, while the probe positions were measured using a laboratory-built micrometer cathetometer.

### III. MEASUREMENTS

#### A. CONVENTIONAL HALL AND RESISTIVITY MEASUREMENTS

##### 1. Pure Crystals

Measurements of the semiconducting properties of CdTe began with the determination of the resistivities of several "pure" CdTe crystals, over the temperature range from room temperature or slightly below to about 360°C. Curves of  $\log_{10} \rho$  vs  $1000/T$  are shown in figures 4, 5 and 6 for specimens 1, 5 and 6 (all "pure"). The forms of these curves are all dissimilar in the extrinsic region, and one (sample 5, figure 5) has no intrinsic range in the temperature region studied. This crystal was investigated both in the dark and under an illumination of about 1 lumen/cm<sup>2</sup> from a standard tungsten lamp. Photoconduction appears in the crystal below about 90°C, the maximum dark to light resistance ratio being about four. The intrinsic activation energies of 1.57 and 1.60 eV for samples 1 and 6 agree within the accuracy of measurement.

Silver paste current electrodes were used on these specimens, with platinum wire voltage probes. Analysis of sample 1 after measurement showed the presence of silver from the electrodes and in subsequent experiments, specimens were kept at high temperature for the minimum time necessary.

##### 2. Bismuth Impurity Crystals

Figure 7 shows a curve of  $\log_{10} \rho$  vs  $1000/T$  for crystal #2 (CdTe + 0.1 mol % Bi). Curves were made, as in the case of sample 5, both in the dark and under the illumination conditions stated above. The intrinsic activation energy of 1.59 eV agrees well with that of specimens 1 and 6 (above). Significant photoconduction appears below

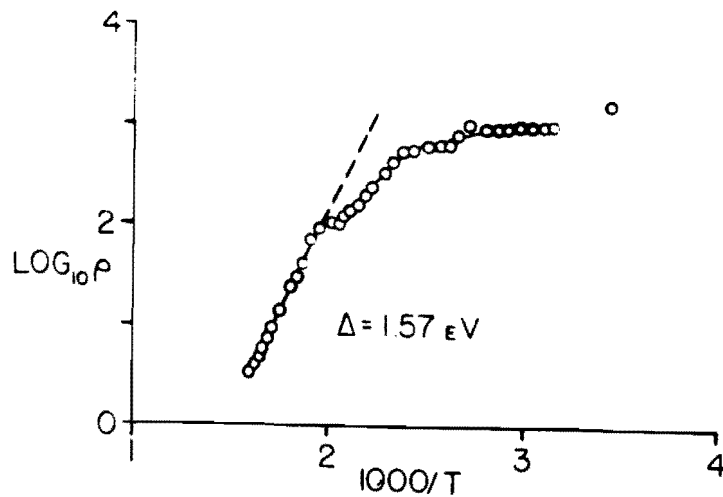


FIG. 4-SAMPLE 1 (PURE)

$\text{LOG}_{10} \rho$  vs  $1000/T$

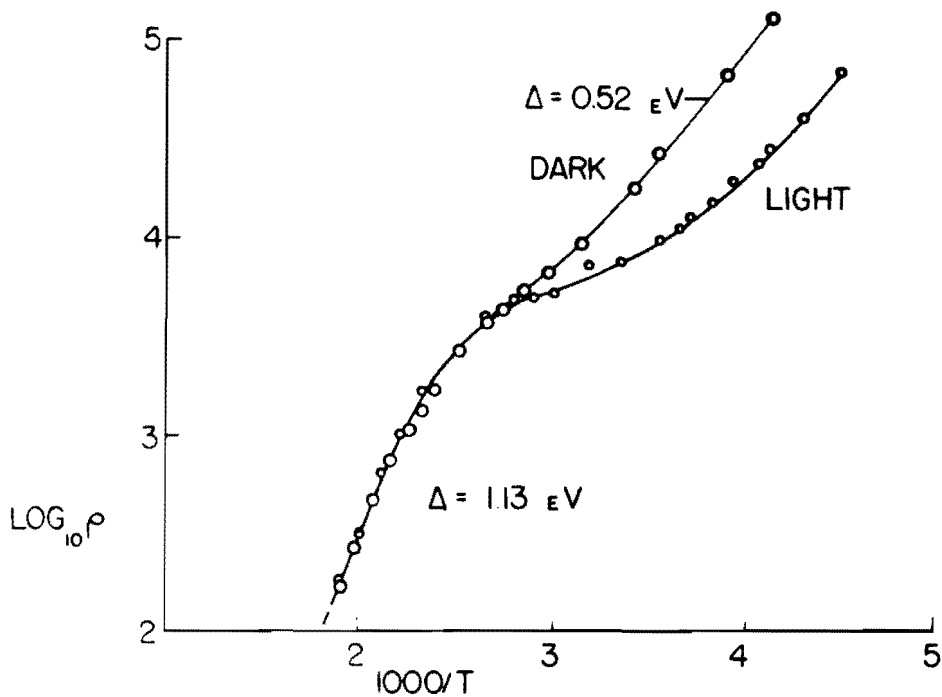


FIG 5-SAMPLE 5 (PURE)

$\text{LOG}_{10} \rho$  vs  $1000/T$

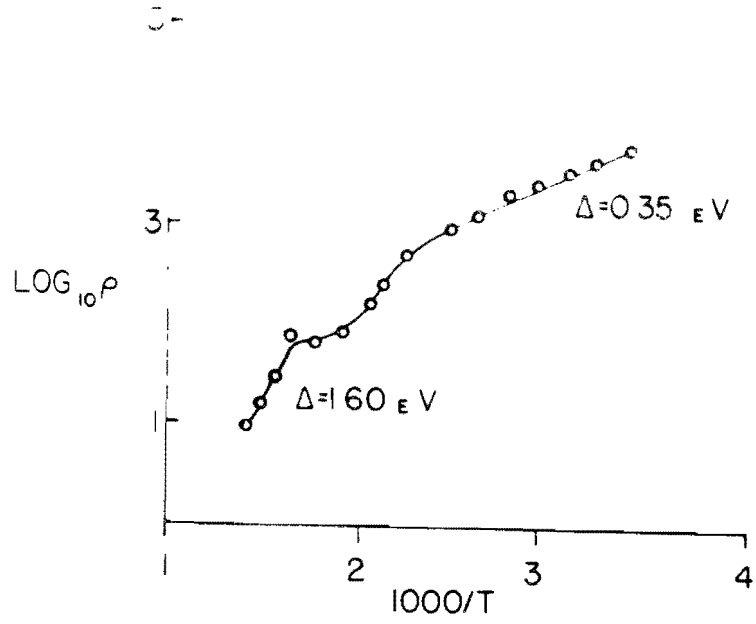


FIG. 6- SAMPLE 6 (PURE)

$\text{LOG}_{10} \rho$  vs  $1000/T$

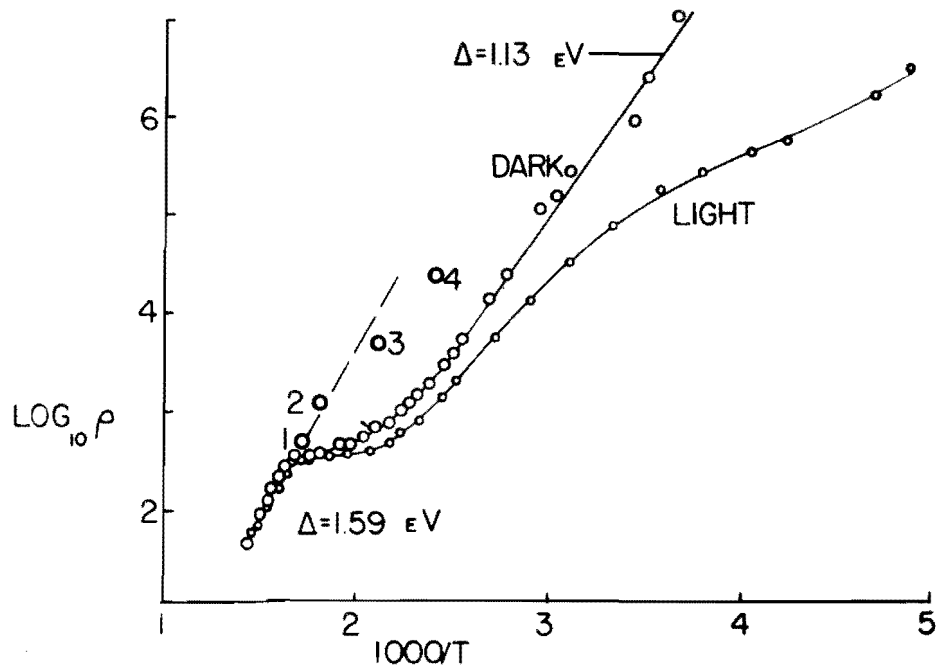


FIG. 7- SAMPLE 2 (Bi)

$\text{LOG}_{10} \rho$  vs  $1000/T$

about 250°C, the maximum value of  $\rho_{\text{dark}}/\rho_{\text{light}}$  being about 50. The possibility of even larger ratios at lower temperatures was impossible to determine because of the very high dark resistance of the crystal.

Measurements of anomalous effects in this and other crystals will be given in a separate section.

No quantitative Hall coefficient measurements were made on specimens 1, 2, 5 or 6, owing to poor geometry of the specimen (#2) and to the unsatisfactory contacts then available.

### 3. Hot-Pressed Specimens

Measurements were made with several specimens of hot-pressed CdTe, the preparation of which is described above. Both the "large-crystal" and "small-crystal" specimens were used, the values of resistivities vs temperatures being essentially the same. A typical plot of  $\log_{10} \rho$  vs  $1000/T$  for specimen 11 ("small crystal") is given in figure 8. The calculated value of E is 0.74 eV for the middle temperature range. No measurements were carried out at higher temperatures corresponding to the intrinsic region.

Measurements of Hall coefficient were extremely erratic in the hot-pressed specimens, undoubtedly because of their polycrystallinity. This was particularly true of the "large-crystal" specimens. Some Hall measurements were, however, carried out on specimen #11. The indicated mobilities calculated from these measurements are shown in figure 9, which displays  $\log_{10} \mu$  vs  $\log_{10} T$ . The equation of the straight line in the figure is

$$\mu = CT^{-3/2}$$

This specimen exhibited p-type conduction, with the calculated concentration of free positive holes at room temperature being  $5.7 \times 10^{13}/\text{cc}$ .

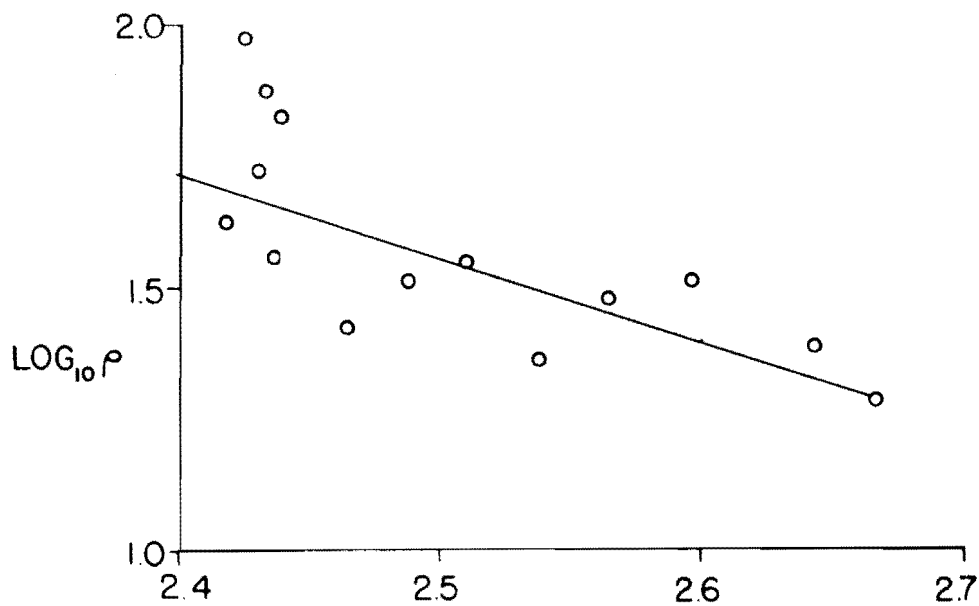
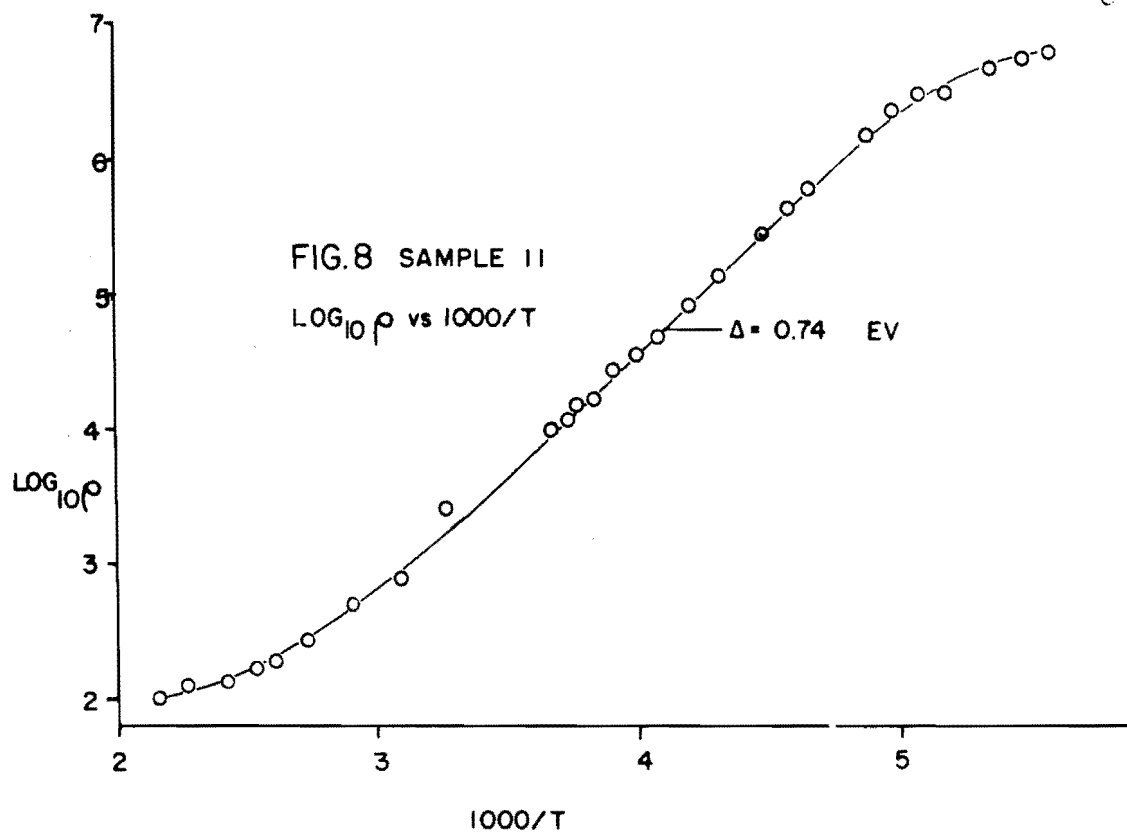


FIG 9- SAMPLE II (HOT-PRESSED)

$\text{LOG}_{10} \rho$  vs  $\text{LOG}_{10} T$

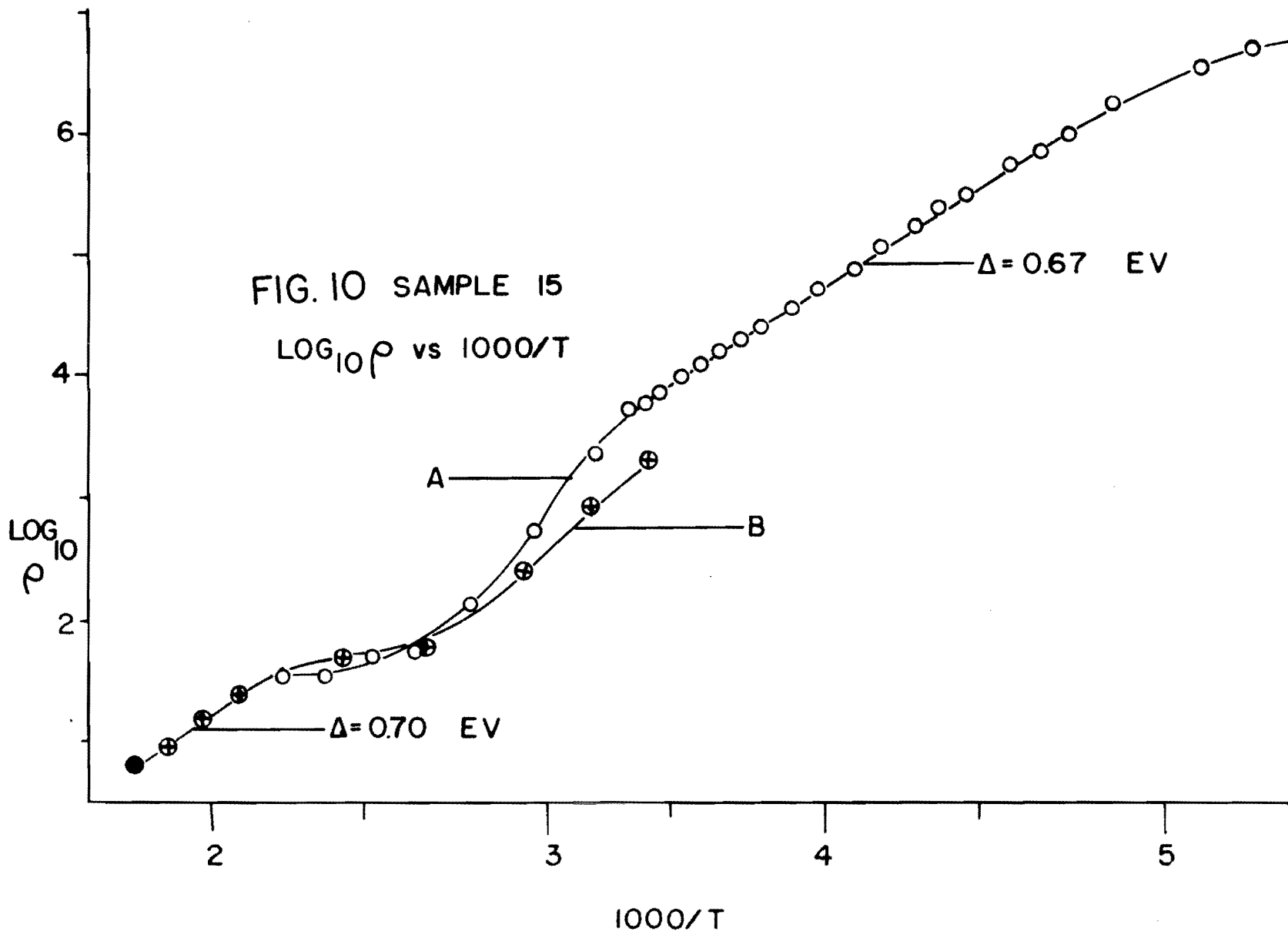
#### 4. Copper Impurity Samples

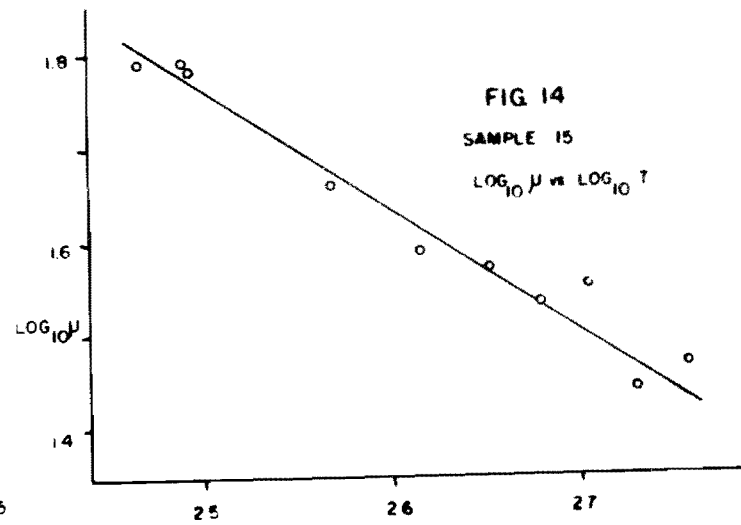
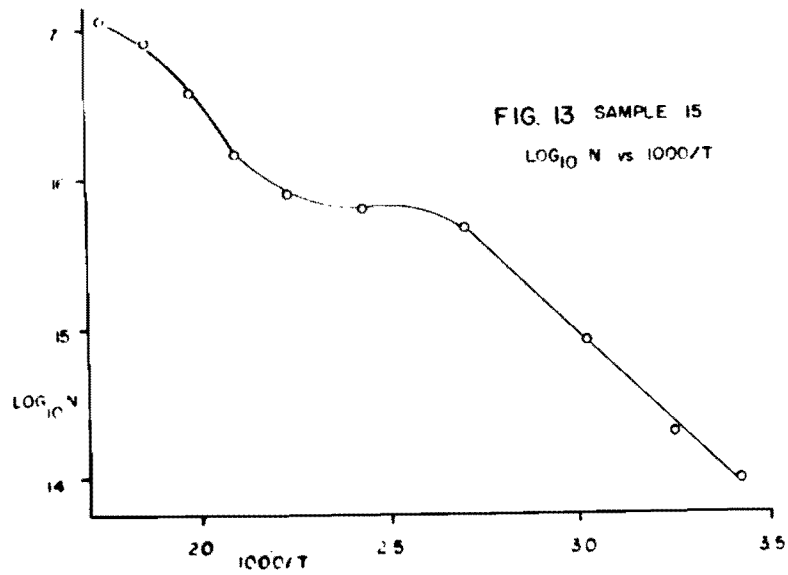
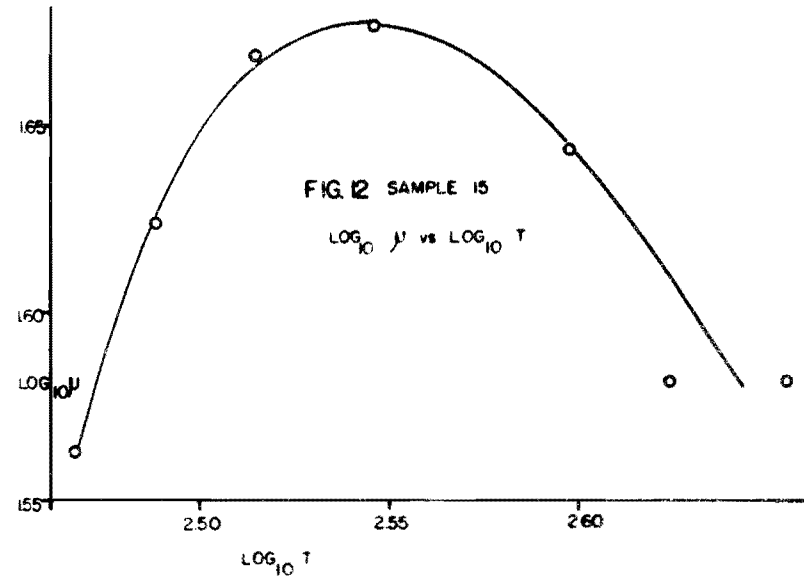
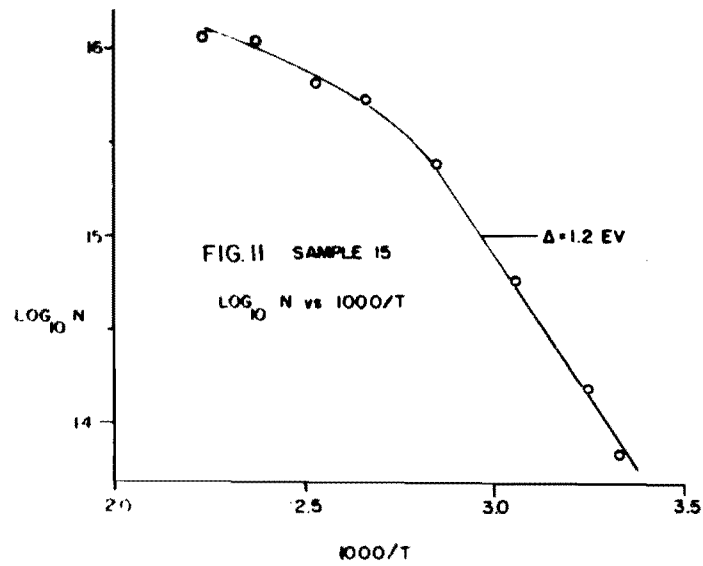
Resistivity curves for the first Cu impurity sample (#15) are shown in figure 10. Curve A was taken beginning at low temperature, and shows a value of E in the low-temperature range of 0.67 eV. The sample was heated to 179°C during this measurement. Hall coefficient data taken during this experiment showed p-type conduction, with a room temperature value of  $N = 5 \times 10^{13}$  holes/cc. A plot of  $\log N$  vs  $1000/T$  is given in figure 11 for the high-temperature region. Figure 12 gives some values of  $\log_{10} \mu$  vs  $\log_{10} T$ . The change of sign of the slope of this curve suggests a change from impurity scattering at low temperatures to lattice scattering at higher temperatures, but the results are not satisfactory for a calculation of the exact equation.

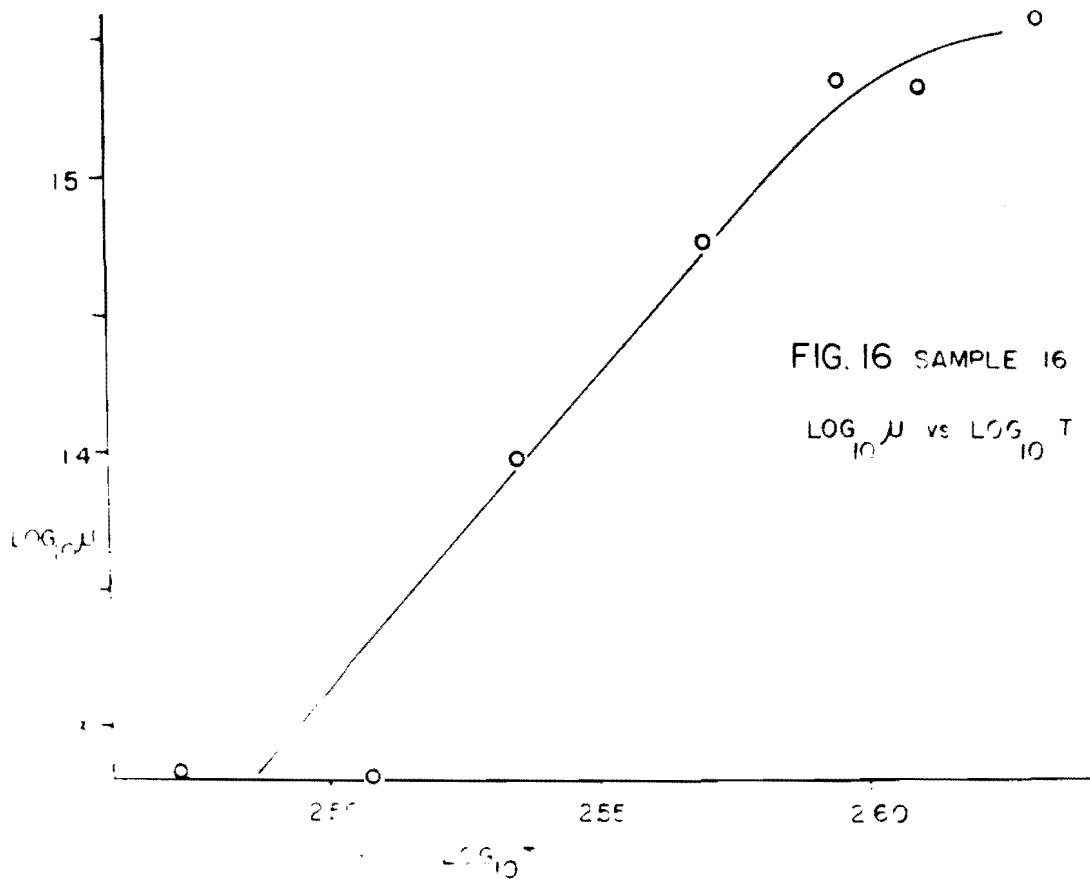
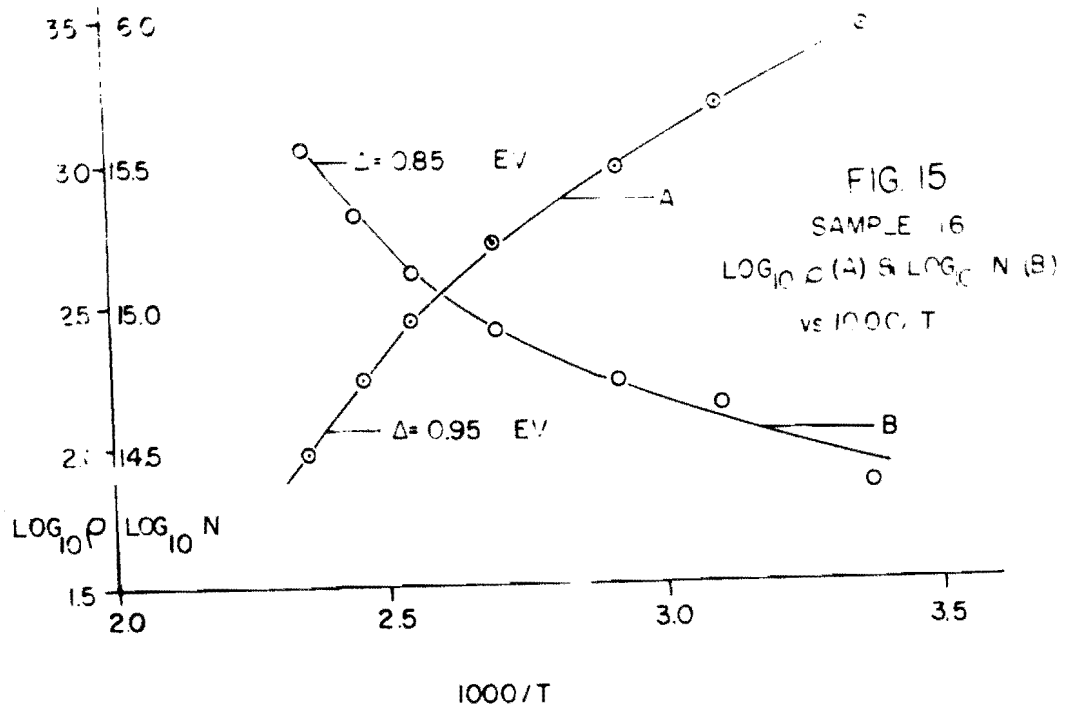
Curve 10B was taken with increasing temperature after cooling the sample after curve A. An apparent activation energy of  $E = 0.70$  eV is obtained for the high-temperature range. Hall coefficient measurements made during this experiment gave values of  $\log_{10} N$  shown in figure 13. The calculated activation energy is  $E = 0.95$  eV, which is not in agreement with the high-temperature activation energy calculated from curve B. This disagreement is partially due to the decrease in mobility with increasing temperature. A curve of  $\log_{10} \mu$  vs  $\log_{10} T$  is given in figure 14. The temperature dependence can be expressed as

$$\mu = CT^{-1.30}$$

The resistivity curve for another sample of CdTe + 0.1 mol % Cu (#16), taken after soaking for several hours at 150°C, is given as curve 15A, which shows an E of 0.85 eV.  $\log_{10} N$  is given in curve 15B as a function of reciprocal temperature, the calculated value of E being 0.95 eV. The discrepancy between the two values is again probably due







to changes in mobility, which, in this sample, increased with increasing temperature. The temperature dependence of the mobility is shown by figure 16.

## 5. Indium Impurity Samples

Measurements were made on a specimen (#9) of pure CdTe crystal into which indium was diffused in a sealed silica container at high temperature. These measurements showed n-type conduction with a very low apparent mobility (about  $2 \text{ cm}^2/\text{v sec}$ ). Substitution of this value in equations (16) and (17) indicates that both holes and electrons were present.

Hall coefficient and resistivity measurements were made on a specimen (#18) of single crystal CdTe with 0.1 mol % indium added, from liquid air temperature to  $67^\circ\text{C}$ . These results are summarized in figures 17, 18 and 19. Figure 17 represents the temperature dependence of the resistivity. The behavior of the resistivity is not primarily a function of the number of carriers, but is controlled by the mobility, the temperature dependence of which is shown in curve 18. The mobility obeys the relation  $\mu = CT^{0.88}$ . This type of relation is typical of impurity scattering. Figure 19 shows the temperature dependence of the number of carriers (electrons), calculated assuming 100% impurity scattering. The apparent activation energy was calculated using equation (10) to be of the order of 0.004 eV. The concentration of carriers at room temperature was calculated to be  $1.53 \times 10^{17}$  electrons/cc. The very low apparent activation energy for this indium specimen is due to its n-type character and indicates that the ionization of the impurity centers is essentially complete at room temperature. Since each indium ion represents one ionizable conduction electron, the concentration of

FIG. 17 SAMPLE 18

$\text{LOG}_{10} \rho$  vs  $1000/T$

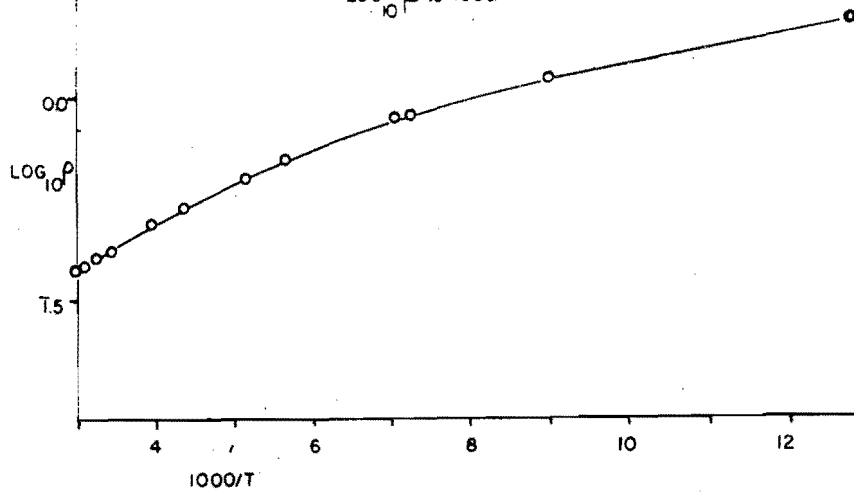


FIG. 18 SAMPLE 18

$\text{LOG}_{10} J$  vs  $\text{LOG}_{10} T$

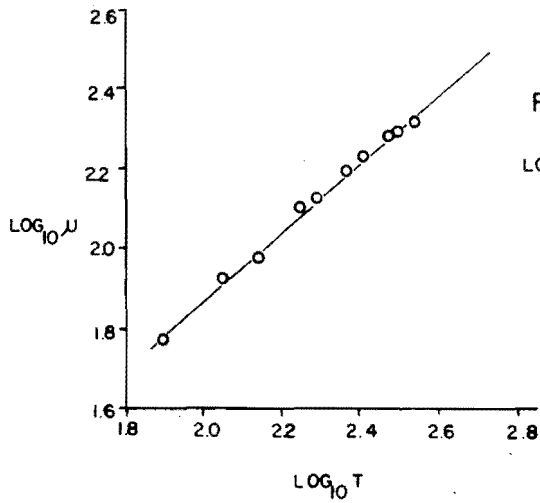
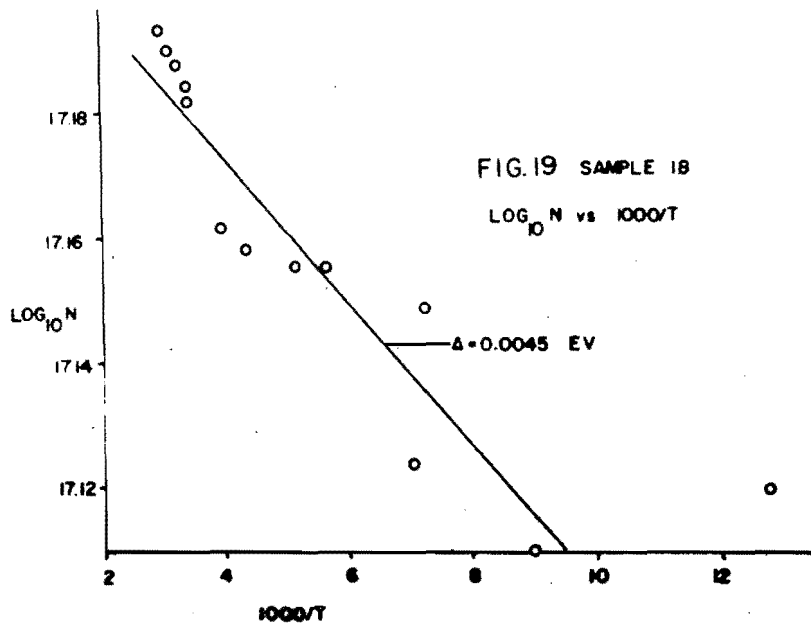


FIG. 19 SAMPLE 18

$\text{LOG}_{10} N$  vs  $1000/T$



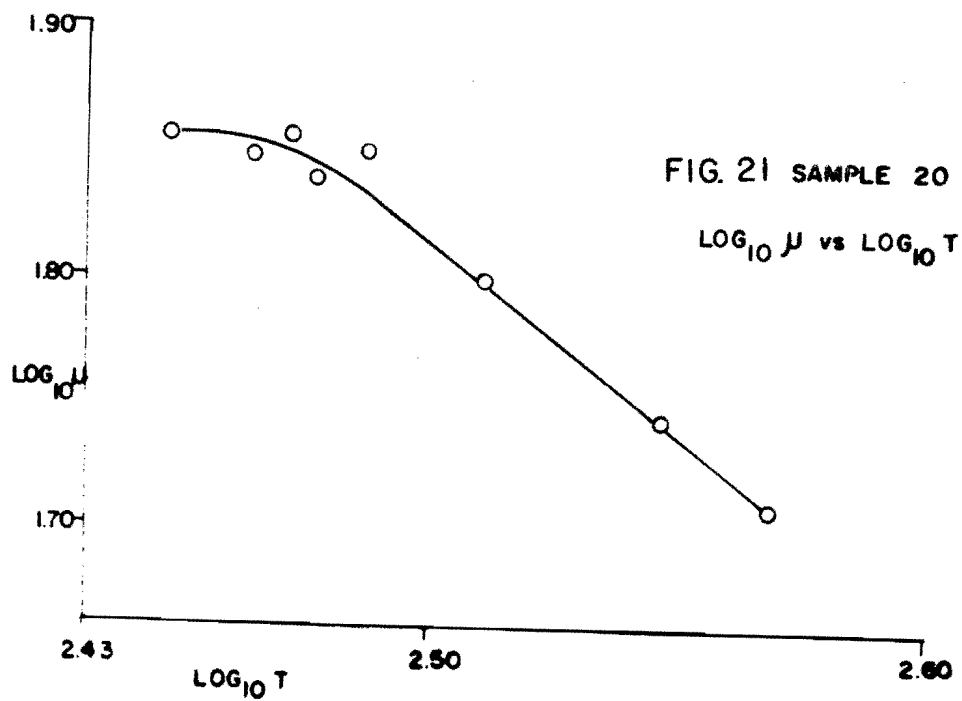
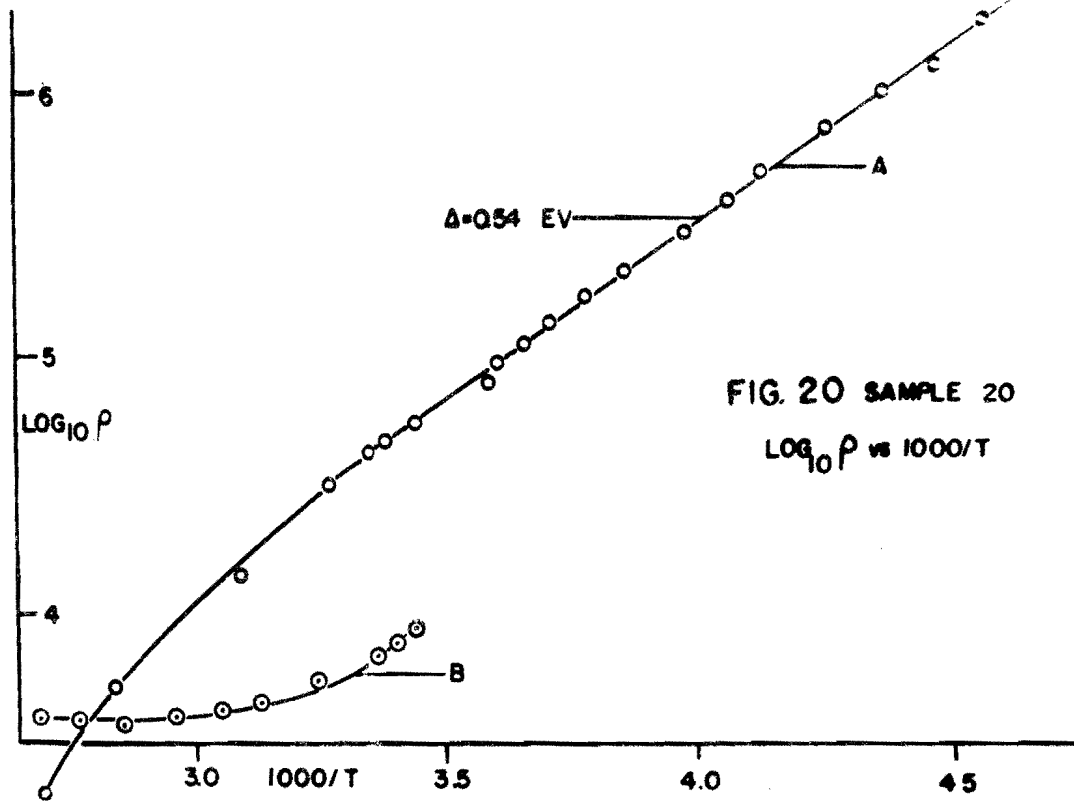
indium atoms in this crystal must have been of the order of  $10^{17}/\text{cc}$ . The reason for this low value is the failure of the indium to dissolve completely in the melt from which the crystal was made. Several very small lumps of metal were recovered from the upper surface of the crystal which, upon spectroscopic analysis, proved to be indium.

#### 6. Silver Impurity Crystals

Two specimens were investigated consisting of CdTe with 0.1 mol % Ag (specimens #20 and #21). These were the first specimens to which the gold-stripe, spring-platinum electrodes were attached (see Cutting and Electrodes). Results of the measurements of sample #20 are shown in figures 20 and 21. Curve 20A shows the resistivity taken as a function of increasing temperature (the sample not having been previously heated). An apparent activation energy of 0.55 eV was obtained in the low-temperature region, with a room temperature value of  $N = 2.17 \times 10^{12}$  holes/cc.

Curve 21 shows the temperature dependence of the mobility, which obeys the relation  $\mu = CT^{-1.52}$ . Curve 20B was taken after soaking the sample at  $100^\circ\text{C}$  for 18 hours. This mild heat treatment is seen to have had a remarkable effect upon the resistivity. From the behavior of the sample during measurements, it was thought that the heat treatment was also partially responsible for the dip in Curve 20A, which commences at about  $35^\circ\text{C}$ . According to Hall coefficient measurements, this change was caused by an increase in the number of carriers, and had little to do with the mobility.

Subsequent measurements, made after leaving the crystal at room temperature for 13 days, showed that the room temperature resistivity had increased to approximately the value indicated by Curve 20A. The



large resistivity change brought about in this crystal due to the heat treatment is, then, probably connected with anomalous effects noted in specimen #18 (see Quenching Experiments).

The dependence of  $\log_{10}\rho$  vs  $1000/T$  for an Sb impurity crystal (specimen #4) is shown in figure 22. There was no intrinsic behavior in the temperature range investigated. The low temperature value of  $E$  was 0.86 eV, and Hall measurements, while unreliable, indicated p-type character.

## B. ANOMALOUS RESISTANCE CHANGES

### 1. "Polarization" Phenomena

Resistivity -- In making the measurements described under "Bismuth Impurity Crystals", anomalous changes were noticed in the resistivity as a function of time. An investigation of these "polarization" effects was carried out in an attempt to determine whether or not these effects were systematic and reproducible. The results are shown below.

Specimen #2 (Bi impurity) was held at constant temperature for several hours. The current was then passed through the specimen and measurements of resistance made as a function of time. Curves of the results of these experiments made at several temperatures are given in figures 23-26. After the resistance had reached a steady minimum (A curves), the current was reversed, measurements being made as before. The results are shown in the B curves. The resistance first increased to a maximum value, which is about the same as the initial resistance in the "A" type of curve, and then decreased to a minimum value comparable to the minimum value of the A curves. These curves will hereafter

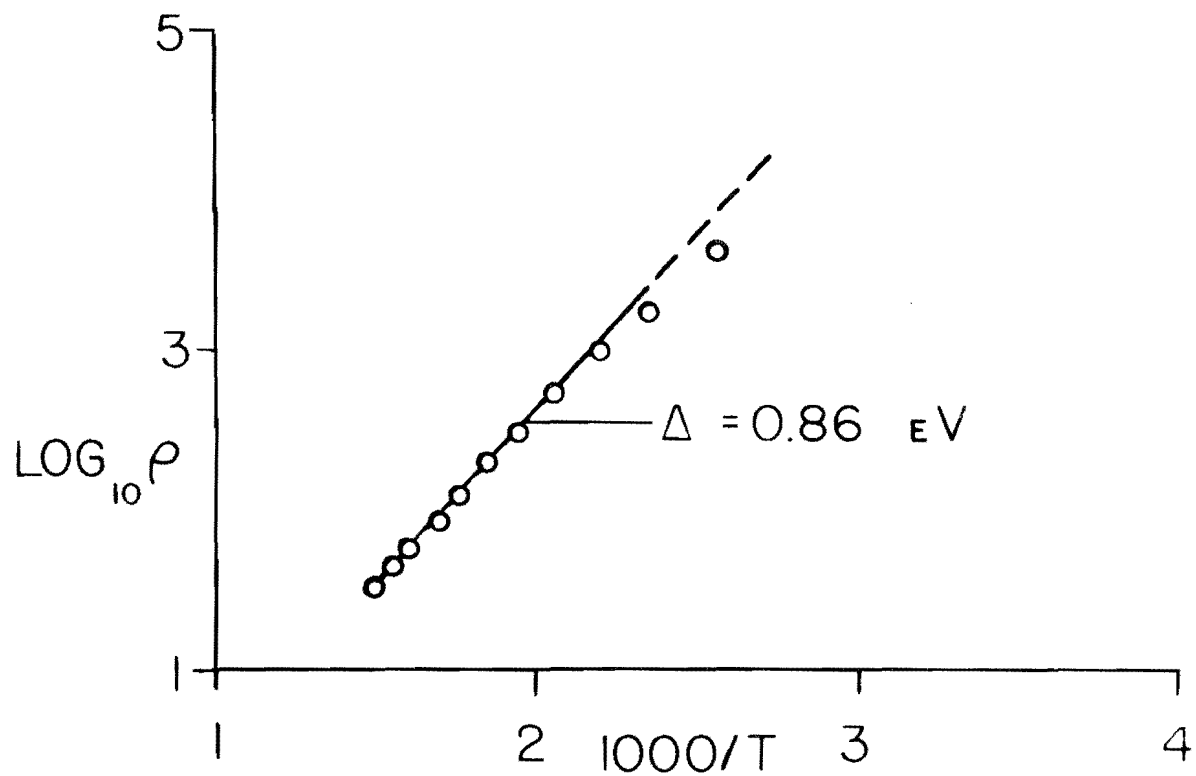


FIG. 22-SAMPLE 4 ( $S_B$ )

$\text{LOG}_{10} \rho$  vs  $1000/T$

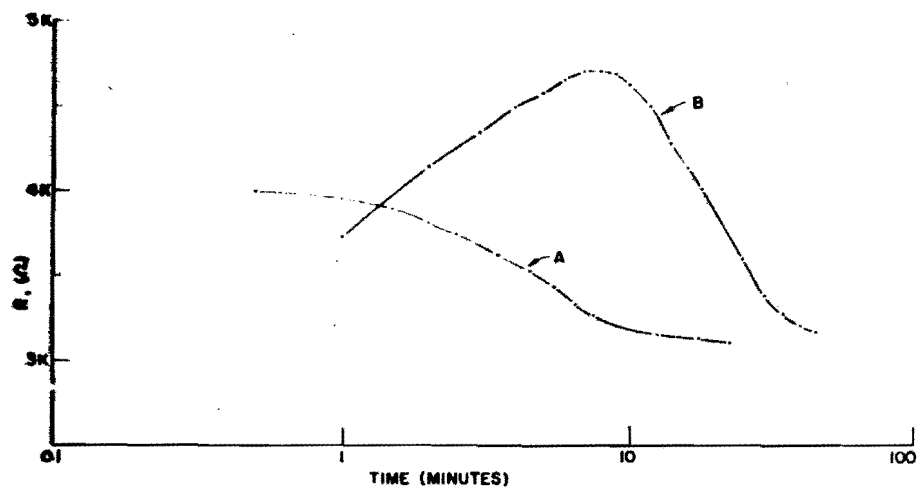


FIG. 23 RESISTANCE OF SAMPLE 2 (CdTe+Bi) vs. TIME AT 298°C.

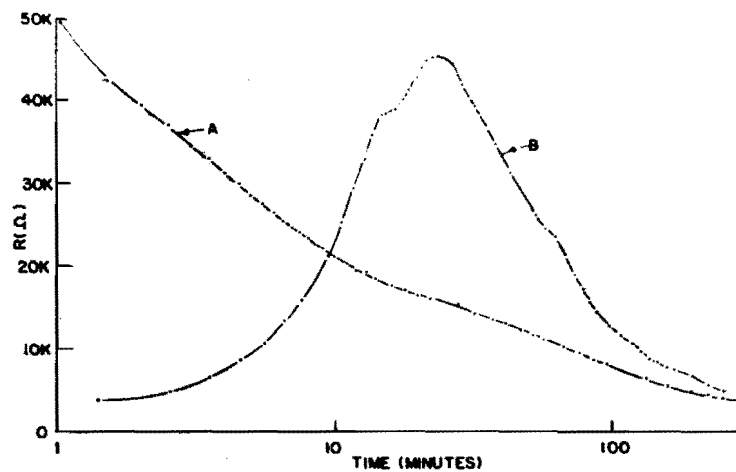


FIG. 25 RESISTANCE OF SAMPLE 2 (CoTe) vs. TIME AT 198°C.

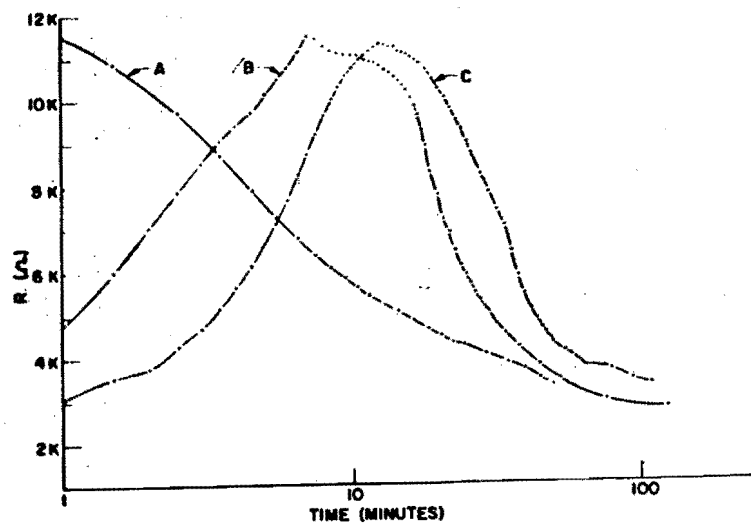


FIG. 24 RESISTANCE OF SAMPLE 2 (CdTe+Bi) vs. TIME AT 268°C.

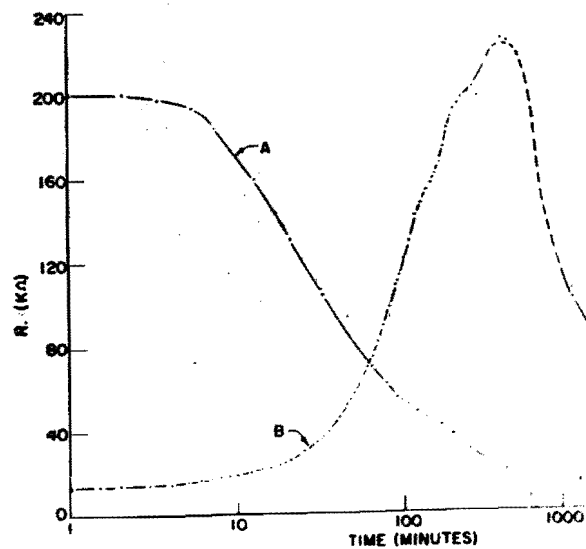


FIG. 26 RESISTANCE OF SAMPLE 2 (CdTe+Bi) vs. TIME AT 144°C.

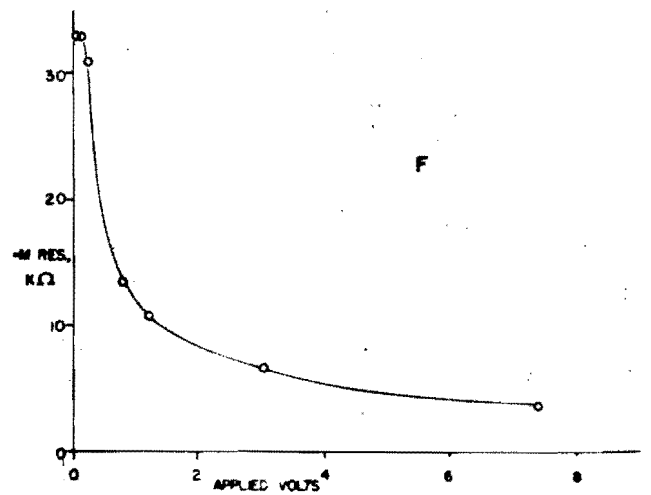
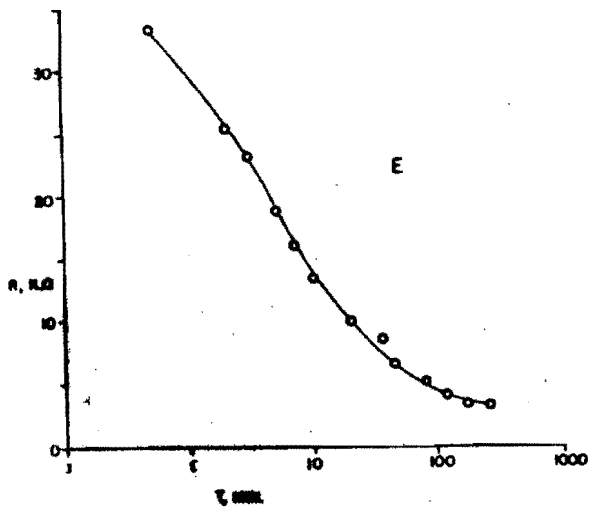
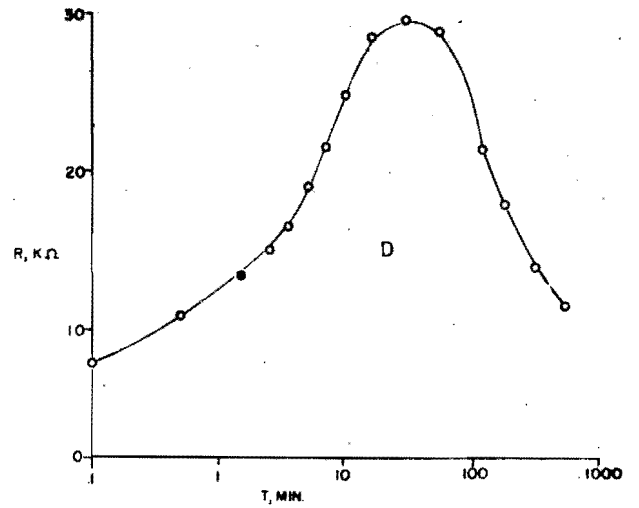
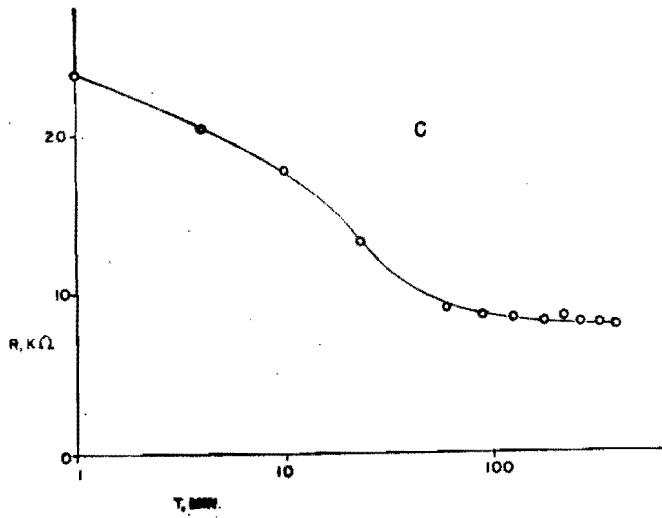
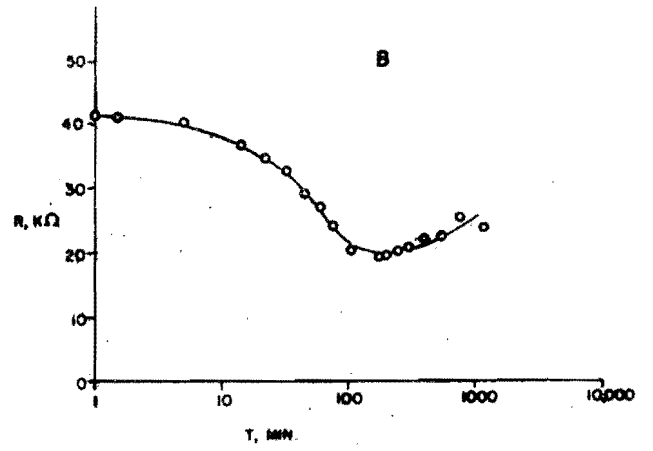
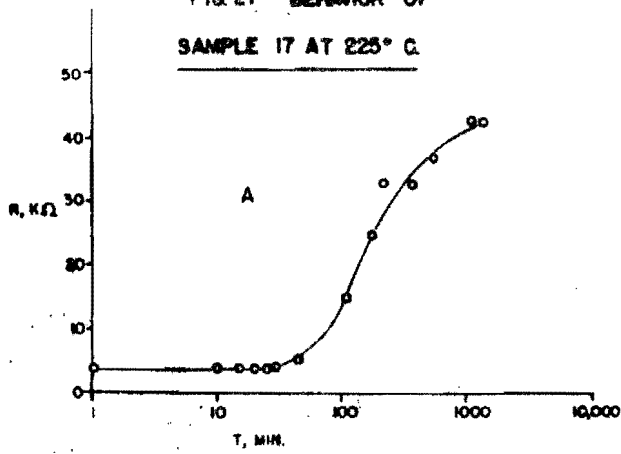
be referred to as the "direct" and "reversal" curves, respectively. If, after one reversal curve, a further reversal curve is made, the results are approximately the same (figure 24C). This is true of additional reversal curves.

It can be seen that both the times involved and the ratio of maximum to minimum resistance decrease greatly at low temperatures. Additionally, the effects noted seem to occur only in the temperature range corresponding to extrinsic conduction in the specimens. This is illustrated by the points marked 1, 2, 3 and 4, in figure 7. These points represent values of the resistance at the peaks of the reversal curves. The curves in figure 7, themselves, show values which correspond to the minimum resistances measured in the direct and reversal curves, due to the fact that during these experiments the current was left on throughout the measurement. Further points of the same type as 1-4, taken at lower temperatures, trace out a plot which is essentially parallel to the low temperature portion of curve 7 (dark).

Because of the peculiar nature of the results obtained with sample #2, it was decided to repeat the measurements, using another crystal which was cut from an adjacent portion of the same crystal slab. This was specimen #7, which was prepared with silver paste current electrodes and platinum wire voltage probes. This crystal was heated to about 375°C for the purpose of making measurements of resistivity as a function of temperature, which measurements produced results similar to those shown for specimen #2. An attempt was then made to reproduce the time-dependent resistance measurements found in the previous specimen. The results obtained were identical in form to those previously determined and will not be reproduced here.

Somewhat later it was hypothesized that the properties measured might have been produced as a result of heating the crystal during the measurement of resistivity as a function of temperature. Consequently, it was decided to repeat the measurements, using this time a crystal which had not been heated previously. This specimen (#17) was taken from another portion of the same crystal batch as that used for the two previous bismuth impurity crystals. After preparation of the crystal with chemically deposited gold current electrodes and platinum wire potential probes, it was heated rapidly to 225°C and measurements of resistivity immediately commenced as a function of time. The results are shown in figure 27. The current was turned on at the beginning of Curve A, whereupon, after an initial induction period, the resistance increased by about one order of magnitude. At the end of this curve, the polarity of the crystal was reversed, after which the resistance first decreased, and then increased slightly (Curve B). The potential across the crystal was then increased and the resistance decreased again (Curve C). The behavior of the crystal during these first three experiments was atypical of the results found with the other Bi impurity crystals. However, subsequent experiments produced results consistent with those obtained in the other specimens. These measurements are represented by the next two curves. Curve D was taken upon reversal of the polarity after the measurements in Curve C, and shows the characteristic form of a reversal curve, the resistance first rising and then falling to a minimum value. After this series of measurements, the crystal was left at the measurement temperature for several days, in order that it might reach the "equilibrium-current-off" condition. The measurements were then commenced again, the result being the "direct"

FIG. 27 BEHAVIOR OF  
SAMPLE 17 AT 225° C.



curve E. This curve is of the same type as the direct curves found in the other crystals. Measurements were now made of the dependence of the equilibrium-current-on resistance upon the applied field. First the crystal was brought to equilibrium under the highest applied field to be investigated. Subsequent measurements were taken by reducing the field, allowing time for equilibrium to be established (resistance measurements serving as the criterion) and then the equilibrium resistance measured. This was done for several values of the applied field, the results being given in Curve F. The equilibrium value of resistance is seen to be a strong function of the applied field at low values of field, gradually flattening in the high-field region. This dependence of equilibrium resistance upon applied field had not been noticed in the other bismuth impurity specimens investigated. No specific attempt had been made before to detect the dependence, but the direct and reversal curves usually had been measured under an applied field which falls on the steep part of this curve. The field dependence found in this specimen is considered as another instance of atypical behavior, for the above reasons, and also as a result of measurements made on another crystal, to be reported below.

Frequent attempts were made to measure the Hall coefficients of the bismuth impurity crystals reported above, with disappointing results, in that the data were never sufficiently reliable for calculations to be made. It was possible to determine, however, that the crystals all showed p-type conduction. This is in agreement with the large low-temperature activation energies found in these crystals, which mark them as probably p-type (40).

Results similar in form to the ones described above for the bismuth impurity specimens were found in one other crystal by another member of the laboratory, although no quantitative data were obtained. This specimen was a "pure" crystal, and constituted the only specimen other than those containing a trivalent impurity in which this behavior was observed. However, the results may have been due to a trace of unintentional trivalent impurity.

The existence of the effects reported above only in crystals containing intentional trivalent impurity suggested that the presence of trivalent ions might be necessary for the production of the effect. The addition of trivalent ions to CdTe would be expected, however, to produce n-type conduction. The presence of p-type conduction constituted a contradiction of this expectation, and it was decided that some other mechanism must be responsible for the p-type character.

It has been noted above that heat treatment of CdTe in the absence of a protective Cd atmosphere caused the evolution of Cd vapor, leaving behind Cd vacancies in the crystal, and these vacancies have been proven to produce p-type conduction. It was therefore hypothesized that the Bi impurity crystals investigated had, during some stage of preparation or measurement, suffered depletion in Cd, with the resultant development of p-type character. In order to test this contention, it was decided to heat-treat a crystal containing trivalent impurity which had already been proven to exhibit well-behaved n-type character, in an attempt to produce in it the results obtained in the Bi impurity crystals. According to Kroger and de Nobel (40), the evolution of Cd vapor becomes appreciable above 300°C, and therefore this temperature was decided as the proper one for the heat treatment.

Use was made of specimen #18, which consisted of CdTe + 0.1 mol % In. This crystal, like the Bi impurity crystals, was expected to exhibit n-type semiconductivity, since part of the Cd<sup>+2</sup> had been replaced by In<sup>+3</sup>, producing excess ionizable electrons. Hall and resistivity measurements made with this crystal using helium as a transfer gas at low temperature showed n-type conduction, and are summarized at room temperature by

$$\rho = 0.429 \text{ cm} \quad N_0 \approx N = 1.53 \times 10^{17} / \text{cm}^3$$

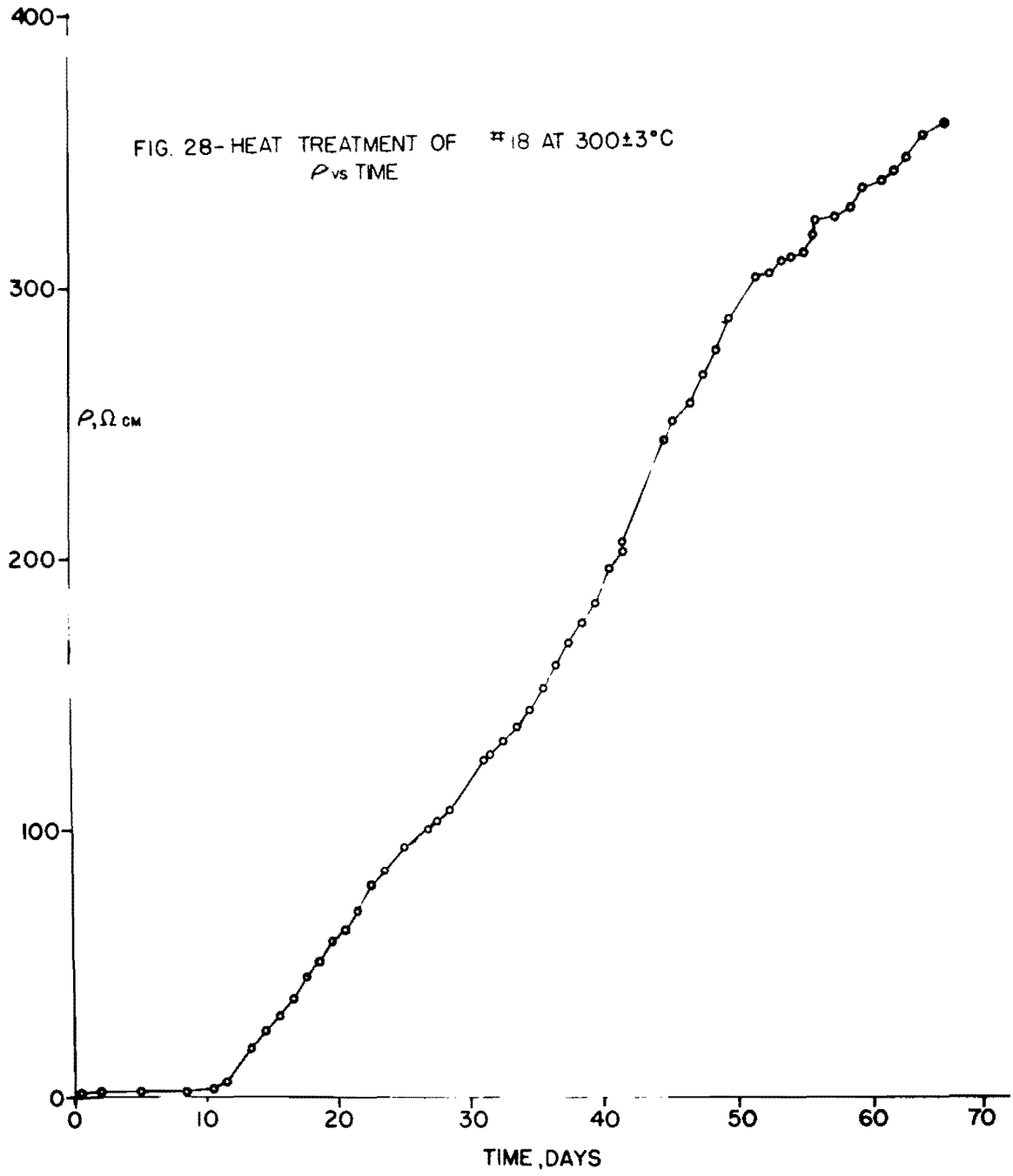
$$E = 0.0045 \text{ eV} \quad \mu_n = 189 \text{ cm}^2 / \text{v sec.}$$

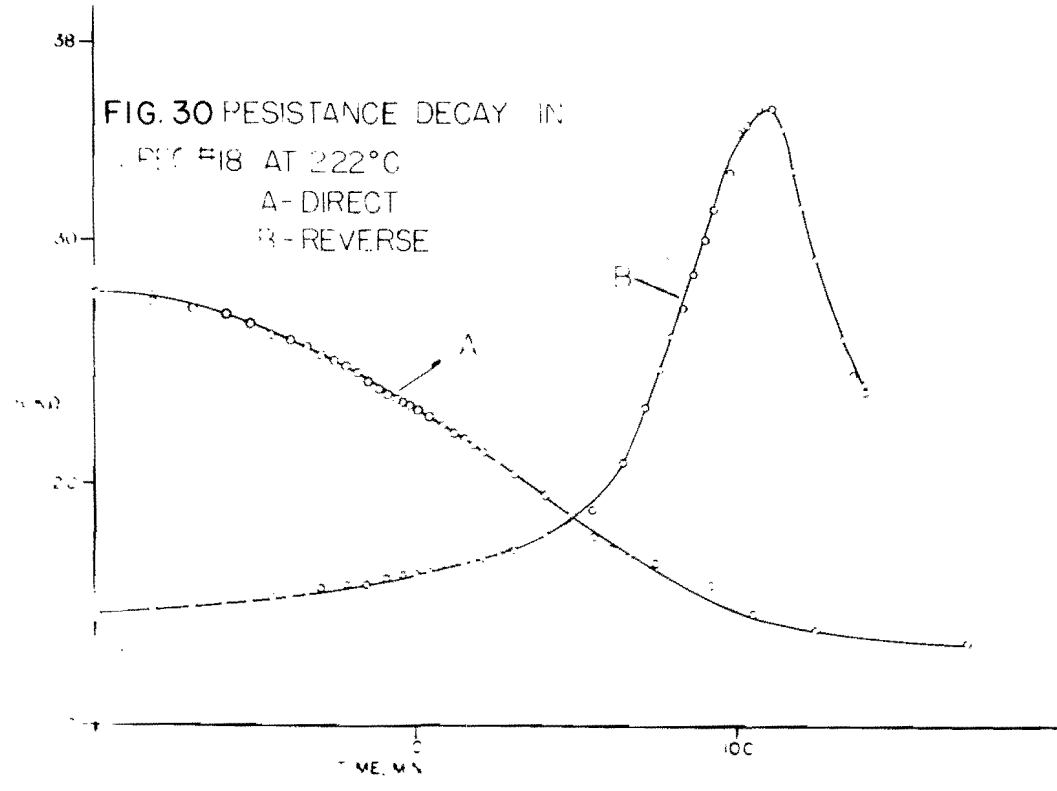
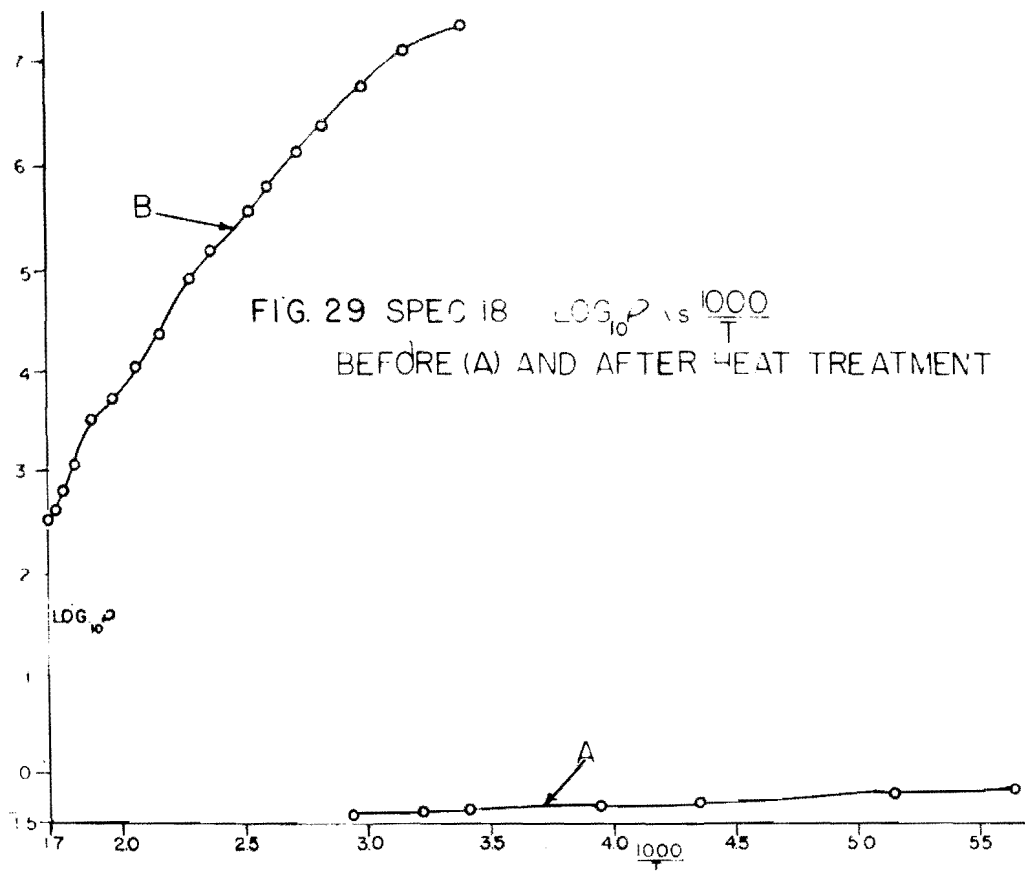
(see In impurity crystals).

The crystal was heated at  $300 \pm 3^\circ\text{C}$  and measurements of resistance were made as a function of time, using a photographic recording technique. At five-minute intervals a timer turned on the current for 10 seconds, measurements being made after about 9 seconds. These measurements included time, temperature, voltage and current. Results are shown in figure 28.

After an initial induction period of about 10 days, the resistance began increasing, assuming after a few days a linear time rate of change. During the 63 days of this experiment, the resistivity changed from 1.34 to 346 ohm cm, and the conductivity changed from n- to p-type, as expected. The room temperature resistivity increased by a factor of  $1.1 \times 10^8$ . Typical temperature coefficients of resistivity for the crystal are shown in figure 29, before (Curve A) and after (Curve B) heat treatment. The indicated high-temperature activation energy is about 1.6 eV, which agrees well with values calculated for other crystals. Curve B was taken under equilibrium-current-off conditions.

FIG. 28- HEAT TREATMENT OF #18 AT  $300 \pm 3^\circ\text{C}$   
 $\rho$  vs TIME





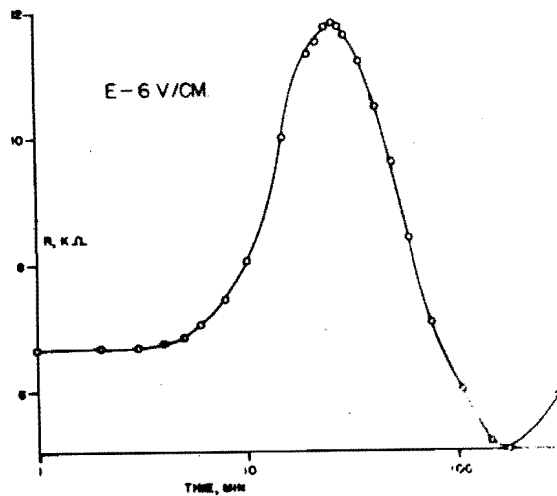
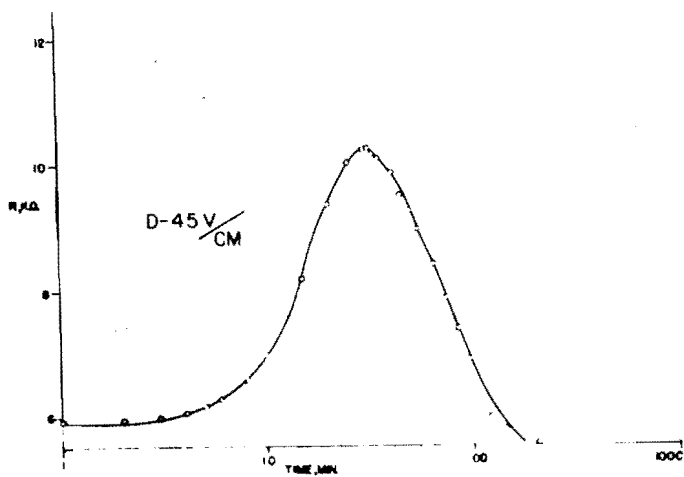
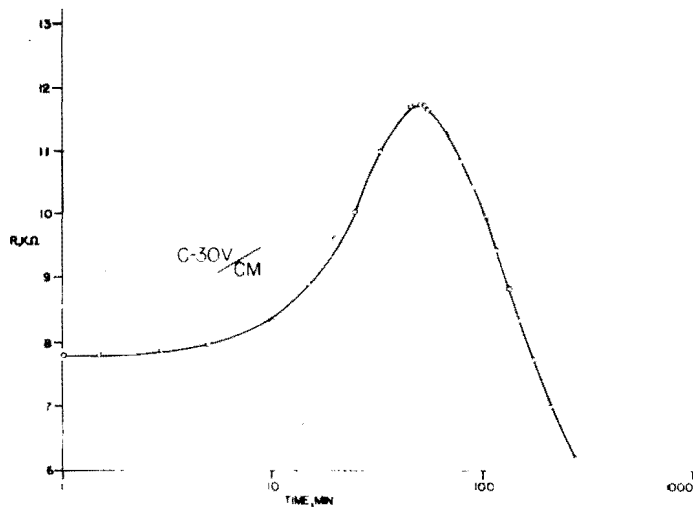
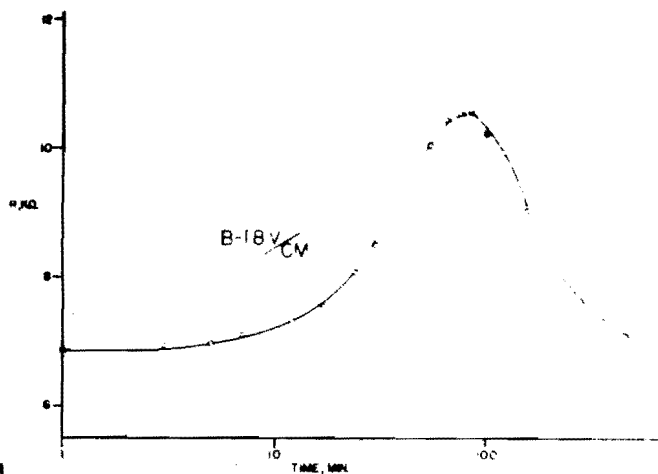
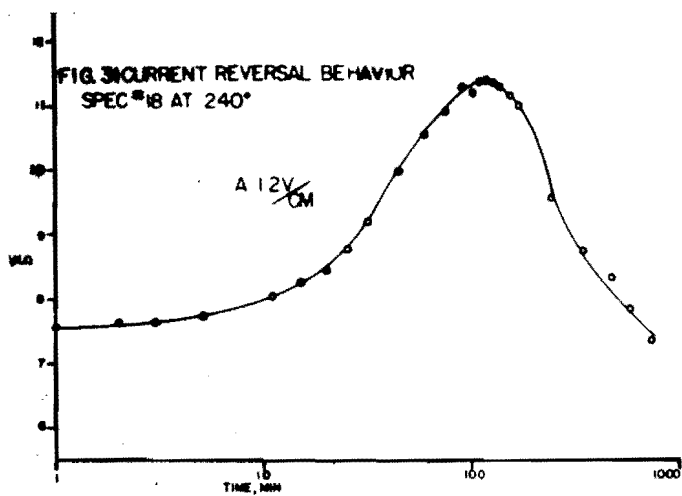
Following heat treatment, experiments were commenced to detect possible time changes of resistance similar to those found in the CdTe + Bi crystals. Results of these measurements are shown in figure 30. The current was turned on at the beginning of Curve A, and reversed at the end, the measurements in Curve B being started immediately after the reversal. The structures of these curves are identical with those in the CdTe + Bi crystals.

It might be expected that the times involved in the decay measurements would be related to the value of the electric field applied to the crystal during measurement, since it is the current flow which causes the resistance changes. Consequently, a series of measurements was made at constant temperature as a function of the applied field. The problem existed of establishing some reproducible point on the resistance curves which would serve as a signpost for the measurement of time. The peak of resistance after reversal was chosen as being the most accurately measured and reproducible point.

Accordingly, for each experiment, the crystal was first brought to the equilibrium-current-on condition (polarized, for lack of a better term) under the applied field to be investigated. Immediately thereafter the current was reversed and resistances measured as a function of time, in such a way that for each reversal experiment the current was passed through the crystal in the same direction.

Results of this series of measurements at 240°C are shown in figure 31 for applied fields of from 1.2 to 6.0 v/cm. In order to eliminate the effect of possible space charge effects and discontinuous voltage drops across the current electrodes, the current was adjusted by reference to the voltage across the voltage-measuring probes, which

FIG. 3 CURRENT REVERSAL BEHAVIOR  
SPEC #18 AT 240°



served as the criterion for maintaining constant field conduction. The degree of "polarization" was found to be independent of field for applied fields within the above limits, contrary to the results reported for specimen #17 above. If one calculates the product of applied field and time to maximum resistance after reversal (the "reversal time"), one finds the product to be essentially constant, viz.

Curve	Field (v/cm)	time (min)	product (v min/cm)
A	1.2	120	144
B	1.8	81	146
C	3.0	50	150
D	4.5	31	150
E	6.0	26	156

Such results immediately suggest that the time-field product is a fundamental property of the material at this temperature.

It was indicated that in the bismuth-doped crystal, the values of the polarization time and the reversal time decreased rapidly with increasing temperature. It was considered to be important to determine the temperature coefficient of the reversal time. Accordingly, measurements were made of the reversal time as a function of temperature, under conditions of constant applied field. Typical curves are shown in figure 32 A-E for temperatures from 200° to 320°C. It can be seen that the reversal time is a strong negative function of temperature. A more complete temperature coefficient of the reversal time is given in figure 33. The abscissa is  $1000/T$  and the ordinate is  $P$ , the applied voltage-time product. The Curve A is a plot for the first series of measurements made, and displays several interesting features. The curve is very

FIG 32 POLARIZATION REVERSAL IN #18  
AS A FUNCTION OF TEMPERATURE

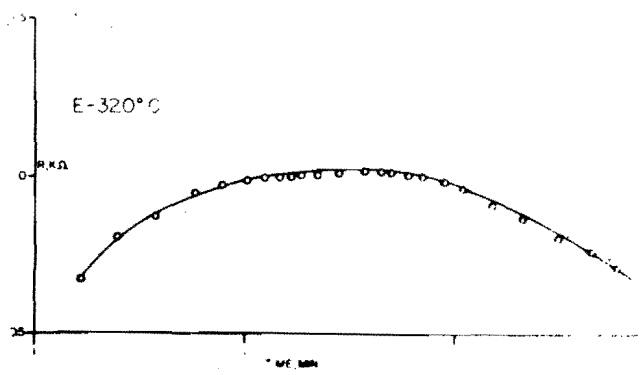
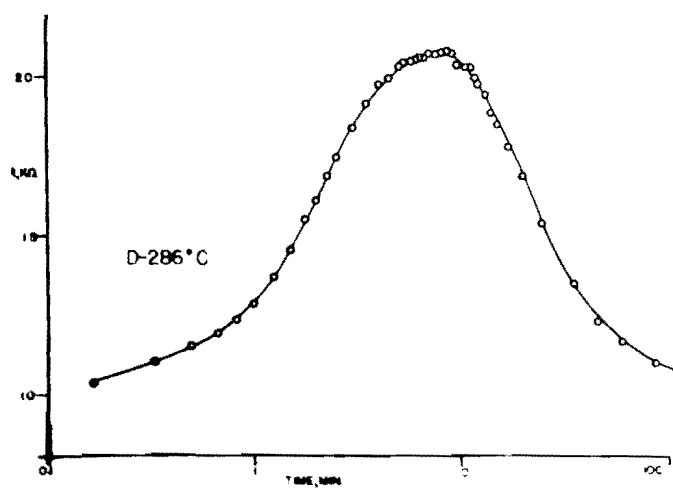
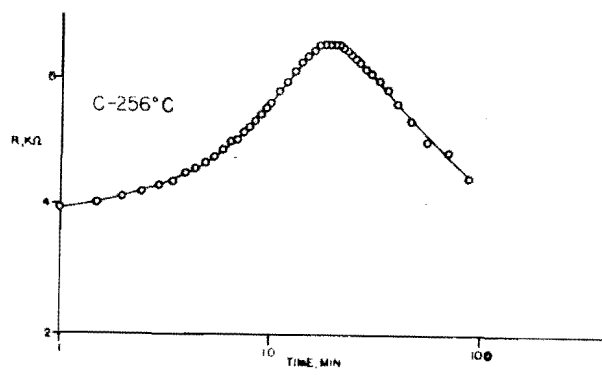
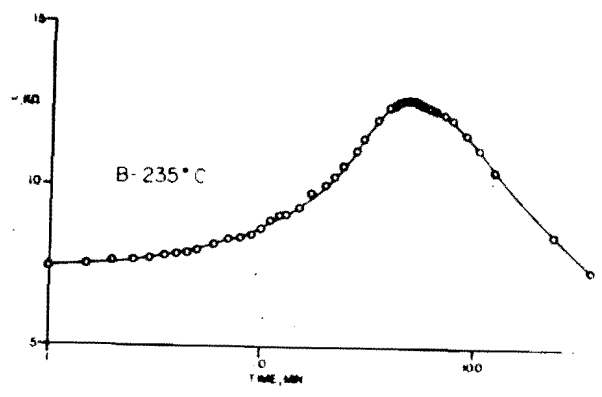
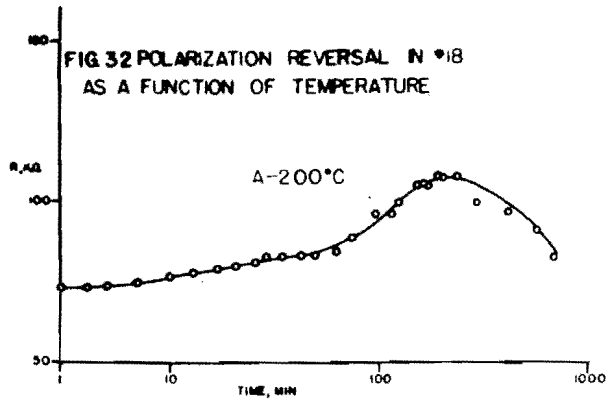
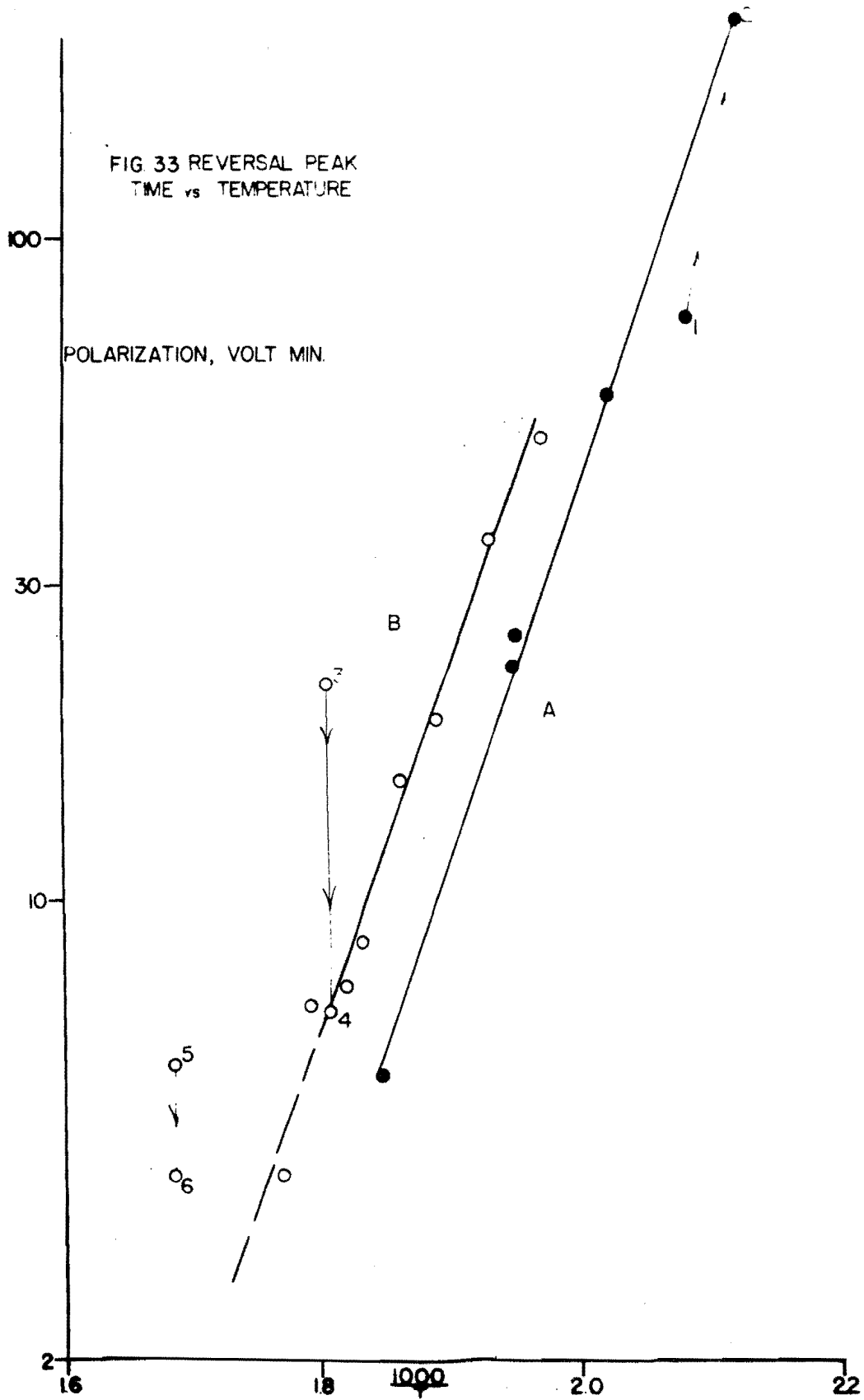


FIG 33 REVERSAL PEAK  
TIME vs TEMPERATURE



nearly linear, obeying the relation  $P = P_0 \exp (E/2kT)$ , where  $E = 2.32$  eV. This linear relation suggests that an activation energy  $E$  can be calculated from these data.

The second effect observed is an apparent memory associated with the previous heat treatment to which the crystal had been subjected. This is illustrated by point (1), Curve A. Prior to this measurement, the crystal had been heated to  $320^{\circ}\text{C}$  for several hours and then soaked overnight at  $205^{\circ}\text{C}$  preparatory to the measurement. The time obtained from this measurement was about 40% less than would be expected from the other data. Subsequent soaking of the crystal for three days at  $200^{\circ}\text{C}$  produced an equilibrium after which point (2) was obtained.

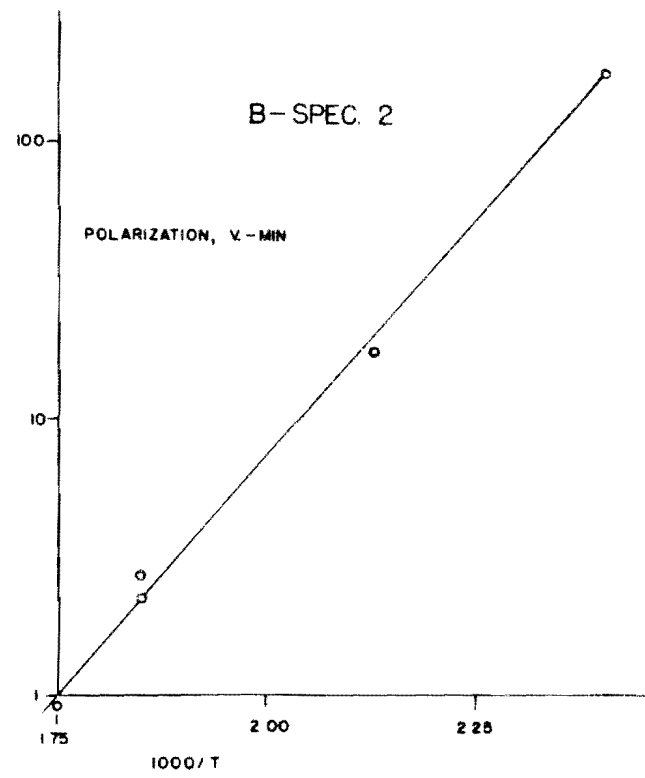
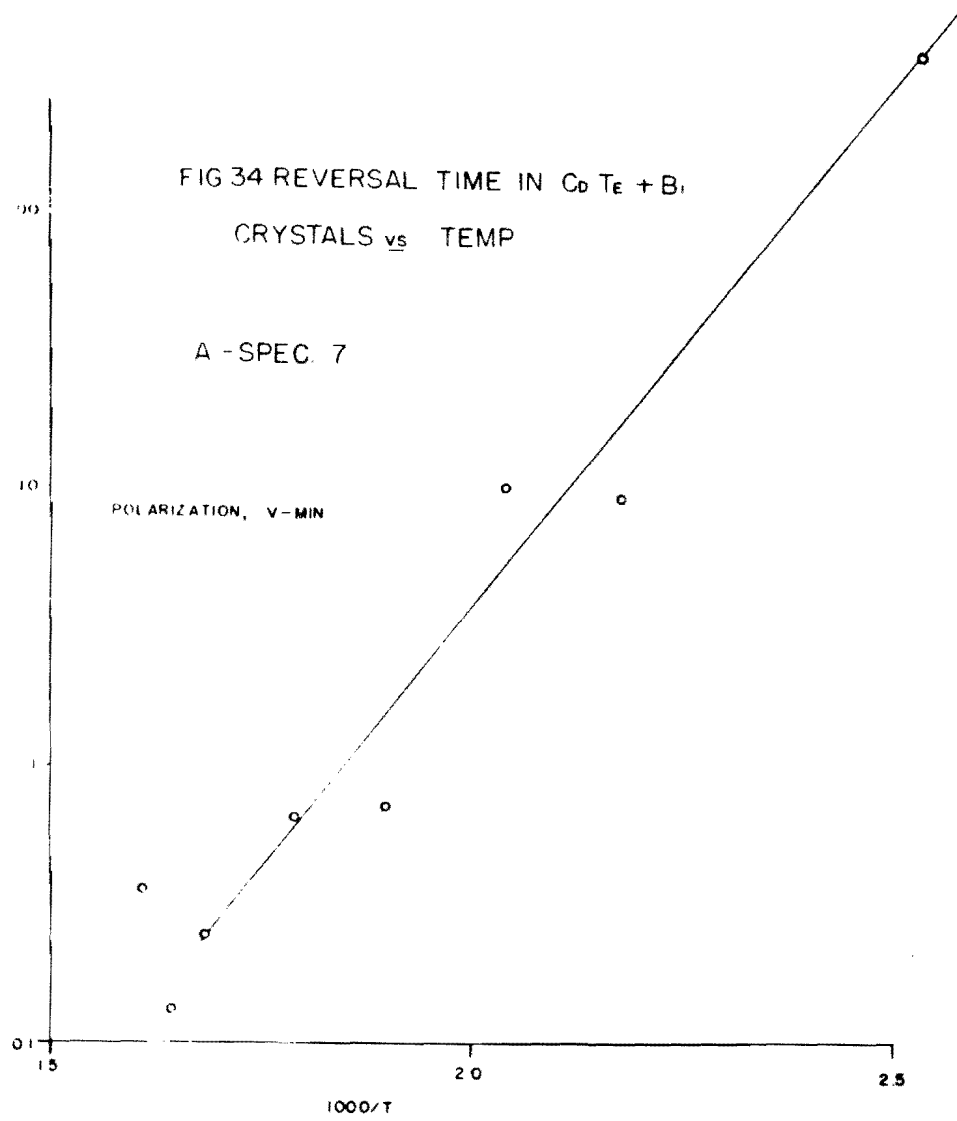
Curve B is a similar series, but is seen to be displaced in the direction of greater time by a factor of approximately two. This may have been the result of further heat treatment, during which the crystal was held at  $280^{\circ}\text{C}$  for four days in order to attain equilibrium. The apparent activation energy for this curve in the middle temperature region is 2.18 eV. The reproducibility and precision of these measurements, however, are such that this value can be considered as in agreement with the value from Curve A, within the limits of experimental error. Measurement of reversal time is more difficult at temperatures above about  $290^{\circ}\text{C}$ , owing to the tendency for the peaks to flatten in this range (see figure 32E). Curve B shows the same memory effect, (points 3, 4, 5 and 6), as that described above for Curve A. Point 3 was obtained after raising the temperature from  $200^{\circ}\text{C}$  and soaking at the measurement temperature ( $281^{\circ}\text{C}$ ) for two hours before commencing the polarization. The value obtained is above the curve by a factor of three; that is, the crystal "remembers" the long time associated with  $200^{\circ}\text{C}$ , the

last temperature at which it was polarized, just as point (1) on Curve A shows a memory for the previous high temperature of polarization. After point (3) the crystal was held at the measurement temperature for four days and then point (4) was determined. The crystal had now apparently attained equilibrium. Similar behavior is exhibited by points (5) and (6). Point (5) represents a seventeen-hour soak, after which the crystal was held at temperature an additional two days before point (6) was determined.

The temperature dependence found in specimen #18 led to a re-evaluation of the data obtained for specimens #2 and #7 (both CdTe plus Bi). Since these results were not obtained under constant applied voltage, it was necessary to arrive at an estimate of the average applied voltage by graphical integration of the voltage-time curve for each temperature.

Results for specimen #7 are shown in figure 34A, the ordinate ("polarization") being (time to reversal) x (applied potential). A linear plot is obtained, with an activation energy of 1.5 eV. Figure 34B shows a similar plot for specimen #2, again approximating a straight line, with an apparent activation energy of  $E = 1.38$  eV. As was the case with specimen #18, these two activation energies probably cannot be differentiated, owing to the limited accuracy of the measurements. If the results for specimens #2 and #7 are plotted on the same axes, (taking account of the difference in separation of the electrodes) it is found that the experimental points for one specimen agree fairly well with those for the other specimen. Similar plots of the same data for crystal #17 show a wide discrepancy between this crystal and the other two.

FIG 34 REVERSAL TIME IN  $\text{CoTe} + \text{Bi}$   
CRYSTALS vs TEMP

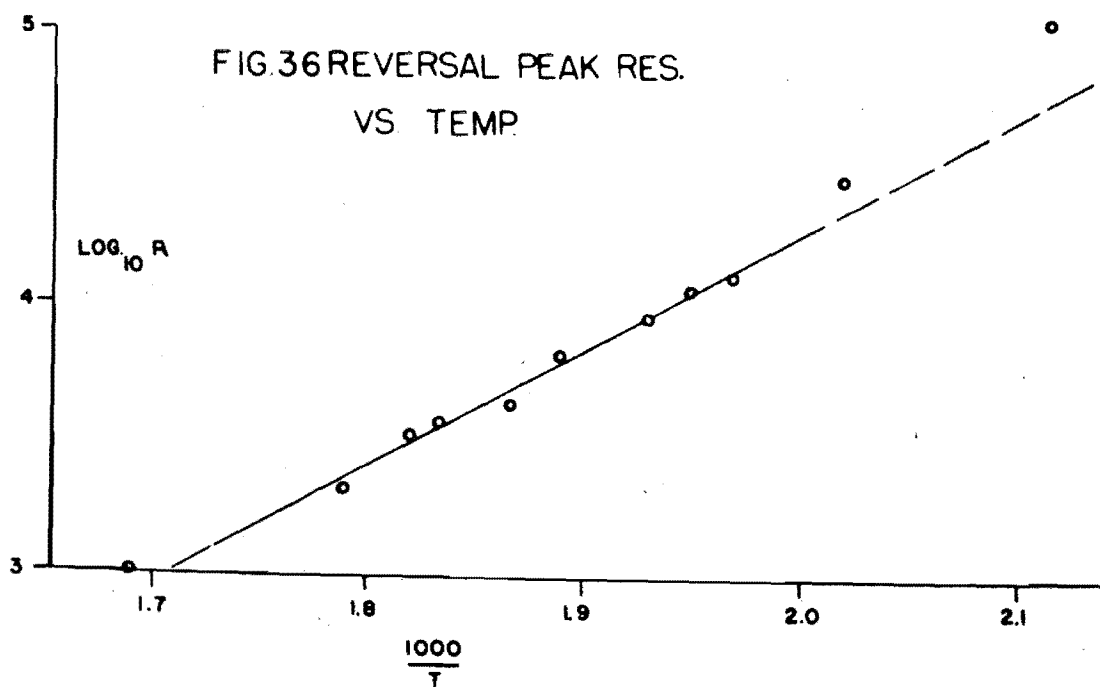
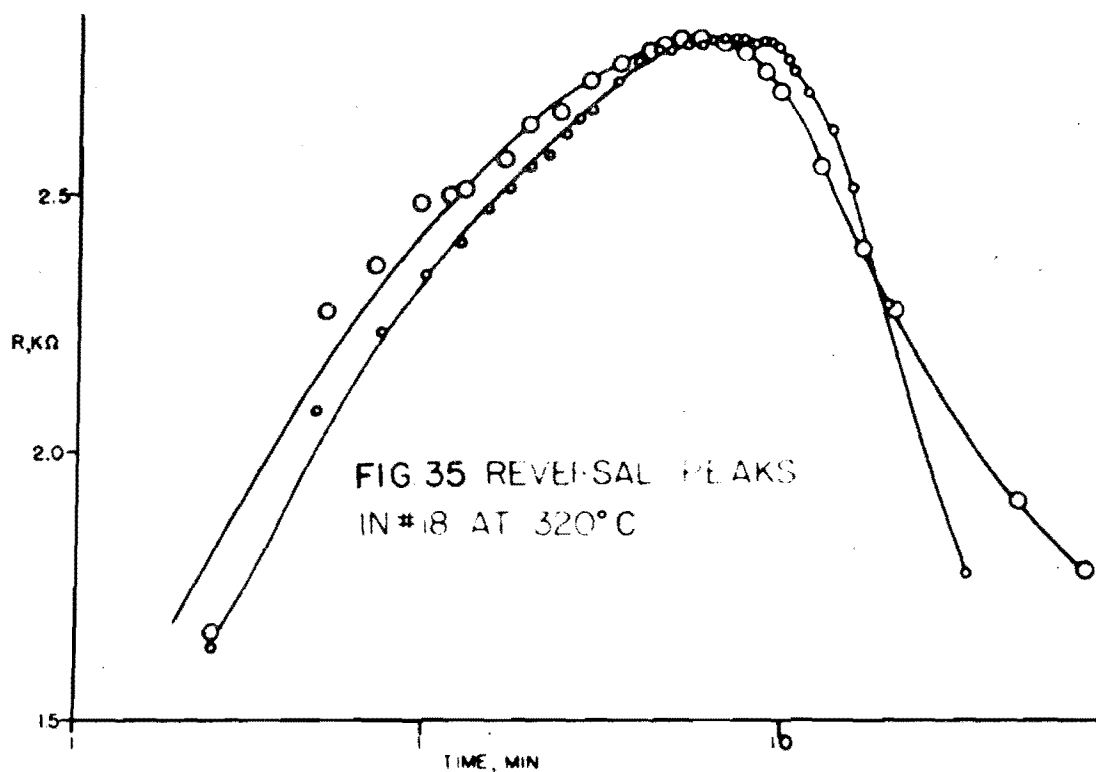


A plot of the peak in resistance after reversal for specimen #18 (In impurity) is shown in figure 36. The apparent activation energy is 1.67 eV, compared to the value of 1.6 eV obtained from the high temperature portions of such curves as figure 29B. Similar plots of the equilibrium-current-on (polarized) values yielded approximately the same value.

Other features of interest are found in the resistance curves after reversal. One is their virtual independence of the direction of current flow as is the case of Bi-doped specimens reported above. This is illustrated in figure 35, which consists of two consecutive curves, made under constant voltage conditions with opposite directions of current flow.

Another illustration of the reversal characteristic is shown in figure 37, measurements being made at 273°C. Curve A is a normal reversal curve; at point (1) the current was reversed, whereupon the resistance tended to a peak; at point (2) the current was again reversed, this time producing a much more pronounced peak. This peak is significant, since the reversal came at a point where the resistance equalled the original equilibrium-current-off (unpolarized) value. Apparently the condition of the crystal at this point was not the same as in the unpolarized case, even though the resistances are equal. If it were, Curve C should be a simple "direct" curve of the type shown in figure 30A.

In order to test the stability of the crystal condition at an arbitrary fixed point on the reversal curve, a new treatment was imposed at point (3). This scheme consisted of reversing the current each minute precisely on the half-minute and measuring resistance precisely on the minute. The crystal now alternated between two tendencies,



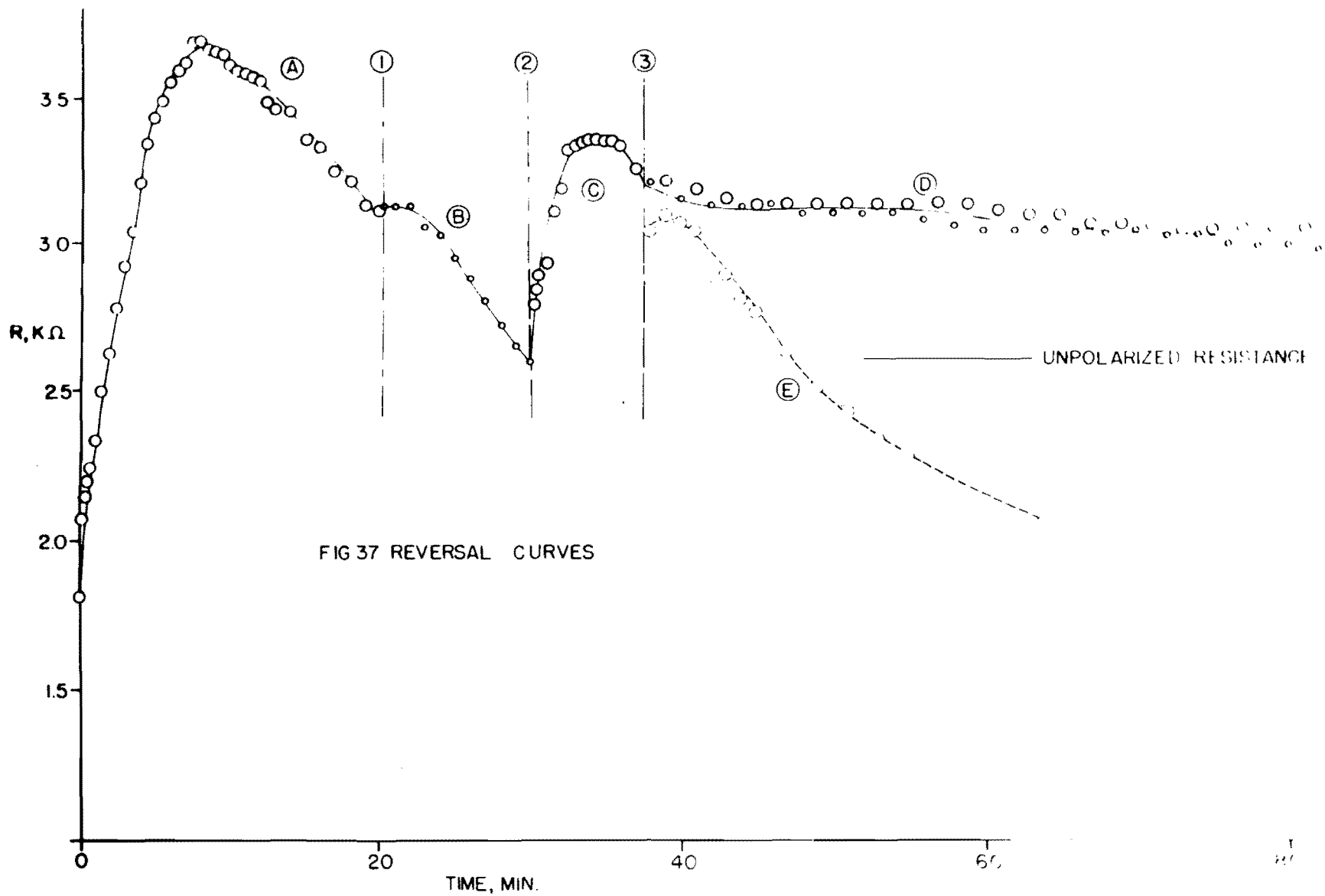
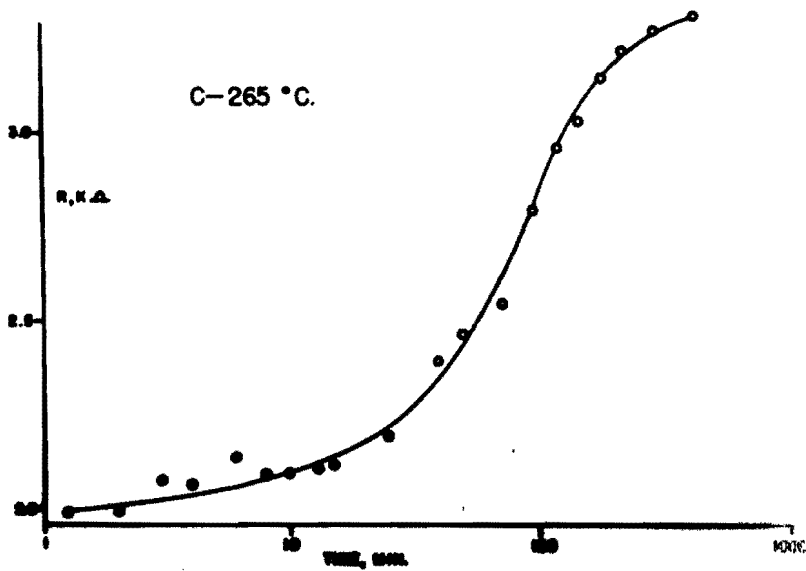
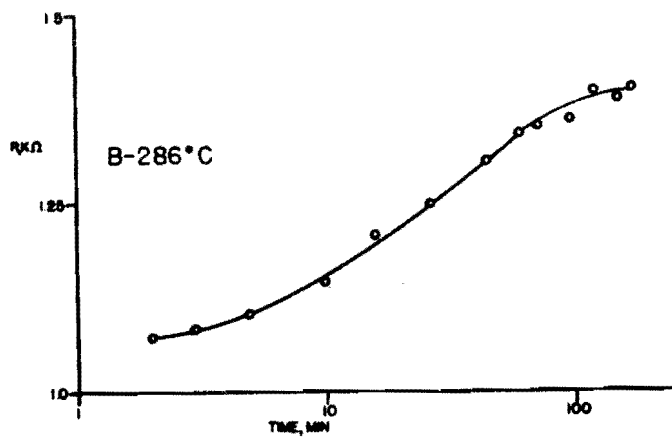
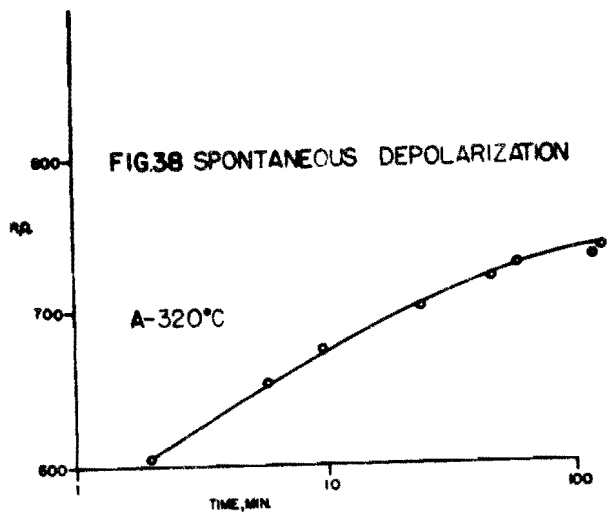


FIG 37 REVERSAL CURVES

to polarize and to depolarize, the long-term effect being similar to the application of zero field. After 50 minutes of this treatment, the reversal cycle was stopped such that the direction of current flow was the same as in Curve C. If segment D of the figure is removed entirely, the continued polarization (Curve E) fits continuously with segment C, as if the crystal had been held in suspension during the cycling period.

The slight downward drift of Curve D represents the tendency of the crystal to return to the unpolarized condition (spontaneous depolarization, to be discussed below). Further evidence of this has been found in a similar series of measurements, with the following results. If the resistance at point (3) is greater than that in the unpolarized case, then the gradual shift during the cycling period is down (toward unpolarized value). If it is less, then the drift is upward (again toward the unpolarized value).

As indicated above, the return to the unpolarized condition in the absence of an applied field (spontaneous depolarization) has been investigated. These measurements consisted of polarizing the crystal with an applied field of 6 v/cm (same as figure 32), removing the field, and measuring resistance as a function of time, applying, for the very short time interval during which the resistance is measured, a field small enough not to effect significantly the polarization of the crystal. These fields were of the order of a few mv/cm. Results are shown in figure 38 for three temperatures. The temperature dependence is approximately that to be expected, although the time necessary for depolarization at constant temperature is much less than the time observed to achieve equilibrium when changing temperature. Apparently,



two different processes are involved, for which the equilibrium time constants are vastly different.

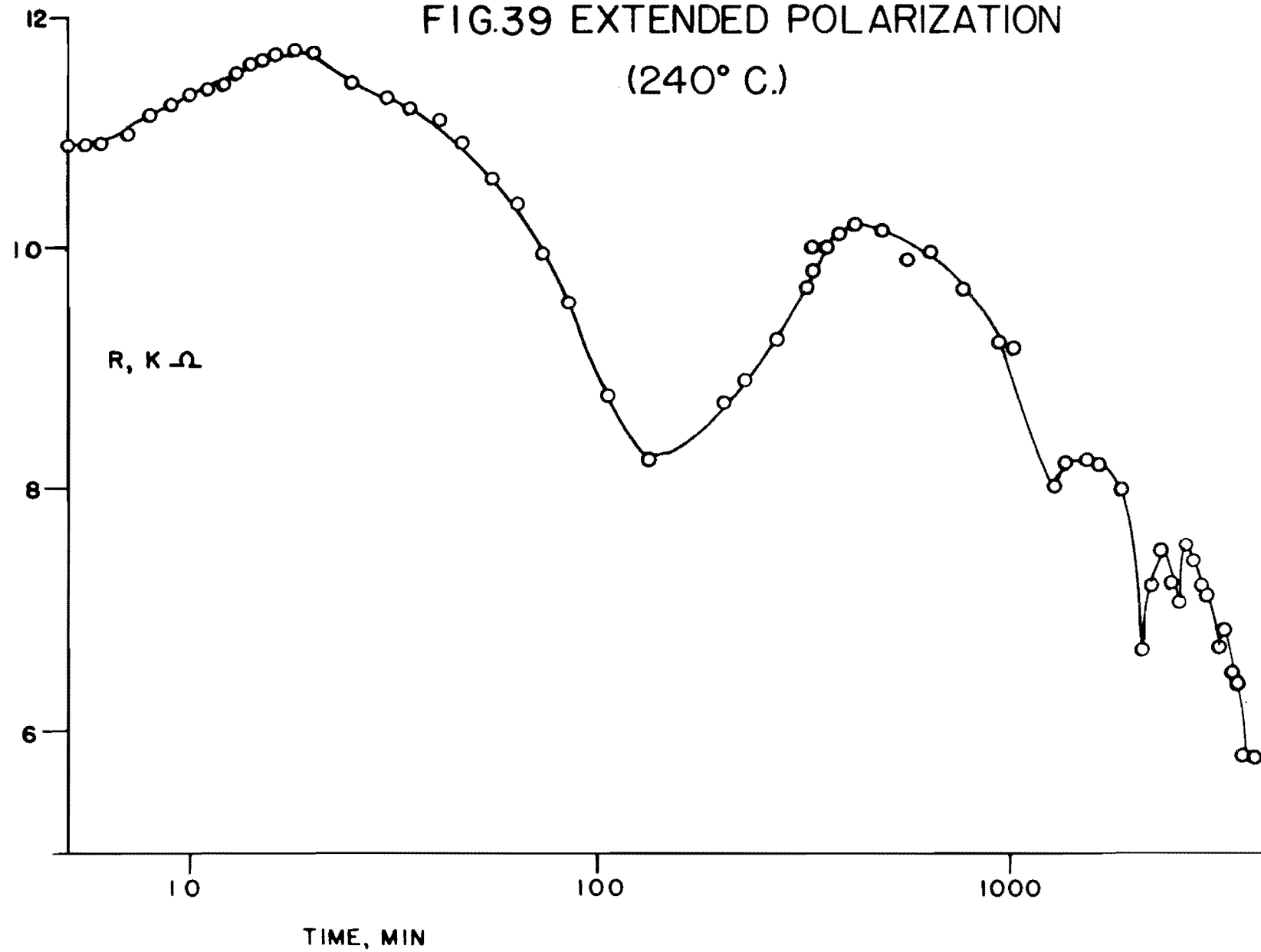
If one calculates the time constants from each depolarization curve, an exponential plot of the time constant against the reciprocal of temperature is obtained with a slope indicating an apparent activation energy of about 2.3 eV, which agrees satisfactorily with the values calculated from figure 33.

During the polarization and reversal measurements for specimen #18, it was found that, after polarization, the resistance began to rise again (figure 31E, for example). This prompted an experiment in which the polarization was continued for long periods of time. The results of this experiment (at 240°C) are shown in figure 39. The resistivity, after reaching a minimum, passed through several subsidiary peaks, which became less and less distinct. The resistance continued to change after two to three days (normal reversal time under these conditions was about 40 minutes).

The broad initial peak of this curve is a memory of a previous polarization which in this case had persisted for twenty-four hours at a temperature where the measured depolarization time is about 3-5 hours. This vestigial peak is found in many cases when insufficient time is allowed between experiments. After this long polarization the crystal exhibited atypical behavior for several days, after which it returned to its former state.

Hall Measurements -- Previous attempts to measure Hall coefficient in crystals showing the polarization effect have failed due to the large drift in Hall probe voltage imposed by the drift in resistance. Development of a more precise probe setting technique, however, made it

FIG.39 EXTENDED POLARIZATION  
(240° C.)



possible to position Hall voltage probes opposite each other with a precision of  $\pm 0.001$  inch, so that the I.R. component of the Hall voltage became much smaller. This enabled measurements to be made during polarization, as long as the temperature was low enough that the resistance drift during individual measurements was small (long polarization time).

The result of such a series of measurements is shown in figure 40, at  $220^{\circ}\text{C}$ . Curve A is for direct polarization, and Curve B for current reversal. Curves 1 are resistance; 2, Hall coefficient; and 3, indicated Hall mobilities. These measurements suffer from low precision, and also from the fact that they can be made only in the high temperature range in which the specimen is already approaching the intrinsic region where Hall measurements, in the absence of some independent information about the number of carriers or mobility, become less meaningful, due to the presence in the crystal of both electrons and positive holes. Certain features can be noted, however.

The Hall coefficient is positive, and from previous measurements (40), it appears that the mobility ratio  $b = \mu_n / \mu_p$  must be at least 4. In the expression for Hall coefficient

$$R = - \frac{3\pi}{8} \frac{(nb^2 - p)}{(nb + p)^2} \frac{1}{e}, \text{ then}$$

the term  $(nb^2 - p)$  must be negative. Substituting the value 4 for  $b$  we get

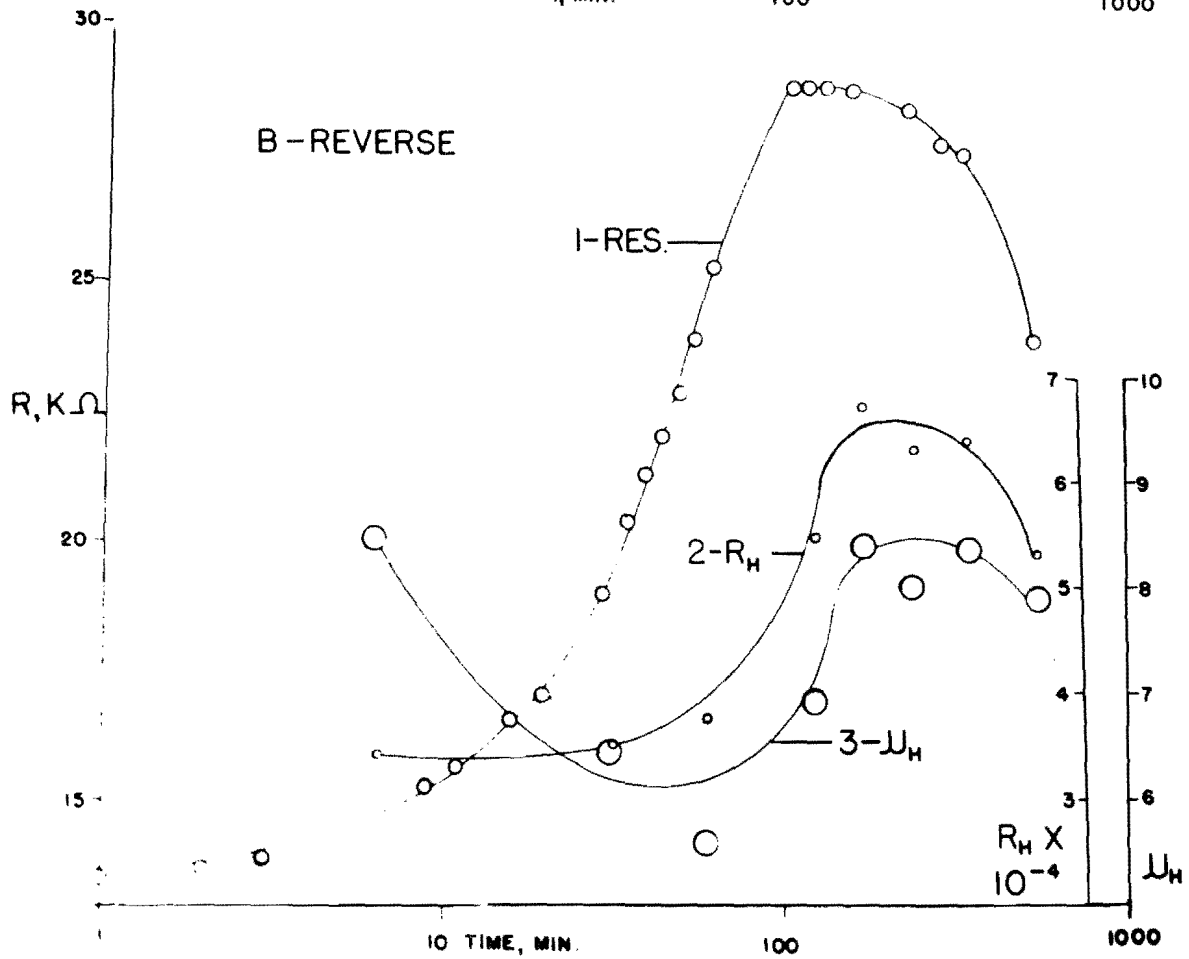
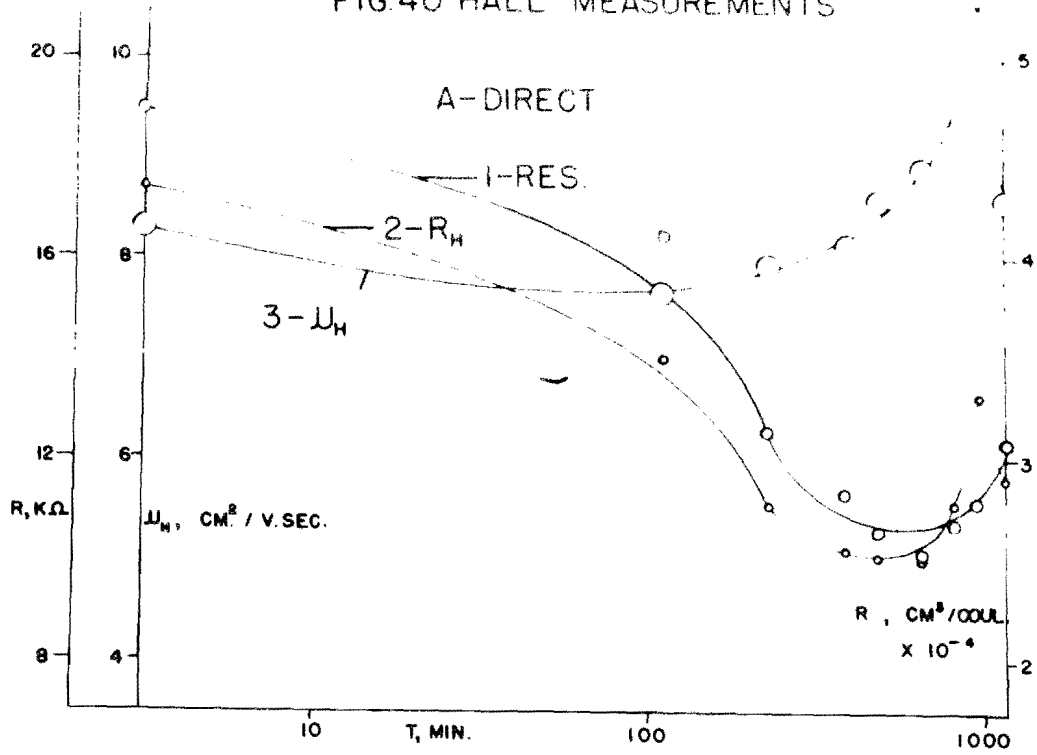
$$16n - p < 0, \quad \text{or } p > 16n$$

If the Hall constant were zero, the expression for conductivity

$$\begin{aligned} \sigma &= p\mu_p + n\mu_n && \text{would become} \\ \sigma &= 16n\mu_p + n(4\mu_p) = 16n\mu_p + 4n\mu_p \\ &= 4\mu_p (4n + n) \end{aligned}$$

$$(R_H = 0)$$

FIG.40 HALL MEASUREMENTS



In this case ( $R_H = 0$ ), the contribution of the positive holes to the conduction is more than 4 times that of the electrons. Since  $R_H > 0$ , the hole contribution is even more.

The data also indicate that the operative factor in the resistance change is the change in concentration of free positive holes, and not a change in the carrier mobility.

## 2. "Quenching" Experiments

Boer (77) has found in CdS a lag of the resistance behind the temperature when a crystal is heated or cooled quickly. In the case of heating at a very high rate ( $5^\circ/\text{sec}$ ) from room temperature to the measuring temperature a conductivity/time curve is obtained which is very similar to the polarization curves reported here with the conductivity changing by 3 to 4 orders of magnitude. The time constant of the conductivity build-up (resistance decay) is an inverse function of temperature. The time necessary to reach a stationary resistance value is about ten times as great at  $294^\circ\text{C}$  as at  $348^\circ\text{C}$ , indicating an activation energy of about 2.6 eV, calculated as above. The band gap in this temperature range is quoted as being 2 eV. The author calls this effect "intrinsic defect semiconductivity" and indicates that the current carriers are ionized from thermally induced lattice defects.

Experiments have been performed in an attempt to detect possible similar behavior in CdTe crystals. The crystal used was sample #18 (In impurity), the anomalous behavior of which has been described above. The procedures used in these experiments were approximately the same as those reported by Boer (see Apparatus, Measurement Techniques).

The results in terms of  $\log_{10} \rho$  vs  $1000/T$  are shown in figure 41. Pretreatment of the specimen consisted of heating it at a moderate

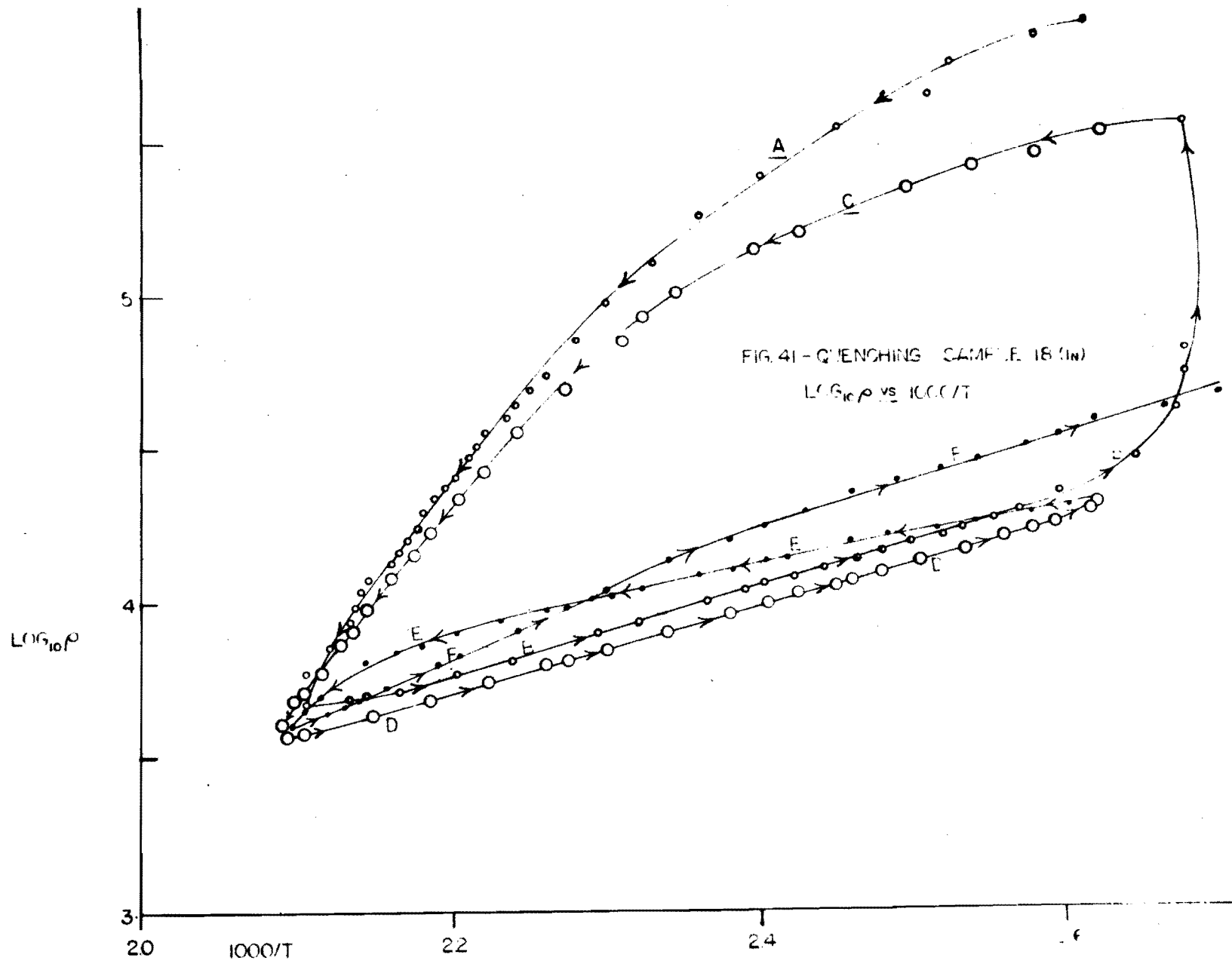


FIG. 41 - QUENCHING SAMPLE 18 (IN)  
 $\text{LOG}_{10} \rho$  VS  $1000/T$

rate to 200°C, and then cooling to 100°C very rapidly, during which treatment it was discovered that the behavior was similar to that reported by Boer. The sample was then allowed to soak at 100°C for five days, in order that the crystal should reach equilibrium at this temperature.

Next, the temperature was raised rapidly to 200°C, measurements of resistance being made every few seconds. The behavior of the resistivity is shown in Curve A, which shows the resistivity decreasing, at a gradually increasing rate. Equilibrium was then established at this new temperature, after which the temperature was lowered rapidly, the measured resistance being pictured in Curve B. This curve lies much lower than the heating curve, and has the property of being straight over the greater part of its length, which suggests that a meaningful activation energy can be calculated from its slope. The value of E for this curve is 0.58 eV.

Then, the crystal was allowed to soak at 100°C for one day, during which time the resistance progressed toward the equilibrium value for this temperature (near-vertical portion of Curve B). At the end of this time, the resistance was still short of the equilibrium value. The temperature was then raised rapidly to 200°C, then immediately reduced to 100°C, then immediately raised again to 200°C (Curves C, D and E). The behavior of the first two of these curves is quite similar to the first series of experiments. Curve E, before which no time had been allowed for equilibrium to be established, follows the same general path as the rapid cooling curve. After this curve, the temperature was lowered suddenly to 100°C (Curve F), whereupon the resistance followed the same type of path as in the cases above. The

calculated values of  $E$  are very nearly the same (0.58 eV) for all of the rapid cooling curves.

A similar pair of experiments is represented by figure 42. The temperature range was  $100^{\circ}$  to  $250^{\circ}\text{C}$ . The forms of the curves are identical with those given above, except for a larger difference between the two series of resistance values. The apparent activation energy of the rapid cooling curve is 0.57 eV.

One further pair of similar experiments was performed, this time between  $100^{\circ}$  and  $300^{\circ}\text{C}$ , the results of which are shown in figure 43. These two curves have the same general form as those previously given, but the apparent activation energy of the rapid cooling curve is now 1.37 eV. In addition, the high-temperature portion of this curve has a greater slope than the low-temperature portion; that is to say, its slope is more nearly the same as that of the rapid heating curve. This may be due to the faster response of the specimen to the rapidly changing temperature at these high temperatures.

In order to determine the equilibrium curve of resistance as a function of temperature for this specimen, a protracted cooling of the specimen was undertaken, during which resistance measurements were made at various points. The specimen was first allowed to soak at  $250^{\circ}\text{C}$  for 20 days, so as to be sure of temperature equilibrium at the beginning of the measurements.

At each value of temperature, the resistance was measured as a function of time until the change became negligibly small, after which the temperature was lowered to the next temperature to be investigated. The time required for the establishment of equilibrium conditions was an inverse function of temperature, becoming as large as several days at the lowest temperatures investigated.

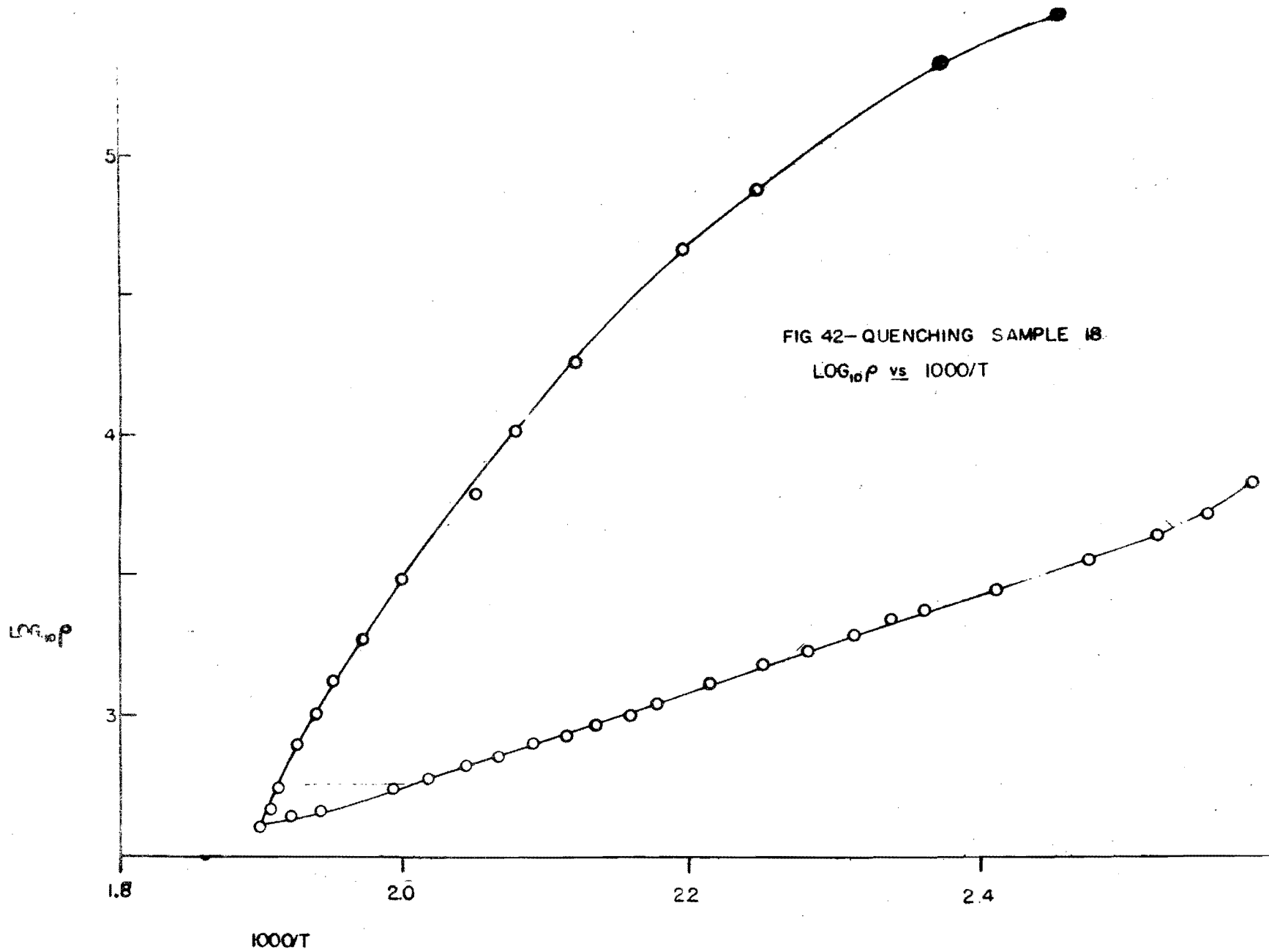
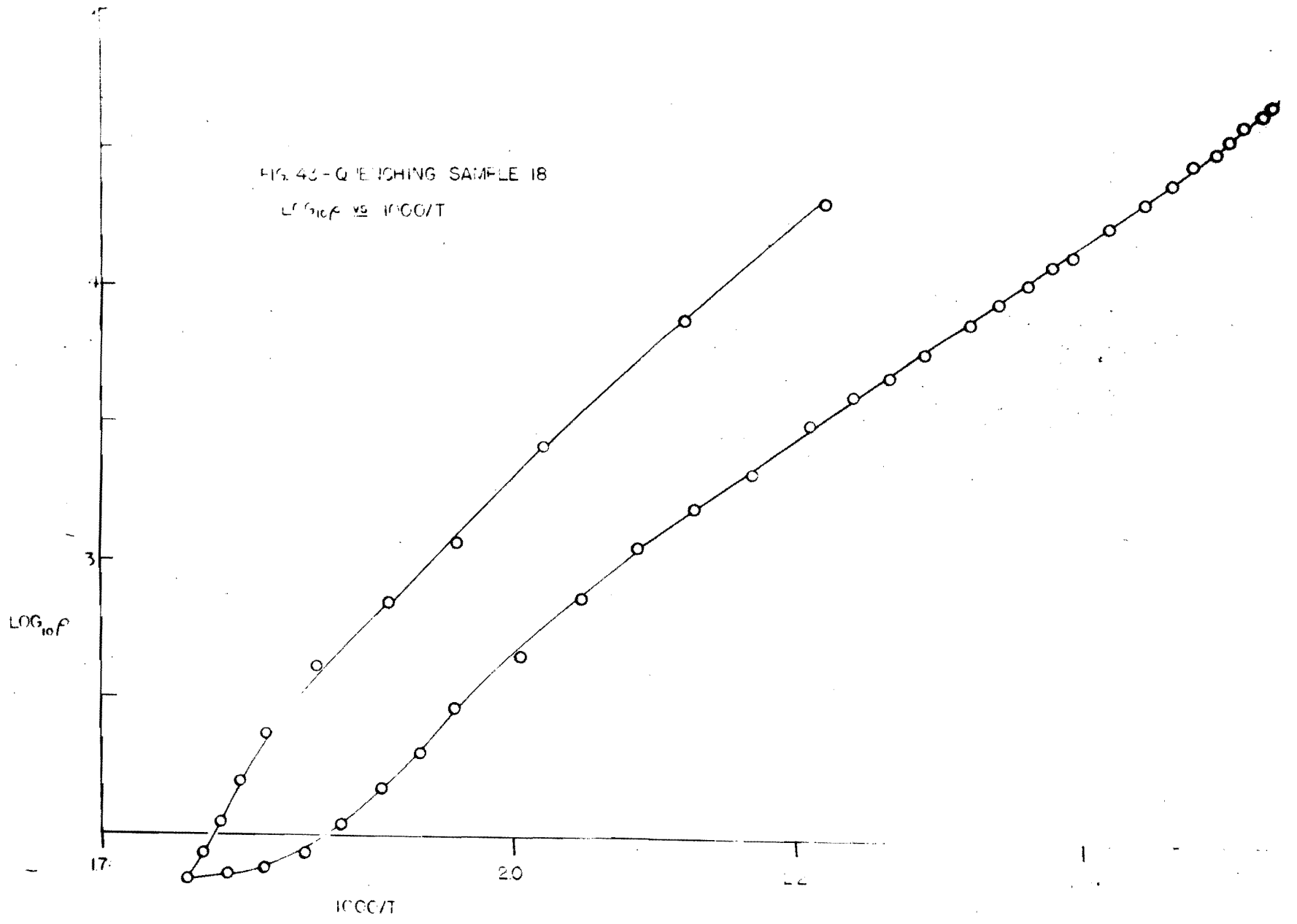
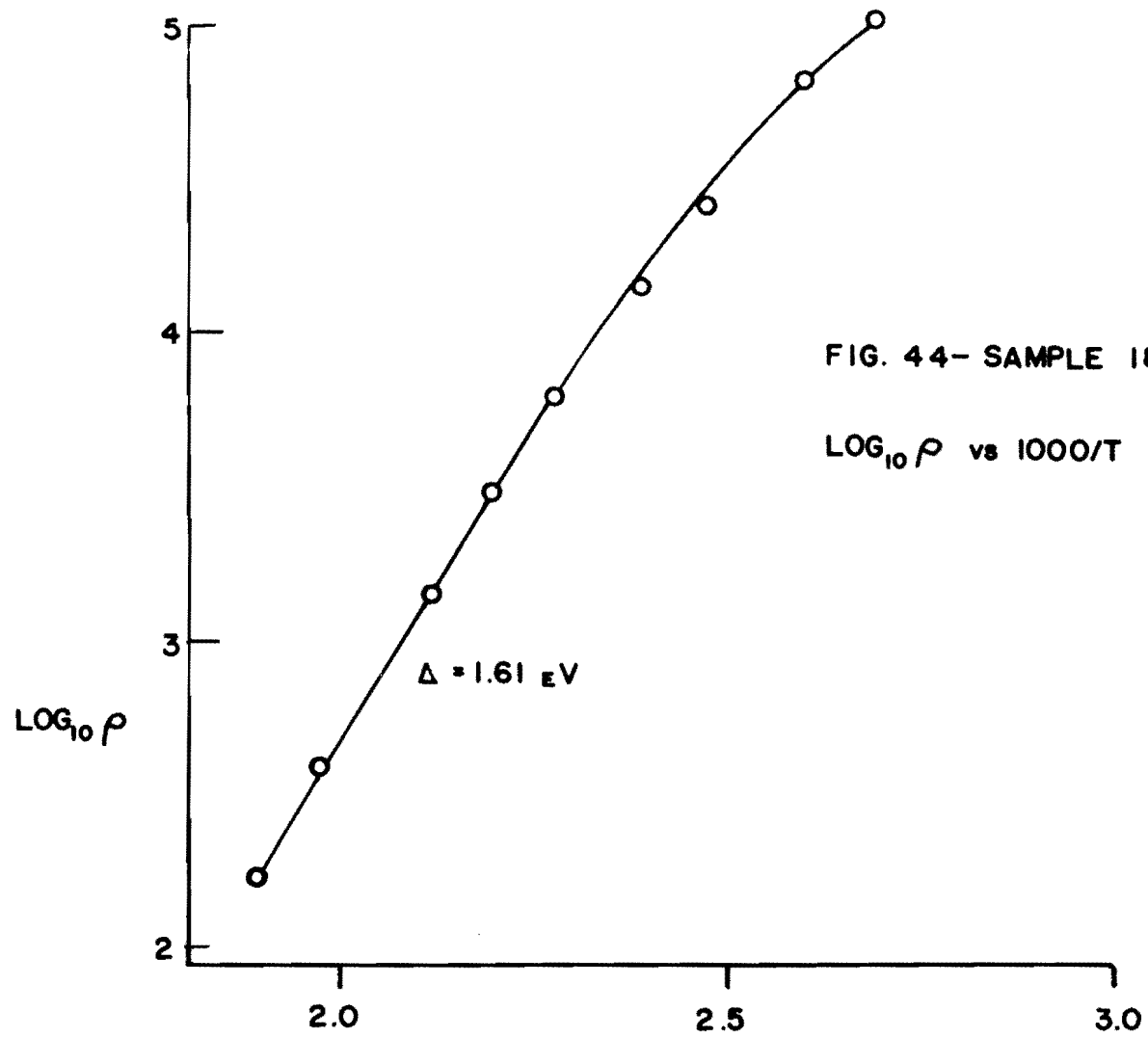


FIG. 43-Q'ENCHING SAMPLE 18

$\text{LOG}_{10} P$  vs  $10^3 C/T$





The results of this experiment are shown in figure 44, the values plotted being the equilibrium resistivity. The specimen apparently had an intrinsic region at temperatures above about 170°C, the calculated value of activation energy being 1.61 eV, which agrees well with the values reported above. The low-temperature portion of the curve is not straight enough for the calculation of a meaningful activation energy.

It has been mentioned above that continued heat treatment of the In impurity specimen produced a lengthening of the measured reversal time. This behavior continued during the course of the quenching experiments just described, due to the necessary heat treatment to which the crystal was subjected. After the completion of these experiments it was found that the resistance-time characteristic had altered by at least several orders of magnitude.

#### IV. DISCUSSION

##### A. CONVENTIONAL HALL AND RESISTIVITY MEASUREMENTS

The intrinsic activation energies reported here averaged  $1.59 \pm 0.02$  eV, which is about 0.1 eV greater than the average of those reported by other workers. The low-temperature activation energies of pure specimens #5 and #6 (0.52 and 0.35, respectively) are in good agreement with the results of Kroger and de Nobel (40) for excitation of positive holes from Cd vacancies.

Results obtained from the hot-pressed specimens show them to be p-type, probably due to a combination of monovalent impurity and Cd vacancies.

The two activation energies measured in the Cu impurity specimen #15 (figure 10) are the same, within the limits of experimental error. The break between the two portions of the resistivity curve is seen (in figure 11 and 12) to be due to changes in both the number of current carriers and the carrier mobility. The data of figures 15 and 16, obtained from the other Cu impurity specimen, are again apparently affected by the same type of discontinuity.

The p-type conduction found in the Cu and Ag impurity specimens is to be expected from specimens of CdTe containing a monovalent impurity, although the calculated activation energies in many cases exceed those reported for similar specimens by other workers. This might perhaps be due to a failure of the assumption of negligible donor concentration in these specimens. If this were the case, the solution of equation (9) would not be of either of the simple forms given, but would be obtainable only through a much greater multiplicity of measurements. This would

allow the exact evaluation of the pre-exponential term of the equation, as performed by Kroger and de Nobel, who, even then, were unable to reach a satisfactory conclusion. However, it seems unlikely that the assumption of negligible donor concentration could be far wrong, due to the heavy doping of these crystals. The extrinsic activation energies calculated for the pure specimens, and more particularly the Sb and Bi impurity specimens (which were known to contain a significant concentration of donor impurity) may be in more serious doubt.

It has been observed that the temperature dependence of the carrier mobility in the Cu- and Ag-doped and hot-pressed specimens, in general, obeyed the relation to be expected from specimens in which the mobility is determined by lattice scattering.

The p-type behavior found in all but the In impurity crystal is almost certainly due, to a greater or lesser extent, to the presence of Cd vacancies in these specimens.

The measurements made before heat treatment of the In impurity specimen (#18) show the n-type conduction to be expected from specimens containing a trivalent impurity, which is apparently not compensated by Cd vacancies. The activation energy calculated for this specimen is probably not reliable, since the equation used for its calculation is not applicable to materials in which the impurity centers are almost completely ionized. However, the activation energy is probably of the order of  $kT$  at the lowest temperature at which measurements were made ( $kT \approx 0.008$  eV). A precise determination of the activation energy of this specimen would necessitate measurements at much lower temperatures. The mobility in this specimen has been seen to obey a temperature dependence indicating the predominance of impurity scattering, although the

numerical values of the mobility are lower by a factor of about three than the results of Kroger and de Nobel. This discrepancy may be due to the greater concentration of donor centers in the In impurity crystal.

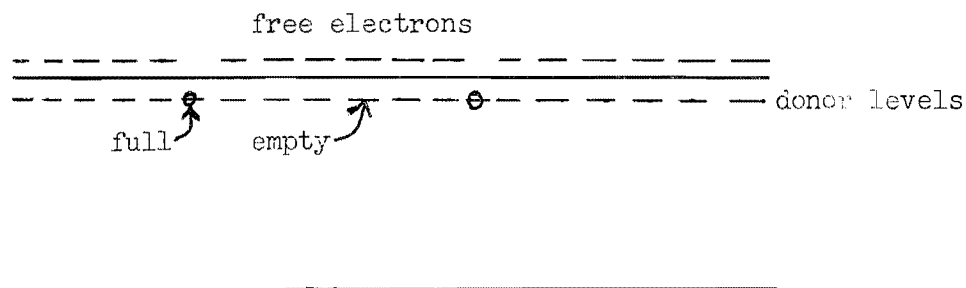
#### B. POLARIZATION AND QUENCHING EXPERIMENTS

Behavior of this type has not been previously reported, except for the quenching experiments of Boer (77). It might be suggested that the effects noted were the result of the peculiarity of one specimen, and/or that they were due to contamination from the electrodes.

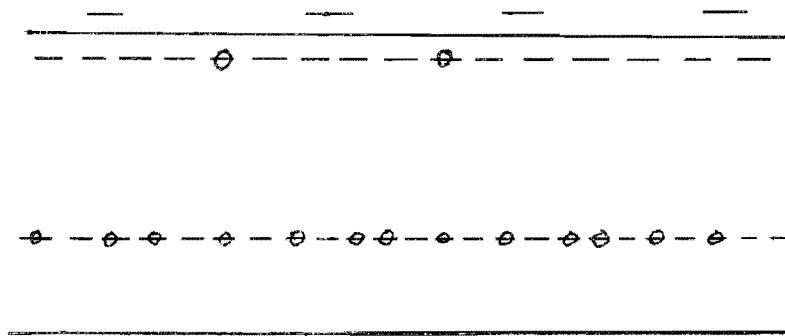
The first objection is not valid, since the effects were found in four different crystals, of two different compositions, the last of which was studied particularly extensively. As for the second objection, the effects were found in crystals bearing several different types of electrode: pressed platinum foil (#2), silver paste (#7), and chemically-deposited gold (#17, #18).

This establishes the reality of the effect and eliminates the possibility of artifact due to electrodes or other causes. It appears that the presence of both donor and acceptor centers produce these effects. Let us consider this further, for the case of the In impurity specimen (#18).

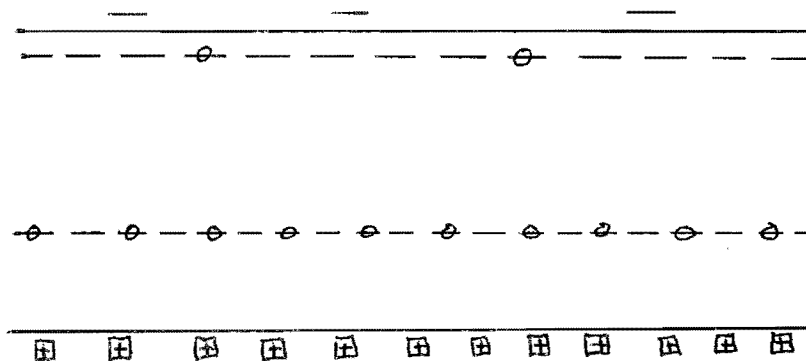
The band picture of this specimen before heat treatment was the following:



where, of the approximately  $10^{17}$  donors present, almost all were ionized because of the very low activation energy. During the heat treatment at a constant temperature of  $300^{\circ}\text{C}$ , Cd vacancies were introduced in the crystal, while  $\text{Cd}^0$  vapor was evolved. These vacancies constituted acceptor centers, into which dropped electrons from the conduction band. As this process continued, the reduction in free electron concentration resulted in an increase in the resistivity:



However, during this process, the product of the concentration of free electrons and the concentration of free positive holes remained constant, since it is a property of the crystal lattice for any constant temperature (equation (6), Introduction). Therefore, as the concentration of free electrons decreased, the concentration of free positive holes increased. Following from this, the band picture of the crystal at the time of the measurements was approximately thus:

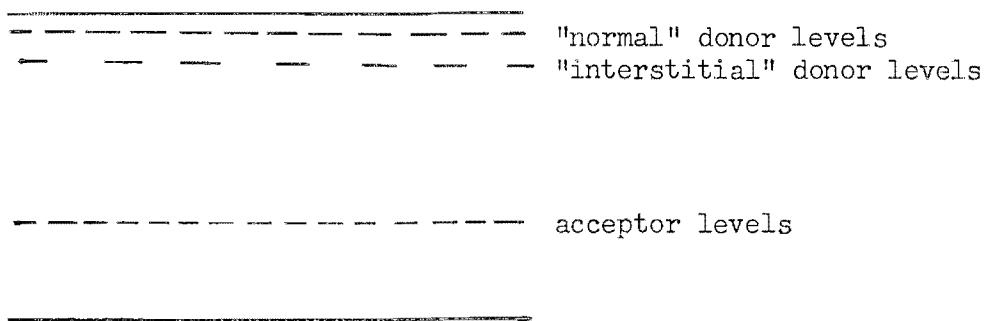


where the concentration of free holes exceeds the concentration of free electrons.

It would normally be expected that the resistivity of the crystal would pass through a maximum, and then begin to decrease as the crystal crosses the boundary between n- and p-type character. The fact that it does not suggests that at the beginning of the polarization experiments the crystal was not at equilibrium, and that the interior of the crystal was still n-type, while the surface layer (which was closest to the atmosphere into which the Cd vapor was escaping) had become p-type. It would be expected that the Hall coefficient measurement would be affected primarily by the condition of the surface layers, and that the effects observed are a property of these layers and not of the core of the crystal. Additionally, as the polarization experiments progressed, the resistivity of the material did begin to fall again, suggesting that the entire crystal had become p-type. This decrease is barely discernible in measurements made at the same time as the Hall measurements, and became much greater at the end of the investigation, particularly in figure 44, which shows a decrease of about a factor of 12.

A possible mechanism for the effects observed can now be described. Under the influence of an applied electric field or thermal agitation at high temperatures, a few In ions jump from their normal lattice positions into interstitial positions in the crystal (the interstices in the zincblende structure have six-fold coordination and so are larger than the normal lattice sites, which have four-fold coordination). These interstitial cations would constitute Frenkel defects (78). It may be assumed that they exist in the interstices as  $\text{In}^{3+}$  ions, whereas

in their lattice positions they had a much lower effective average charge, due to the mixed ionic-covalent bonding of the lattice. Because of the increased effective charge of the  $\text{In}^{3+}$  ions, their coulombic attraction for free electrons would be much greater, and so they would represent ionized donor centers, but with much greater activation energy than that which they possessed while still in normal lattice positions. The band picture of the crystal would thus be



The probability of free electrons dropping from the conduction band to one of these deeper "interstitial" donor levels would be much greater than that of its dropping into a shallow "normal" donor level, and the overall effect would be a marked reduction in the number of free electrons in the conduction band. However, since  $np = C_T$  (where  $C_T$  is constant at constant temperature), a decrease in  $n$  must be accompanied by an increase in  $p$  and, by differentiation,

$$n dp + p dn = d(C_T) = 0,$$

$$dp/dn = -p/n$$

Since  $p \gg n$ , then  $dp \gg (-)dn$ , and the number of positive holes would be greatly increased, with a resultant decrease in the resistivity (as in figure 30A, for example). Upon the reversal of the current direction, the interstitial  $\text{In}$  ions would first tend to jump back into normal

cation positions (reversing the above process), and the resistivity would increase. Then the movement to interstitial positions would proceed in the opposite direction, and the resistivity would again decrease. This behavior is the same as that found in the reversal curves (figures 30B, 31, 32, etc.).

The jumping of In ions from interstitial to normal lattice positions would be an activated process, due to the potential barriers between the two types of site, and the activation energy calculated from the reversal curves is apparently that for the jumping process (the calculation of this activation energy has followed the relation associated with the thermal creation of Frenkel defects (79)). The spontaneous depolarization curves would be expected to show the same activation energy, which was observed.

The secondary peak observed in the extended polarization experiment (figure 39) would, according to this model, be associated with the diffusion of In ions from normal lattice sites to Cd vacancies, in which their behavior would be similar to that in the unpolarized condition.

The proposed model accounts for the essential features of the results obtained, not only in the In impurity crystal, but in the Bi impurity crystals as well. While there is no reason to suppose that Cd ions do not also move to interstitial positions, where they would behave in essentially the same manner, the activation energies calculated for the Bi impurity crystals are different from those of the In-doped crystals. This would not be expected unless the impurity played a dominant role in the production of the effects. However, the activation energy may be not only a function of the impurity present, but also due in part to some other parameter.

The behavior observed in the quenching experiments is probably related to the other properties discussed above. It is likely that the decrease in the low-temperature resistivity is due to the freezing-in of interstitial ions, and that the activation energies observed in the rapid-cooling curves represent the recombination of the excess positive holes created as a result of the interstitial ions produced thermally at higher temperatures.

The model proposed above cannot be made directly to account for the following observed features:

1. The increase in reversal time in the In impurity specimen brought about by continued heating of the crystal.
2. The ultimate disappearance of the reversal effects which was observed after the quenching experiments.
3. The long times required to attain temperature equilibrium for the measurement of reversal times, which in all cases greatly exceed the observed depolarization times.

These features might be explainable by further development of the proposed model. However, further elucidation of the polarization and quenching effects would require extremely extensive further work, particularly as regards the production of specimens of sufficient variety and of proper impurity content.

## V. SUMMARY

Conventional Hall coefficient and resistivity measurements were carried out in single crystals of CdTe, both "pure" and with added impurities, and in hot-pressed polycrystalline specimens. In most cases, the sign of the current carriers was consistent with the valence of the added impurity. Discrepancies in certain trivalent impurity crystals are explained on the basis of an excess of Cd vacancies. The mobilities for electrons averaged about  $200 \text{ cm}^2/\text{v sec}$ , and those of holes about  $40 \text{ cm}^2/\text{v sec}$ , both at room temperature.

Anomalous changes in resistivity as a function of applied electric field and heat treatment in crystals containing both donors and acceptors were found and investigated. A rough model is developed which accounts for most of the effects observed.

## VI. BIBLIOGRAPHY

1. L. Pauling, The Nature of the Chemical Bond, Cornell Univ. Press, Ithaca, 1945, p. 69.
2. F. Seitz, The Modern Theory of Solids, McGraw-Hill, New York, 1940, p. 139.
3. H. Lorentz, Amsterdam Proc. 1904-1905; cf. reference 2.
4. A. Sommerfeld, Z. Physik 47, 1 (1928); cf. reference 7.
5. F. Richtmyer and E. Kennard, Introduction to Modern Physics, McGraw-Hill, New York, 1947, p. 248.
6. de Broglie, Phil. Mag. 47, 446 (1924); Ann de Physique 3, 22 (1925); cf. reference 5, p. 236.
7. A. Dekker, Solid State Physics, Prentice-Hall, Englewood Cliffs, 1957, p. 214.
8. loc cit, reference 5, p. 102.
9. W. Hume-Rothery, Atomic Theory for Students of Metallurgy, The Institute of Metals, London, 1948, p. 182.
10. C. Kittel, Introduction to Solid State Physics, John Wiley and Sons, New York, 1956, p. 295.
11. C. Kittel, Introduction to Solid State Physics, John Wiley and Sons, New York, 1953, p. 275.
12. W. Shockley, Electrons and Holes in Semiconductors, Van Nostrand, New York, 1950, p. 22.
13. Verwey et al, Chem. Weekbl. 44, 705; Philips Res. Repts. 5, 173 (1950); cf. reference 16.
14. P. Selwood et al, J. Am. Chem. Soc. 71, 693 (1949); cf. reference 16.
15. G. Koch and C. Wagner, Z. Phys. Chem. 38B, 295 (1937); cf. reference 16.
16. F. Kroger and H. Vink, Physica 20, 950 (1954).
17. P. E. Klaus, Phys. Rev. 109, 1944 (1958).
18. W. Brattain. Rev. Mod. Phys. 23, 203 (1951).
19. J. de Boer and W. Van Geel, Physica 2, 286 (1935); cf. reference 18.
20. B. Nijboer, Proc. Phys. Soc. 5, 1575 (1939); cf. reference 18.
21. F. Seitz, Phys. Rev. 73, 549 (1948).

22. W. Harrison, Phys. Rev. 104, 1281 (1956).
23. M. Sclar, Phys. Rev. 104, 1548 (1956).
24. M. Sclar, Phys. Rev. 104, 1559 (1956).
25. E. Conwell and V. Weisskopf, Phys. Rev. 69, 258 (A) (1946); 77, 388 (1950).
26. T. Dauphine and E. Mooser, Rev. Sci. Inst. 26, 660 (1955).
27. J. McDonald and J. Robinson, Phys. Rev. 95, 44 (1954).
28. W. Dunlap, Phys. Rev. 79, 286 (1950).
29. O. Lindberg, Proc. I.R.E., 40, 1414 (1952).
30. P. Banbury et al, Proc. Phys. Soc. 66A, 753 (1953).
31. T. J. Gray et al, The Defect Solid State, Interscience, New York, 1957, p. 33.
32. ibid, p. 72.
33. H. Jones, Phys. Rev. 81, 149 (1951).
34. V. Johnson and K. Lark-Horovitz, Phys. Rev. 69, 258 (1946); 79, 176 (1950).
35. F. Blatt, Phys. Rev. 105, 1203 (1957).
36. L. Hunter, Phys. Rev. 94, 1157 (1954).
37. W. Zachariasen, Z. Phys. Chem. 124, 277 (1926); Chem. Abstr. 21, 842 (1927).
38. J. Mellor, A Comprehensive Treatise on Inorganic and Theoretical Chemistry, Longmans, Green and Co., London, 1931, Vol. 11, p. 51.
39. International Critical Tables II, 430.
40. F. Kroger and D. de Nobel, J. Electronics 1, 190 (1955).
41. C. Hodgman et al, Handbook of Chemistry and Physics, Chemical Rubber, Cleveland, 1957, p. 500.
42. J. McAteer and H. Seltz, J. Am. Chem. Soc. 58, 2081 (1936).
43. D. de Nobel and D. Hoffman, Physica 22, 252 (1956).
44. C. Goodman, Proc. Phys. Soc. 67B, 258 (1954).
45. L. Pauling, The Nature of the Chemical Bond, Cornell Univ. Press, Ithaca, 1945, p. 69.

46. C. Goodman and R. Douglas, *Physica* 20, 1107 (1954).
47. R. Frerichs, *Phys. Rev.* 72, 594 (1947).
48. F. Moglich and R. Rompe, *Z. Phys.* 119, 472 (1942); *Chem. Abstr.* 38, 295 (1944).
49. R. Bube, *Proc. I.R.E.*, 43, 1836 (1955).
50. R. Frerichs and R. Warminsky, *Naturwiss.* 33, 251 (1946); *Chem. Abstr.* 43, 35 (1949).
51. R. Frerichs, *Naturwiss.* 33, 28 (1946); *Chem. Abstr.* 43, 3294 (1949).
52. P. Gorlich and J. Heyne, *Optik* 4, 206 (1948); *Chem. Zentr.* 1950, 1, 1449; *Chem. Abstr.* 46, 8954 (1952).
53. G. Kretschmar and L. Schilberg, *J. Appl. Phys.* 28, 865 (1957).
54. E. Schwartz, *Nature* 162, 614 (1948).
55. F. Van Doorn and D. de Nobel, *Physica* 22, 338 (1956).
56. E. Rittner, *Phys. Rev.* 96, 1708 (1954).
57. R. Bube, *Phys. Rev.* 98, 431 (1955).
58. H. Miyasawa and S. Sugaike, *J. Phys. Soc. Japan* 9, 648 (1954); *Chem. Abstr.* 49, 10728 (1955).
59. T. J. Gray et al, *O.N.R. Annual Rept.*, Contract #Nonr 1503(01), Project #NR015-215 (1955).
60. L. Pensak, *Phys. Rev.* 109, 601 (1958).
61. B. Goldstein, *Phys. Rev.* 109, 601 (1958).
62. R. Waring, *Brit. Patent* 454343, Sept. 29, 1936; *Chem. Abstr.* 31, 1562 (1937).
63. L. Wesch, *Reichsamt Wirtschaftsbaus*, *Chem. Ber. Prof-Nr.* 15, 487 (1942); *Chem. Abstr.* 41, 5022 (1947).
64. C. Jacobson, *Encyclopedia of Chemical Reactions*, Reinhold, New York, **Vol. II**, p. 13, 31; cf. reference 38.
65. D. Jenny and R. Bube, *Phys. Rev.* 96, 1190 (1954).
66. J. Appel, *Z. Naturforsch.* 9a, 265 (1954); cf. reference 67.
67. J. Appel and G. Lautz, *Physica* 20, 1110 (1954).
68. Boltaks, *Zhur. Tekh. Fiz.* 25, 2329 (1955); *Chem. Abstr.* 50, 9074 (1956).

69. cf. reference 59, 1954.
70. cf. reference 59, 1956.
71. R. Smith, Phys. Rev. 97, 1525 (1955).
72. G. Diemer, Philips Res. Repts. 10, 194 (1955).
73. W. Dunlap, Phys. Rev. 94, 1531 (1954).
74. C. Fuller, J. Appl. Phys. 27, 544 (1956).
75. C. Fuller and J. Severiens, Phys. Rev. 96, 21 (1954).
76. G. Quincke, Ann. Phys. 24, 347 (1885); 34, 401 (1888); cf. P. Selwood, Magnetochemistry, Interscience, New York, 1956, p. 10.
77. K. Boer, Z. Naturforsch. 10a, 898 (1955).
78. cf. reference 31, p. 7.
79. cf. reference 10, p. 479.

This report was submitted by John L. Stull as thesis requirement for the degree of Doctor of Philosophy in Ceramics, State University of New York College of Ceramics, Alfred University, Alfred, New York.



~~Thomas J. Gray  
Project Director~~



~~John L. Stull  
Research Fellow~~